

UCSF

UC San Francisco Electronic Theses and Dissertations

Title

Synthetic Biology Approaches to Understand and Engineer Immune Cells

Permalink

<https://escholarship.org/uc/item/515254dg>

Author

Reddy, Nishith

Publication Date

2023

Peer reviewed|Thesis/dissertation

Synthetic Biology Approaches to Understand and Engineer Immune Cells

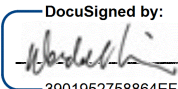
by
Nishith Reddy

DISSERTATION
Submitted in partial satisfaction of the requirements for degree of
DOCTOR OF PHILOSOPHY

in
Biological and Medical Informatics

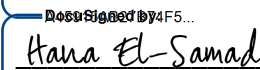
in the
GRADUATE DIVISION
of the
UNIVERSITY OF CALIFORNIA, SAN FRANCISCO

Approved:

DocuSigned by:

3901952758864EF... Wendell Lim
Chair

DocuSigned by:

Arthur Weiss

DocuSigned by:

52F8E320792C4C4... Hana El-Samad

Committee Members

Copyright 2023

By

Nishith Reddy

ACKNOWLEDGEMENTS

Although science is often presented as a linear series of steps, the reality of the scientific process is a more complex exploration of ideas with many twists and turns along the way. My scientific journey during my Ph.D. was made possible by the incredible support I received that helped shape that exploration. This thesis would not have been possible without their support.

First, I would like to thank my thesis advisor, Wendell Lim. Wendell helped me to see the artistry in doing science. Through his mentorship, I learned to better explore a space of new ideas, but also find my footing when I get lost. He taught me the value of communicating science clearly and learning new languages necessary to engage with diverse fields. His unwavering excitement for pushing the limits of the science and high standards for quality continue to inspire and motivate me. Beyond science, Wendell supported me when I ran into personal challenges during my time at UCSF. Thank you for all your mentorship both scientifically and otherwise over the last few years.

Many other people from the Lim lab were essential to my Ph.D. work. Noleine Blizzard was one of my biggest advocates and helped me with most aspects of my Ph.D.: organizing meetings, hitting deadlines for projects or grants, and checking on my general wellbeing. Over the years, I had the opportunity to work with many talented people in the Lim lab, including fellow graduate students (Joe Choe, Jasper Williams, Ki Kim, Hersh Bhargava, Devan Shah, Riley Stockard), postdocs (Greg Allen, Milos Simic, Rogelio Hernandez-Lopez, Kyle Daniels, Geoff O'Donoghue, Aileen Li, Ricardo Almeida, Nick Frankel, Wes McKeithan, Jungmin Lee, Phil Pauerstein, Toshi Tamada), lab managers (Pilar Lopez, Sim Sidhu, Michael Broeker), animal specialists (Wei Yu,

Yurie Tonai), and master's student (Daniela Cabanillas) among other current or past Lim lab members. I relied on many of these people for help and learned a lot from them. My Ph.D. would not have been possible without them.

My thesis would not have been possible without many engaged collaborators that helped push the projects forward. These collaborators include Matthias Hebrok, Audrey Parent, Hasna Maachi, Yini Xiao, Matthew Spitzer, and Jaqueline Yee. Their involvement in the projects were critical to advancing the science and I learned a lot from them in the process. My thesis committee, Art Weiss and Hana El-Samad, provided critical feedback throughout my Ph.D. The integrative program in quantitative biology (IPQB), quantitative biology consortium (QBC), and larger community at UCSF helped to support my development as a scientist. I also met many great people at UCSF and in San Francisco that made my time here exciting and enjoyable.

I want to thank Aishwarya Shah for her companionship and encouragement that motivated me throughout my Ph.D. She has been my biggest supporter and helped me get through my most challenging times. I could not have done this without you. Thank you for all the encouragement and fun memories we created together over the years.

Lastly, I would like to thank my family Krishna Reddy, Hema Reddy, and Navya Reddy. My parents encouraged my curiosity for science from a young age and played an important role in making me who I am today. Without their sacrifices, I would not be here. Thank you for all your support.

Acknowledgement of previously published work in this dissertation.

Chapter 2 contains material from a published article with contributions from several authors:

Allen, G. M.⁺, Frankel, N.W.⁺, **Reddy, N.R.**, Bhargava, H. K., Yoshida, M.A., Stark, S.R., Purl, M., Lee, J., Yee, J. L., Yu, W., Li, A.W., Garcia, K.C., El-Samad, H., Roybal, K.T., Spitzer, M.H., Lim, W.A (2022). Synthetic cytokine circuits that drive T cells into immune-excluded tumors. *Science*, 378, eaba1624.

⁺ denotes equal contribution of the author

Chapter 3 contains material for a manuscript in preparation for submission with contributions from several authors:

Reddy, N.R., Maachi, H., Xiao, Y., Yu, W., Simic, M.S., Cabanillas, D.A., Tonai, Y. , Parent, A.V., Hebrok, M., Lim, W.A. Engineering synthetic suppressor T cells capable of locally targeted immune suppression. *In preparation*.

Synthetic Biology Approaches to Understand and Engineer

Immune Cells

By Nishith Reddy

ABSTRACT: In recent years, synthetic immunology has allowed us to probe the complex interactions between immune cells and their environment, and to develop novel strategies for treating diseases. Cell-based immunotherapies, particularly chimeric antigen receptor (CAR) T cells, have made advances in the clinic for treatment of hematological malignancies. However, there is a broader potential for cell-based immunotherapies to impact the treatment of many challenging diseases such as solid tumors or autoimmunity. Immune cells can be engineered with synthetic circuits to carry out more precise molecular recognition and therapeutic action. Synthetic reconstitution of immune signaling by engineering systems from the bottom-up allow us to identify molecular features sufficient to achieve particular sets of behaviors. Here, we engineered T cells using synthetic Notch (synNotch) receptors that induce the local production of therapeutic payloads. First presented is an exploration of T cell circuits that induce the production of pro-inflammatory cytokine IL-2 specifically at the site of a tumor, bypassing tumor suppression to clear challenging solid tumors without inducing systemic toxicity. Second presented is the study of T cell circuits that drive local immune suppression to block off-target CAR T cell toxicity or protect transplants from cytotoxic T cell killing without systemic immune suppression. Together, these studies demonstrate how synthetic T cell circuits can be used to perturb immune microenvironments for therapeutic applications.

TABLE OF CONTENTS

Chapter 1. Introduction	1
Chapter 2. Synthetic cytokine circuits that drive T cells into immune-excluded tumors	3
References.....	23
Chapter 3. Engineering synthetic suppressor T cells capable of locally targeted immune suppression	78
References.....	98
Chapter 4. Concluding Remarks	124

LIST OF FIGURES

Chapter 2. Synthetic cytokine circuits that drive T cells into immune-excluded tumors.

Fig. 2.1. Synthetic synNotch→IL-2 circuits can drive local T cell proliferation independent of TCR activation or cooperatively with T cell killing.
..... 40

Fig. 2.2 Autocrine synthetic IL-2 circuits strongly improve T cell cytotoxicity against multiple models of immune-excluded syngeneic tumors.
..... 42

Fig. 2.3. Synthetic Notch based cytokine delivery is required for effective control of KPC tumors.
..... 44

Fig. 2.4. Synthetic IL-2 circuit enables T cell infiltration into immune excluded tumors.
..... 45

Fig. 2.5. Profiling of tumor micro-environment shows expansion and activation of CAR T cells with autocrine IL-2 circuit.
..... 47

Fig. 2.6. Bypassing tumor immune suppression mechanisms with a synthetic IL-2 delivery circuit	49
Fig. 2.S1. Driving immune cell expansion with synNotch→IL-2 circuits.	59
Fig. 2.S2. Local autocrine proliferation in vivo driven by synthetic IL-2 circuit	61
Fig. 2.S3. Local paracrine proliferation in vivo driven by synthetic IL-2 circuit.	63
Fig. 2.S4. Tumor killing enhanced by synthetic IL-2 circuits in individual mice.	64
Fig. 2.S5. Enhanced local proliferation of tumor-reactive TCR T cells when co-delivered with synthetic IL-2 circuit T cells.	66
Fig. 2.S6. In-vitro characterization of engineered mouse T cells used in syngeneic tumor model experiments.	68
Fig. 2.S7. Individual mouse tumor volume data for experiments showing that syngeneic tumor killing is enhanced by synthetic IL-2 circuits (synNotch=>mIL-2).	69

Fig. 2.S8 Orthotopic syngeneic tumor killing enhanced by synthetic cytokine circuits	70
.....	
Fig. 2.S9. Comparison of alternative strategies to deliver IL-2 to enhance T cell cytotoxicity against tumors.	71
.....	
Fig. 2.S10. Evaluating toxicity: SynNotch-->IL-2 circuit does not produce systemic toxicity or worsen CAR toxicities.	72
.....	
Fig. 2.S11. Comparison of effect of constitutive vs inducible IL-2 on T cell behavior.	73
.....	
Fig. 2.S12. Enhanced local infiltration of T cells in immunocompetent melanoma and pancreatic tumors.	74
.....	
Fig. 2.S13. CyTOF analysis of autocrine and paracrine IL-2 circuits in KPC tumors.	75
.....	
Fig. 2.S14. CyTOF analysis of treated KPC pancreatic tumors	77
.....	
Fig. 2.S15. Repeat CyTOF analysis of treated KPC pancreatic tumors	79
.....	

Fig. 2.S16. CyTOF analysis of spleens in mice treated.	80
Fig. 2.S17. Estimation of synthetic cytokine circuit strength and induction of CD25	82
 Chapter 3. Engineering synthetic suppressor T cells capable of locally targeted immune suppression.	
Fig. 3.1. Engineering synthetic suppressor T cells that drive antigen-induced expression of immune suppressive payloads.	101
Fig. 3.2. Combinatorial induction of both CD25 and TGFβ1 by the same suppressor cell leads to more effective suppression of CAR T cells in vitro.	103
Fig. 3.3. Synthetic suppressor cells block CAR T cell killing in vivo in locally targeted manner.	105
Fig. 3.4. Synthetic suppressor cells protect beta cells from T cell-mediated destruction in vitro.	107

Fig. 3.5. Synthetic suppressor cells locally protect hPSC-derived beta cell transplants from T cell-mediated killing in vivo.	109
Fig. 3.6. Potential application of synthetic suppressor cells for local immune tolerance.	110
Fig. 3.S1. Analysis of synthetic suppressor cell payload production, IL-2 consumption, proliferation, and differential payload effects on CD4+ vs CD8+ CAR T cells.	117
Fig. 3.S2. Additional analysis of combination payload suppressor cells (synNotch → IL-10 + CD25 or synNotch → TGFβ1 + CD25).	119
Fig. 3.S3. Synthetic suppressor cells overcome heterogeneity in SynNotch priming antigen on target cells.	121
Fig. 3.S4. CD19+ enriched beta cell clusters are functional and activate synthetic suppressor cells in vitro.	122
Fig. 3.S5. Analysis of hPSC-derived beta cell transplants.	123

Chapter 1 - Introduction

Translating molecular immunology into therapeutic interventions

The immune system requires a careful balance between inflammation and tolerance signals within tissues to maintain homeostasis. Immune surveillance has evolved complex communication between distinct immune cell types to effectively respond to infections or cancer but must simultaneously regulate improper activation that could drive autoimmunity. This process operates on multiple spatial scales throughout the body, within peripheral tissues, lymphoid tissues, and systemically, to shape the immune thresholds required to mount a response. The mechanisms underlying immune surveillance and its regulation remains an open area of study.

In the past several decades, many molecular signals underlying immune responses have been identified through genetic and biochemical studies. These studies have opened up the possibility for therapeutic interventions that directly target the immune response. Understanding how particular molecular features influence a given immune phenotype can allow for the design of therapies with predictable action. Immune cells rely on a diverse set of signals: for example, *paracrine signals* (e.g. cytokines or chemokines) can coordinate cell proliferation, trafficking, differentiation, or cytotoxic activity; *juxtacrine signals* (e.g. costimulatory receptors or adhesion molecules) can shape interactions at cell-cell interfaces to direct precisely targeted behaviors; *intracellular signaling pathways* (e.g. nuclear factor of activated T cells signaling) can integrate multiple extracellular or intracellular signals to inform cellular decision making.

However, therapeutic interventions that systemically perturb a particular immune signal without consideration of the spatiotemporal dynamics of the immune response

can be ineffective at treating immunological disorders. For example, administration of cytokines like IL-2 to boost immune responses against cancer can exhibit dose-limiting toxicities since they can drive undesired immune activation in off-target tissues [1]. Spatiotemporal control of therapies could overcome the toxicities of systemic delivery of these agents to more effectively treat immune disorders.

The field of immunotherapy has rapidly evolved over the past decade, leading to revolutionary advances in cell-based therapies for the treatment of cancer [2]. Among these, engineered T cell therapies has emerged as a promising approach for targeted and programmable therapeutic responses. The ability to engineer T cells to recognize and eliminate cancer using chimeric antigen receptors (CAR) has opened up new avenues for treatments with the potential for enhanced specificity and efficacy compared to traditional biologics or small molecules. These therapies have opened the field of synthetic immunology, the ability to generate custom immune responses to both understand our immune system and design effective therapeutic interventions.

Synthetic immunology: Building the immune system to understand it

Synthetic biology has revolutionized our ability to unravel the intricacies of complex biological systems by allowing us to deconstruct *and* reconstruct biological signaling. Importantly, synthetic biology allows us to explore both what exists in nature and what could possibly exist in biology to understand the theoretical space of biological solutions to achieve a given higher-order functions [3]. This process of reconstructing biological systems from the bottom-up allows use to explore more generalizable design principles for how biology must be wired. Engineering these systems is possible due to

the inherent modularity of biological systems. We can use modular components (e.g. proteins, genes, cells) and combine them in different configurations to program a desired behavior. Building synthetic circuits using a set of components allows us directly map what minimal signals are sufficient for a given function and establish quantitative relationships between components.

Synthetic immunology encompasses the application of synthetic biology techniques to manipulate and augment the immune system, enabling us to engineer new immune functions with unprecedented precision [4]. The archetypal example is CAR T cells, which use synthetic receptors (CARs) formed of modular protein domains to direct T cells to recognize and eliminate specific cancer cells. By harnessing the power of synthetic biology, we have been able to engineer T cells to target cancer cells with remarkable accuracy, resulting in success in the clinical for certain types of cancer.

However, synthetic immunology can be extended beyond CAR T cell therapies. For example, synthetic Notch (synNotch) receptors provide an additional layer of control and specificity in directing immune cell behavior [5]. By introducing synNotch receptors into immune cells, we can induce custom cellular programs based on specific molecular triggers in the environment, such as a cancer or tissue-specific antigen. This level of customization through synNotch circuits allows for the development of more tailored and effective immunotherapies. In addition to engineering targeted immune responses, synthetic immunology also offers an unprecedented opportunity to deepen our understanding of the immune system itself. By building artificial immune circuits and observing their behavior, we can unravel the intricate networks, signaling pathways, and feedback mechanisms that regulate immune function. This reverse-engineering

provides valuable insights into the complex interplay of cells and molecules within the immune system, shedding light on both its normal functions and alternative wirings.

Beyond CAR T cells: Synthetic receptors and custom molecular programs

Cell therapies have the potential to treat many immune disorders and extend beyond CAR T cell therapies against hematological cancers. Using synthetic circuits, we can endow T cells with new capabilities such as cytokine production or consumption that enable them to remodel immune microenvironments for therapeutic benefit. In this thesis, we explore two T cell engineering projects aimed at addressing two distinct, but parallel, challenges: (1) promoting cytotoxic immune responses against challenging solid tumors and (2) suppressing immune responses in inflammatory disease. These projects illustrate the ability to engineer T cells with customized programs to carry out precise responses spatially without detrimental systemic effects. These cellular programs reconstitute key immune signaling mechanisms and provide insight into how they might be wired naturally and how they may be rewired to improve T cell function for diverse therapeutic applications.

PROJECT 1: Design principles of T cell cytokine circuits against cancer

The first project (chapter 2) focuses on engineering T cells to locally produce pro-inflammatory signals to combat immune-excluded solid tumors [5]. Despite significant advances in cancer immunotherapy, many solid tumors remain resistant to treatment due to immune suppression within the tumor microenvironment. Tumor suppression can block both the activation of effector T cells through their T cell receptors (TCR) and

consume pro-inflammatory cytokines like IL-2 needed for T cell responses. Systemic administration of IL-2 can enhance T cell tumor expansion and killing but can be prohibitively toxic. By engineering T cell circuits that produce IL-2 locally using a tumor-specific synNotch circuit, we designed T cells that can overcome tumor immune suppression to drive tumor clearance without systemic toxicity. In the process of engineering these T cell circuits, we identify the essential requirements for effective tumor clearance: T cell production of IL-2 must be delivered in an autocrine configuration and TCR/CAR-independent manner.

PROJECT 2: Design principles of immune suppressive T cell circuits

The second project (chapter 3) focused on engineering T cells capable of local immune suppression with the potential to treat inflammatory or autoimmune disorders. While immune suppression is a challenge for cancer treatment, it can be desirable in the context of autoimmunity or transplant rejection. By engineering T cells to produce immune suppressive payloads locally using synNotch, we can achieve targeted and localized immune suppression, minimizing the risk of systemic toxicity associated with conventional immunosuppressive therapies. We explore a diverse set of suppressive payloads and pairwise combinations induced by synNotch circuits in CD4+ T cells. The most effective T cell circuits identify minimal requirements for designing immune suppressor cells, particularly that engineered cells must produce both an inhibitory cytokine such as IL-10 or TGF1 and a sink for pro-inflammatory cytokine IL-2, CD25. These circuits recapitulate key features of natural immune suppressor cells called regulatory T cells (Tregs). These synthetic suppressor T cells could be programmed to

recognize a tissue of interest to locally target immune suppression for the treatment of diverse inflammatory disease, such as acting as a NOT gate to block off-target CAR T cell toxicity, protecting allogeneic transplants for host immune rejection, and blocking autoimmunity.

References:

1. M. B. Atkins, M. T. Lotze, J. P. Dutcher, R. I. Fisher, G. Weiss, K. Margolin, J. Abrams, M. Sznol, D. Parkinson, M. Hawkins, C. Paradise, L. Kunkel, S. A. Rosenberg, High-dose recombinant interleukin 2 therapy for patients with metastatic melanoma: analysis of 270 patients treated between 1985 and 1993. *J. Clin. Oncol. Off. J. Am. Soc. Clin. Oncol.* **17**, 2105–2116 (1999).
2. Lim, W. A., June, C. H., The Principles of Engineering Immune Cells to Treat Cancer. *Cell.* **168**(4), 724-740 (2017).
3. Elowitz, M., Lim, W. A., Build life to understand it. *Nature.* **468**, 889-890 (2010).
4. Roybal, K.T., Lim, W. A., Synthetic Immunology: Hacking Immune Cells to Expand Their Therapeutic Capabilities. *Annu Rev Immunol.* **35**, 229-253 (2018).
5. Morsut, L., Roybal, K. T., Xiong, X., Gordley, R. M., Coyle, S. M., Thomson, M., Lim, W. A., Engineering Customized Cell Sensing and Response Behaviors Using Synthetic Notch Receptors. *Cell*, **164**, 780-791 (2016).
6. Allen, G. M.⁺, Frankel, N.W.⁺, Reddy, N.R., Bhargava, H. K., Yoshida, M.A., Stark, S.R., Purl, M., Lee, J., Yee, J. L., Yu, W., Li, A.W., Garcia, K.C., El-Samad, H., Roybal, K.T., Spitzer, M.H., Lim, W.A. Synthetic cytokine circuits that drive T cells into immune-excluded tumors. *Science*, 378, eaba1624 (2022).

Chapter 2 - Synthetic cytokine circuits that drive T cells into immune-excluded tumors

One-Sentence Summary: Synthetic circuits that deliver IL-2 locally to tumors allow CAR-T cells to overcome suppressive tumor microenvironments.

Authors: Greg M. Allen^{1-2,+}, Nicholas W. Frankel^{2-3,+}, Nishith R. Reddy²⁻³, Hersh K. Bhargava²⁻⁴, Maia A. Yoshida²⁻³, Sierra R. Stark²⁻³, Megan Purl²⁻³, Jungmin Lee²⁻³, Jacqueline L. Yee⁵, Wei Yu²⁻³, Aileen W. Li²⁻³, K. Christopher Garcia⁶, Hana El-Samad^{2,9-10}, Kole T. Roybal^{2,5,7}, Matthew H. Spitzer^{5,7-9}, Wendell A. Lim^{2-3,7,9*}

Affiliations:

¹ Department of Medicine, University of California San Francisco; San Francisco, CA 94158, United States.

² UCSF Cell Design Institute; University of California San Francisco, San Francisco, CA 94158, United States.

³ Department of Cellular and Molecular Pharmacology, University of California San Francisco; San Francisco, CA 94158, United States

⁴ Biophysics Graduate Program, University of California San Francisco; San Francisco, CA 94158, United States

⁵ Department of Microbiology and Immunology, University of California San Francisco; San Francisco, CA 94158, United States

⁶ Department of Molecular and Cellular Physiology and Structural Biology, Howard Hughes Medical Institute, Stanford University; Stanford, United States

⁷ Parker Institute for Cancer Immunotherapy, University of California San Francisco; San Francisco, CA 94158, United States

⁸ Department of Otolaryngology-Head and Neck Surgery, University of California San Francisco; San Francisco, CA 94158, United States

⁹ Helen Diller Family Comprehensive Cancer Center, University of California San Francisco; San Francisco, CA 94158, United States

¹⁰ Department of Biochemistry and Biophysics, University of California San Francisco; San Francisco, CA 94158, United States

+Equal Contributions

*Corresponding author. Email: Wendell.Lim@ucsf.edu

Contributions to This Chapter: My contribution to this work was in the analysis of SynNotch → IL-2 circuits in the syngeneic mouse tumors models using high dimensional CyTOF analysis to understand the impact of different T cell circuit architectures on remodeling of the tumor microenvironment and characterization of off-target toxicity in the spleen. Main contributions found in Fig. 2.5., 2.S13, 2.S14, 2.S15, 2.S16 and the writing of the associated text.

Abstract:

CAR T cells are ineffective against solid tumors with immunosuppressive microenvironments. To overcome suppression, we engineered circuits in which tumor-specific synNotch receptors locally induce production of the cytokine IL-2. These circuits potently enhance CAR T cell infiltration and clearance of immune-excluded tumors, without systemic toxicity. The most effective IL-2 induction circuit acts in an autocrine and TCR/CAR-independent manner, bypassing suppression mechanisms including consumption of IL-2 or inhibition of TCR signaling. These engineered cells establish a foothold in the tumors, with synNotch-induced IL-2 production enabling initiation of CAR-mediated T cell expansion and killing. Thus, it is possible to reconstitute synthetic T cell circuits that activate the outputs ultimately required for an anti-tumor response, but in a manner that evades key points of tumor suppression.

Main Text:

Chimeric antigen receptor (CAR) T cells have demonstrated remarkable success in the treatment of B cell malignancies (1, 2). Nonetheless, application of CAR or T cell receptor (TCR) engineered T cells to solid tumors has proven far more challenging (3). Many solid tumors create an immune-excluded local microenvironment that blocks the infiltration, activation, or expansion of cytotoxic T cells (4). Within this tumor microenvironment, activation of CAR/TCR pathways are inhibited by local immunosuppressive factors and cells (5–7). While evidence suggests that local administration of high-dose inflammatory cytokines could help reverse tumor suppression (8), combining adoptively transferred T cells with systemic cytokine administration or engineered cytokine production has shown either systemic toxicity or poor efficacy (9–11). There is a clear need to engineer next-generation therapeutic T cells with an enhanced ability to overcome tumor suppression, without exacerbating off-target or systematic toxicity.

Here, we have created synthetic cytokine circuits as a strategy to improve therapeutic T cell activity against immune-excluded solid tumors. Using the recently developed synthetic Notch (synNotch) receptor (12, 13), we have created a bypass signaling pathway in which tumor recognition by synNotch induces local interleukin-2 (IL-2) production (**Fig. 2.1A**). The inflammatory cytokine IL-2 plays a critical role as both an output of T cell activation, and as a promoter of T cell activation and expansion (14–17). Suppressive tumor microenvironments can both reduce IL-2 production and/or competitively consume IL-2 (18–20). Thus, we hypothesized that providing IL-2 in a tumor-targeted, but TCR/CAR-independent manner, could help bypass tumor immune

suppression. Indeed, we find that certain synthetic IL-2 circuits drive highly efficient CAR T cell infiltration and tumor control in immune-excluded solid tumor models, without concomitant systemic or off-target toxicity. Immune profiling shows expansion of CAR T cells only within the tumor, with increased markers of activation and decreased markers of exhaustion. Synthetic IL-2 production likely enables infiltrating T cells to survive and initiate sustained CAR-mediated activation, expansion and tumor killing. This type of synthetic cytokine delivery circuit could provide a powerful general approach for remodeling and overcoming immunosuppressive solid tumors.

Results:

Engineering synthetic IL-2 circuits that drive local T cell proliferation independent of T cell activation

To design a tumor-induced synthetic IL-2 circuit in T cells, we used a synNotch sensor to induce the transcription of an IL-2 transgene (**Fig. 2.1B**). Briefly, synNotch receptors are chimeric receptors with a variable extracellular recognition domain, a Notch-based cleavable transmembrane domain, and an intracellular transcriptional domain (12, 13). Antigen binding induces intramembrane receptor cleavage, releasing the transcriptional domain to enter the nucleus and promote expression of a target transgene.

We built a prototype circuit in primary human T cells, using a synNotch receptor that recognizes the model antigen CD19, combined with a synNotch-responsive promoter driving expression of human IL-2 or an affinity-enhanced variant of IL-2 (known as super-2 or sIL-2) (21). As intended, stimulation of the synNotch receptor *in vitro*

induced strong proliferation of the engineered cell population (**Fig. 2.1C**). Cells with the anti-CD19 synNotch→sIL-2 circuit could function in a paracrine manner, driving the proliferation of co-cultured non-engineered T cells (**Fig. 2.1D**) or NK cells (**Fig. 2.S1C**) *in vitro*. The degree of proliferation was dependent on the type of gamma-chain cytokine payload, with significant T cell proliferation seen with production of either IL-2 or sIL-2 (**Fig. 2.S1D**). Production of the homeostatic cytokine IL-7 (22) led to T cell survival with minimal expansion, while un-tethered IL-15 (23) had no effect. Thus, *in vitro*, a synNotch→sIL-2 circuit T cell can drive its own proliferation, as well as the proliferation of other co-cultured IL-2 responsive cells.

We then tested whether the synNotch→sIL-2 circuit could drive targeted expansion of human T cells *in vivo*, independent of CAR or TCR activation. We established a bilateral K562 tumor model in immunocompromised NOD *scid* gamma (NSG) mice, where only one flank tumor expressed the synNotch target antigen, CD19 (**Fig. 2.1E**). Human primary CD8⁺ T cells engineered with the anti-CD19 synNotch→sIL-2 circuit were tagged with enhanced firefly luciferase (eff-luc) and injected intravenously. Cells with the synthetic IL-2 circuit autonomously identified the target tumor (CD19⁺/right) and locally expanded approximately 100-fold within this tumor (**Fig. 2.1E**). In contrast, no off-target expansion was seen in the contralateral (CD19⁻) tumor. Flow cytometry analysis of tumor infiltrating lymphocytes (TILs) in the target and off-target tumor showed synNotch activation, T cell expansion, and proliferation only in the CD19⁺ tumor (**Fig. 2.S2A-C**). The administered T cells have no CAR or TCR reactivity against tumors, thus the synthetic production of IL-2 alone did not result in killing of the K562 tumors in this immunodeficient NSG mouse model (**Fig. 2.S2D**).

We also found that the anti-CD19 synNotch→sIL-2 circuit was also capable of driving T cell expansion in a paracrine (two-cell type) configuration, in this NSG mouse model. Here we co-injected a population of bystander T cells, which did not express the sIL-2 induction circuit but expressed luciferase to distinguish them from the synNotch→sIL-2 T cells. Co-injected into mice at a 1:1 ratio, the bystander cells also specifically expanded in the targeted (CD19⁺/right) tumor (**Fig. 2.S3A-D**) where the synNotch receptor was locally activated (**Fig. 2.S3E**). This paracrine T cell expansion was not observed in negative control experiments using synNotch T cells that either did not produce sIL-2 or did not recognize CD19 (**Fig. 2.S3F**).

In summary, this work represents one of the first examples in which locally targeted T cell expansion can be induced in a manner uncoupled from TCR or CAR activation.

Synthetic IL-2 circuits can enhance targeted T cell cytotoxicity in vivo

Many engineered T cell therapies show effective cytotoxicity *in vitro* but fail to show sufficient proliferation or persistence to achieve effective tumor control *in vivo*. For example, cells bearing the affinity-enhanced anti-NY-ESO-1 TCR are able to lyse A375 melanoma tumors *in vitro* (24), but have shown limited clinical benefit in patients or preclinical models (25). We hypothesized that the addition of a synthetic cytokine circuit producing IL-2 might enhance tumor control by NY-ESO-1 T cells. Moreover, these T cells might function as a new type of AND gate (26, 27), where a therapeutic T cell exhibits enhanced specificity by requiring two antigens to be present before triggering its full cytotoxic response (the TCR antigen required for T cell activation, and the synNotch antigen required for inducing IL-2 production). In this case, we used an anti-

GFP synNotch \rightarrow sIL-2 synthetic cytokine circuit. By requiring the presence of both the TCR antigen (NY-ESO-1) and the synNotch antigen (in this case, membrane-tethered GFP) (**Fig. 2.1F**), this cellular design strategy should further minimize off-target toxicity. We examined the efficacy of anti-NY-ESO-1 TCR human T cells in NSG mice using a bilateral tumor model of a NY-ESO-1+ melanoma (A375). Only one flank tumor was co-labelled with the synNotch-targeted model antigen (membrane-tethered GFP). Anti-NY-ESO-1 TCR-expressing T cells lacking the synthetic IL-2 circuit were largely ineffective at controlling the growth of both the single (NY-ESO⁺) and dual (NY-ESO⁺/GFP⁺) antigen tumors (**Fig. 2.S4A**). However, when mice were treated with T cells simultaneously expressing both the anti-NY-ESO-1 TCR and the anti-GFP synNotch \rightarrow sIL-2 circuit, the dual-targeted NY-ESO⁺/GFP⁺ tumor now showed a significant reduction in tumor size (**Fig. 2.1F**). Similar tumor reduction was observed when IL-2 was provided in a paracrine configuration, by co-injection of one cell type only expressing the anti-NY-ESO-1 TCR and a second cell type only expressing the synthetic IL-2 circuit. Critically, in either the autocrine or paracrine configuration, the synthetic IL-2 circuit did not cause a reduction in the contralateral NY-ESO⁺/GFP⁻ tumor (lacking the synNotch ligand), highlighting the precisely targeted impact of the synthetic IL-2 circuit.

Using luciferase tracking of anti-NY-ESO-1 TCR T cells, we observed substantially increased intratumoral expansion of T cells only in tumors that were targeted by the synthetic IL-2 circuit (**Fig. 2.S5A**). The synthetic IL-2 circuit was only activated in the targeted double antigen positive tumor (**Fig. 2.S5B**), and we observed a significant increase in T cell activation markers in this targeted tumor (**Fig. 2.S5C**). A synthetic IL-

2 circuit T cell without co-delivery of a tumor reactive cytotoxic T cell population did not produce tumor control in these NSG mouse models (**Fig. 2.S5D**).

Autocrine configuration of synthetic IL-2 circuit is required in immunocompetent tumor models

Although the above results show that synthetic synNotch → IL-2 circuits can significantly enhance T cell activity and expansion in immunodeficient mouse tumor models, we wanted to test whether they could also be effective in immunocompetent mouse models. Important factors influencing IL-2 production and consumption are likely missing in immunodeficient mouse models. Key missing factors include inhibitors of T cell activation (28) and the presence of competing IL-2 consumer cells (e.g. both native T cells, and T regulatory cells), which could significantly lower the effectiveness of synthetically produced IL-2 within tumors (29, 30). To study the effects of local IL-2 production within fully immunocompetent mouse tumor models, we rebuilt our synthetic IL-2 circuit in primary mouse T cells (**Fig. 2.2A**). Primary CD3⁺ mouse T cells were engineered to express an anti-human-CD19 synNotch → mouse IL-2 (mIL-2) circuit. This circuit resulted in synNotch-induced proliferation of mouse T cells *in vitro*, just as was observed previously with human T cells (**Fig. 2.S6A**).

We then chose to deploy this IL-2 circuit in targeting the mouse pancreatic tumor model KPC (Kras^{LSL.G12D/+}; p53^{R172H/+}; PdxCretg⁺) (31, 32), as this immune-excluded tumor exhibits the challenging immunotherapy refractory features of pancreatic ductal adenocarcinoma (PDAC) (33). Like most pancreatic ductal adenocarcinomas, these cells express the tumor target antigen mesothelin (34). Although anti-mesothelin mouse

CAR T cells show robust cytotoxicity against KPC cells *in vitro* (**Fig. 2.S6B**), they show limited to no tumor control of KPC tumors *in vivo* (**Fig. 2.S6C**). Thus, this immune competent mouse model replicates the poor *in vivo* therapeutic efficacy reported in early phase clinical trials of standard anti-mesothelin CAR T cells in pancreatic cancer (3), making it an ideal model in which to test enhancement of the CAR T cells with synthetic IL-2 circuits. We engineered KPC tumor cells that, in addition to endogenously expressing the CAR antigen (mesothelin), also expressed a model synNotch antigen (human CD19).

We first tested CAR T cell enhancement by a paracrine synNotch→mIL-2 circuit. Anti-mesothelin CAR T cells were co-injected with a second T cell population expressing the anti-CD19 synNotch → mIL-2 circuit. Distinct from our studies in immunodeficient mice, these paracrine IL-2 circuit cells failed to improve tumor control in an immune competent context (**Fig. 2.2B, 2.S7A**). Instead, we found that in this fully immunocompetent tumor model, improved CAR T cell-mediated tumor control was only observed with the autocrine configuration of the synthetic IL-2 circuit – i.e. the cytotoxic receptor (CAR) and the synNotch→IL-2 circuit must be encapsulated within the same cell (**Fig. 2.2C, 2.S7B**). We hypothesize that the presence of competing host IL-2 consumer cells (e.g. bystander T cells and T_{regs}) in immune-competent models contributes to this major difference between the autocrine and paracrine circuits (i.e. paracrine circuits might be more sensitive to competing IL-2 sink cells), a model consistent with more in depth tumor profiling data in later sections of this paper.

The autocrine synthetic IL-2 circuit anti-Mesothelin CAR-T cells were extremely potent. In an even more challenging immune-competent mouse model, in which KPC tumors

were engrafted orthotopically in the pancreas, complete tumor clearance was observed upon treatment (**Fig. 2.2D**) —100% of mice survived, compared with 0% with CAR only T cells. Simply increasing the dose of anti-Mesothelin CAR-T cells had a negligible effect compared to addition of the synthetic IL-2 circuit (**Fig. 2.S8A,B**).

This type of autocrine IL-2 circuit also shows similar dramatic therapeutic improvement in treating a different type of immune-excluded solid tumor – B16-F10 OVA intradermal melanoma tumors, treated with OT-1 TCR expressing T cells (**Fig. 2.2E, S7C**). Here again, OT-1 T cells without the cytokine circuit are ineffective *in vivo* in immune competent models (despite *in vitro* cytotoxic activity -- **Fig. 2.S6D**). Only when the OT-1 TCR is co-expressed with the autocrine synNotch→IL-2 circuit, do we observe effective infiltration and tumor clearance in the immune competent model.

Comparison to other strategies of IL-2 co-delivery.

Importantly, this strong therapeutic improvement was not observed with other methods of co-delivering IL-2 with a CAR T cell. We tested systemic co-administration of IL-2 at maximum-tolerated doses (35) (**Fig. 2.3B, 2.S9B**), expression of IL-2 in the CAR T cell from a constitutive promoter (“armored CAR”) (**Fig. 2.3C, 2.S9C**), or expression of IL-2 from a T cell activated promoter such as pNFAT (36) (**Fig. 2.3D, 2.S9D**).

Systemically injected IL-2 led to systemic toxicity without improving CAR T cell activity (**Fig. 2.S10B**). Constitutive production of IL-2 was unable to support T cell proliferation *in vivo* (**Fig. 2.S11A**) likely in part due to significant silencing of the constitutive IL-2 transgene (**Fig. 2.S11B**) (37). IL-2 can have a biphasic effect on T cell survival (38) in

part due to promotion of activation induced cell death (39) and T cell differentiation (40). We find that such negative effects are exacerbated by constitutive IL-2 production (**Fig. 2.S11C**). This suggests that when and how the IL-2 cytokine is produced is critical in determining the outcome.

Importantly, despite its potent anti-tumor efficacy, the synNotch→IL-2 circuit showed no evidence of systemic cytokine toxicity or exacerbation of CAR T cell toxicity, as assessed by mouse survival, body weight, spleen weight, and measurements of hepatotoxicity (**Fig. 2.S10**). Moreover, the required recognition of two antigen inputs (CAR and synNotch antigens) should further enhance the specificity of tumor targeting (as seen by specific targeting to dual antigen tumor **Fig. 2.S7C**, and reduced hepatotoxicity **S10C**). In summary, combining a tumor-reactive TCR/CAR with an autocrine synNotch→IL-2 circuit, results in uniquely potent and localized anti-tumor enhancement.

Synthetic IL-2 circuit drives T cell infiltration into immune excluded tumors

To better characterize how this autocrine synthetic IL-2 circuit improves CAR T cell control of syngeneic pancreatic tumor models, we profiled the tumors in more depth during treatment. We collected KPC pancreatic tumor specimens at the beginning and well into tumor regression (8 days and 23 days after T cell treatment) and measured CD3⁺ T cell infiltration using immunohistochemistry. Tumors treated with standard anti-mesothelin CAR T cells displayed a classic immune-excluded phenotype, with very limited T cell infiltrate inside the tumor core and most T cells gathered at the tumor periphery (**Fig. 2.4, top**). In contrast, tumors treated with CAR T cells containing the

synthetic autocrine IL-2 circuit showed substantially increased infiltration of T cells throughout the tumor core (**Fig. 2.4, bottom**). A similar infiltration and expansion of the CD8⁺ lymphocytes also seen in B16-F10 OVA melanoma tumors sampled 10 days after treatment with OT-1 T cells bearing the synthetic IL-2 circuit (**Fig. 2.S12A**).

To profile the tumors in more detail, we performed flow cytometry and CyTOF analyses on excised and dissociated tumors. To track the endogenous (host) T cells independently from the adoptively transferred CAR T cells, we adoptively transferred congenic Thy1.1 or CD45.1 CAR T cells into Thy1.2 or CD45.2 mice, respectively, allowing us to clearly distinguish endogenous from transplanted T cells by FACS.

These studies showed that the engineered autocrine T cells (expressing both CAR and the synNotch→IL2 circuit) drove substantial intra-tumoral infiltration of both adoptively transferred (engineered) T cells and native host T cells (**Fig. 2.5A, S12B**). In contrast parallel analysis of tumors treated with the paracrine synNotch→IL-2 circuit (CAR and synthetic cytokine circuit are expressed by two separate, co-injected cell types) showed expansion of native T cells only and no expansion of the adoptively transferred CAR T cells (**Fig. 2.5A, 2.S13B**), suggesting that in the paracrine configuration, induced IL-2 was primarily consumed by competing native T cells, leaving little available to drive expansion of the rarer CAR T cells.

Unsupervised clustering (41) of the CyTOF measurements (from the CD45⁺ immune cell infiltrate in KPC tumors) identified that the primary therapeutic effect of the autocrine IL-2 circuit was to enrich the population of activated adoptively transferred CAR T cells (**Fig. 2.5B**). Little change was seen in the myeloid compartments (42), suggesting that synthetic IL-2 production acts primarily to drive T cell infiltration (both native and

adoptive) and not by altering myeloid cell associated immune suppression.

Furthermore, the expansion of T cells was completely constrained to the tumor - no changes were seen in immune cells from isolated spleens by flow cytometry or CyTOF analysis (**Fig. 2.S12A, Fig. 2.S16**), highlighting the focused local activity of the engineered cytokine circuit.

In addition to driving expansion of cytotoxic T cells in these immunologically cold tumors, the synthetic autocrine IL-2 circuit improved the phenotypes of the CAR T cells that infiltrate the tumor. CyTOF analysis showed that the synthetic autocrine IL-2 circuit upregulated markers of T cell activation (CD25), effector activity (Granzyme B) and proliferation (Ki67). Conversely, these IL-2 enhanced T cells also showed reduced expression of markers of exhaustion (Tim3, Lag3, PD-1) (**Fig. 2.5C, 2.S14B**) (43). Most native T cells (non-CAR) found in the tumors, however, appear to act simply as IL-2 sinks – they did not show markers of activation, effector function, proliferation, or exhaustion (**Fig. 2.5C, 2.S14B**), but instead largely exhibited a naïve phenotype (**Fig. 2.S14C,D, 2.S15C**). The phenotype of the regulatory T cell population was mostly unchanged (**Fig. 2.S14D, 2.S15D**). These findings suggest that the tumor has a significant population of native host T cells that, in bulk, compete to consume IL-2 without contributing to the anti-tumor response, (akin to T_{reg} suppression via IL-2 consumption).

Discussion

Cell delivered IL-2 is a powerful tool to synergize with therapeutic T cells

Cytokines such as IL-2 have long been known as powerful stimulators of anti-tumor immunity (44). However, systemic IL-2 delivery is also well known to be highly toxic, leading to a broad set of adverse effects including capillary leak syndrome, thereby greatly limiting its therapeutic use (45). Most current efforts in IL-2 engineering have focused on engineering the cytokine to be more selective for a tumor. Here instead we use a different strategy: harnessing the power of an engineered cell to identify a tumor and locally deliver IL-2 exactly where it is needed. We show that cell-mediated local cytokine (IL-2) delivery can effectively overcome immune suppression, augmenting CAR T cells to efficiently clear multiple immune-excluded tumor models (pancreatic cancer and melanoma) that are otherwise nearly completely resistant to standard CAR T cell treatment.

However, the exact manner of by which the cytokine is produced is critical to its success. First, cytokine production must be dynamically regulated (inducible). Constant production of IL-2 risks exacerbating off-target toxicity. Moreover, constitutive IL-2 expression in T cells has negative effects – it leads to terminal differentiation, fails to drive autonomous proliferation, and is limited by payload silencing. Second, in order to bypass TCR/CAR suppression by the tumor microenvironment, induction of IL-2 production must be independent of the TCR activation pathway (e.g. NFAT promoter induced IL-2 still requires TCR/CAR activation to be triggered). We find that one powerful solution to this constraint is to engineer a synthetic signal transduction pathway that is tumor-triggered, but bypasses the native CAR/TCR activation pathway

(**Fig. 2.6A,B**). Using a synNotch receptor that detects the tumor to drive IL-2 production provides a simple and modular way to achieve this goal. The synNotch IL-2 circuit can maintain payload expression in spite of T cell inhibition or exhaustion (**Fig. 2.S17A**).

Finally, we find that simply having an immune cell that can individually produce high levels of IL-2 in the tumor is not sufficient to overcome suppression. The specific circuit architecture is critical, including exactly which cells produce IL-2. We find that an effective therapeutic response is only observed with an autocrine IL-2 circuit (i.e. synthetic IL-2 induction pathway is contained within the same cell as the anti-tumor CAR/TCR).

Mechanisms underlying autocrine/paracrine circuit differences

Why does the autocrine IL-2 induction circuit perform so much better than the equivalent paracrine circuit in driving T cell infiltration of immunosuppressed tumor models? Both circuits act by the same principle of delivering high levels of IL-2 (**Fig. 2.S17B**) directly to the tumor. Moreover, why do we only see this large difference in autocrine vs paracrine circuit efficacy in the presence of a native immune system?

It is likely that there are multiple mechanisms that contribute to the far better efficacy of the autocrine circuit (**Figure 2.6C,D**). These mechanisms are tightly interlinked, and likely act in a highly cooperative manner, thus making it difficult to precisely pinpoint the relative contribution of each mechanism.

First, it is likely that autocrine cells have *preferential access* to self-produced IL-2, especially in environments with competing IL-2 sinks. Paracrine circuits must physically

transfer IL-2 further through space from a producer T cell to an effector T cell. This becomes challenging in the presence of competing IL-2 consumer cells (e.g. T_{regs} in immune competent models), which can greatly reduce the effective length scale of IL-2 signaling creating gradients that drop off sharply around IL-2 sources (46). Here, in both the autocrine and paracrine circuit, we observe an expansion of host T_{reg} cells (**Fig. 2.5A, S15A**); however, we also see a much larger expansion of naïve T cells (**Fig. 2.S12B, S15A**). These results suggest that host conventional T cells in the tumor can also play a significant role as IL-2 sinks, especially given their vast excess population. Although it is difficult to parse out the relative contribution of these T_{regs} vs conventional T cells as IL-2 consumers, it is not uncommon to observe the presence of large numbers of tumor infiltrating but non tumor-reactive T cells (30). Whatever their relative contribution, these IL-2 consumers are both expected to decrease the effective signaling distance of IL-2 producers (47, 48), which would strongly favor the efficacy of autocrine over paracrine IL-2 production in driving CAR T cell expansion.

Second, it is also likely that autocrine cells are capable of *preferential expansion* in response to the available pool of IL-2. There is a unique proliferative positive feedback loop that could in principle take place with T cells that can induce both IL-2 and TCR/CAR activation. T cell activation can both trigger an initially IL-2 independent proliferative response (49) as well as induce expression of the high affinity IL-2 receptor subunit, CD25 (**Fig. 2.S17C**), which allows T cells to outcompete other T cells for available IL-2. Because an autocrine circuit cell contains both the CAR and synNotch→IL-2 circuit, it has the capability to become both a preferred IL-2 responder (via T cell activation) and strong IL-2 producer (via synNotch activation) within a tumor.

We hypothesize that these dually activated autocrine cells could thereby initiate a powerful population level positive feedback loop that builds up even higher levels of intra-tumoral IL-2 due to preferential expansion of better IL-2 consumers/responders. This population positive feedback would not take place in the paracrine circuit, as the IL-2 producers do not upregulate CD25 (**Fig. 2.S17C**) and their IL-2 production would largely contribute to expanding competing T cells (such as Tregs) that act to suppress T cell based immunity. Several pieces of evidence support this model of preferred expansion of autocrine circuit cells. First, only in the autocrine CAR T cells, do we observe significantly higher expression of the proliferation marker Ki67 (**Fig. 2.5C, S14B**). Second, we notably do not see increased tumor control with an autocrine circuit that produces the homeostatic cytokine IL-7 (**Fig. 2.S17D**). Further experiments will be needed to definitively evaluate the relative contributions of the multiple mechanisms discussed in this model.

Essential requirements to bypass tumor immunosuppression

Our efforts to systematically design CAR T circuits that couple IL-2 production/signaling with CAR signaling in alternative ways also sheds light onto the basic design principles of native T cell activation. The T cell system has evolved to severely restrict improper activation, but at the same time to be able to launch a locally explosive response, once triggered. Population-level positive feedback signaling using a shared cytokine (IL-2) allows this type of digital response between on and off states (50, 51). In this model, T cells must not only be stimulated by the proper antigens, but they must also subsequently produce enough IL-2 to overcome the threshold set by competing IL-2

consumer cells present throughout the microenvironment (52). This control mechanism, however, provides weak points that tumors can take advantage of for immune suppression. Many tumors keep a strong T cell response in check, either by blocking T cell activation (28), or increasing competition for amplification factors like IL-2.

Here we show that it is possible to still reconstitute the pathways required for a strong anti-tumor T cells response (i.e. rewiring the cell such that T cell activation, co-stimulation and IL-2 signaling are still cooperatively stimulated), but in a way that now evades the major tumor suppressive mechanisms. Normally IL-2 is produced after T Cell activation and acts as a critical amplifier of T cell activity. By placing IL-2 production under the control of a new TCR-independent but still tumor-targeted synthetic receptor we can now produce IL-2 immediately and consistently after tumor entry despite suppression of T cell activation. In addition, normally IL-2 consumers apply a selective pressure only allowing strongly activated effector T cells to expand (52). By coupling TCR/CAR activation and synNotch driven IL-2 production in an autocrine IL-2 circuit we can selectively expand the engineered therapeutic T cell population out of a background of competing IL-2 consumers. These rewired cells ultimately activate the same critical pathways (TCR and IL-2 pathways) as seen in native T cell responses but do so in a different temporal order and in response to different inputs allowing them to be far more effective as a tumor-targeted therapy (**Fig. 2.6**). The engineered circuit maintains the explosive cell expansion necessary for a robust anti-tumor activity but triggered in a manner that evades the major mechanisms of immunosuppression.

The power of alternatively wired immune cell circuits.

In summary, we have been able to use flexible synthetic biology tools, such as the synNotch receptor system, to create new, alternative ways to rapidly establish both the TCR and IL-2 pathway activity required for an effective and sustained T cell response. The resulting bypass channel for IL-2 production allows for improved tumor control and reduced toxicity compared to alternative mechanisms of IL-2 delivery. Synthetic cytokine production circuits may represent a general solution for engineering immune cell therapies that can function more effectively in hostile tumor microenvironments, illustrating the power of customizing immune responses in highly precise but novel ways.

References and Notes:

1. S. J. Schuster, M. R. Bishop, C. S. Tam, E. K. Waller, P. Borchmann, J. P. McGuirk, U. Jäger, S. Jaglowski, C. Andreadis, J. R. Westin, I. Fleury, V. Bachanova, S. R. Foley, P. J. Ho, S. Mielke, J. M. Magenau, H. Holte, S. Pantano, L. B. Pacaud, R. Awasthi, J. Chu, Ö. Anak, G. Salles, R. T. Maziarz, JULIET Investigators, Tisagenlecleucel in Adult Relapsed or Refractory Diffuse Large B-Cell Lymphoma. *N. Engl. J. Med.* **380**, 45–56 (2019).
2. N. C. Munshi, L. D. Anderson, N. Shah, D. Madduri, J. Berdeja, S. Lonial, N. Raje, Y. Lin, D. Siegel, A. Oriol, P. Moreau, I. Yakoub-Agha, M. Delforge, M. Cavo, H. Einsele, H. Goldschmidt, K. Weisel, A. Rambaldi, D. Reece, F. Petrocca, M. Massaro, J. N. Connarn, S. Kaiser, P. Patel, L. Huang, T. B. Campbell, K. Hege, J. San-Miguel, Idecabtagene Vicleucel in Relapsed and Refractory Multiple Myeloma. *N. Engl. J. Med.* **384**, 705–716 (2021).
3. A. R. Haas, J. L. Tanyi, M. H. O’Hara, W. L. Gladney, S. F. Lacey, D. A. Torigian, M. C. Soulen, L. Tian, M. McGarvey, A. M. Nelson, C. S. Farabaugh, E. Moon, B. L. Levine, J. J. Melenhorst, G. Plesa, C. H. June, S. M. Albelda, G. L. Beatty, Phase I Study of Lentiviral-Transduced Chimeric Antigen Receptor-Modified T Cells Recognizing Mesothelin in Advanced Solid Cancers. *Mol. Ther. J. Am. Soc. Gene Ther.* **27**, 1919–1929 (2019).
4. S. Mariathasan, S. J. Turley, D. Nickles, A. Castiglioni, K. Yuen, Y. Wang, E. E. Kadel, H. Koeppen, J. L. Astarita, R. Cubas, S. Jhunjunwala, R. Banchereau, Y. Yang, Y. Guan, C. Chalouni, J. Ziai, Y. Şenbabaoğlu, S. Santoro, D. Sheinson, J.

- Hung, J. M. Giltane, A. A. Pierce, K. Mesh, S. Lianoglou, J. Riegler, R. A. D. Carano, P. Eriksson, M. Höglund, L. Somarriba, D. L. Halligan, M. S. van der Heijden, Y. Lorient, J. E. Rosenberg, L. Fong, I. Mellman, D. S. Chen, M. Green, C. Derleth, G. D. Fine, P. S. Hegde, R. Bourgon, T. Powles, TGF β attenuates tumour response to PD-L1 blockade by contributing to exclusion of T cells. *Nature*. **554**, 544–548 (2018).
5. A. Xia, Y. Zhang, J. Xu, T. Yin, X.-J. Lu, T Cell Dysfunction in Cancer Immunity and Immunotherapy. *Front. Immunol.* **10**, 1719 (2019).
 6. A. B. Frey, N. Monu, Signaling defects in anti-tumor T cells. *Immunol. Rev.* **222**, 192–205 (2008).
 7. M. Y. Balkhi, Q. Ma, S. Ahmad, R. P. Junghans, T cell exhaustion and Interleukin 2 downregulation. *Cytokine*. **71**, 339–347 (2015).
 8. L. Tang, Y. Zheng, M. B. de Melo, L. Mabardi, A. P. Castaño, Y.-Q. Xie, N. Li, S. B. Kudchodkar, H. C. Wong, E. K. Jeng, M. V. Maus, D. J. Irvine, Enhancing T cell therapy through TCR signaling-responsive nanoparticle drug delivery. *Nat. Biotechnol.* **36**, 707–716 (2018).
 9. L. Zhang, R. A. Morgan, J. D. Beane, Z. Zheng, M. E. Dudley, S. H. Kassim, A. V. Nahvi, L. T. Ngo, R. M. Sherry, G. Q. Phan, M. S. Hughes, U. S. Kammula, S. A. Feldman, M. A. Toomey, Sid. P. Kerkar, N. P. Restifo, J. C. Yang, S. A. Rosenberg, Tumor Infiltrating Lymphocytes Genetically Engineered with an Inducible Gene

- Encoding Interleukin-12 for the Immunotherapy of Metastatic Melanoma. *Clin. Cancer Res. Off. J. Am. Assoc. Cancer Res.* **21**, 2278–2288 (2015).
10. M. B. Atkins, M. T. Lotze, J. P. Dutcher, R. I. Fisher, G. Weiss, K. Margolin, J. Abrams, M. Sznol, D. Parkinson, M. Hawkins, C. Paradise, L. Kunkel, S. A. Rosenberg, High-dose recombinant interleukin 2 therapy for patients with metastatic melanoma: analysis of 270 patients treated between 1985 and 1993. *J. Clin. Oncol. Off. J. Am. Soc. Clin. Oncol.* **17**, 2105–2116 (1999).
 11. Q. Zhang, M. E. Hresko, L. K. Picton, L. Su, M. J. Hollander, S. Nunez-Cruz, Z. Zhang, C.-A. Assenmacher, J. T. Sockolosky, K. C. Garcia, M. C. Milone, A human orthogonal IL-2 and IL-2R β system enhances CAR T cell expansion and antitumor activity in a murine model of leukemia. *Sci. Transl. Med.* **13**, eabg6986 (2021).
 12. L. Morsut, K. T. Roybal, X. Xiong, R. M. Gordley, S. M. Coyle, M. Thomson, W. A. Lim, Engineering Customized Cell Sensing and Response Behaviors Using Synthetic Notch Receptors. *Cell.* **164**, 780–791 (2016).
 13. K. T. Roybal, L. J. Rupp, L. Morsut, W. J. Walker, K. A. McNally, J. S. Park, W. A. Lim, Precision Tumor Recognition by T Cells With Combinatorial Antigen-Sensing Circuits. *Cell.* **164**, 770–779 (2016).
 14. K. A. Smith, Interleukin-2: inception, impact, and implications. *Science.* **240**, 1169–1176 (1988).
 15. Z. Sun, Z. Ren, K. Yang, Z. Liu, S. Cao, S. Deng, L. Xu, Y. Liang, J. Guo, Y. Bian, H. Xu, J. Shi, F. Wang, Y.-X. Fu, H. Peng, A next-generation tumor-targeting

IL-2 preferentially promotes tumor-infiltrating CD8 + T-cell response and effective tumor control. *Nat. Commun.* **10**, 3874 (2019).

16. G. R. Weiss, W. W. Grosh, K. A. Chianese-Bullock, Y. Zhao, H. Liu, C. L. Slingluff, F. M. Marincola, E. Wang, Molecular insights on the peripheral and intratumoral effects of systemic high-dose rIL-2 (aldesleukin) administration for the treatment of metastatic melanoma. *Clin. Cancer Res. Off. J. Am. Assoc. Cancer Res.* **17**, 7440–7450 (2011).
17. M. C. Panelli, E. Wang, G. Phan, M. Puhlmann, L. Miller, G. A. Ohnmacht, H. G. Klein, F. M. Marincola, Gene-expression profiling of the response of peripheral blood mononuclear cells and melanoma metastases to systemic IL-2 administration. *Genome Biol.* **3**, RESEARCH0035 (2002).
18. T. Saito, H. Nishikawa, H. Wada, Y. Nagano, D. Sugiyama, K. Atarashi, Y. Maeda, M. Hamaguchi, N. Ohkura, E. Sato, H. Nagase, J. Nishimura, H. Yamamoto, S. Takiguchi, T. Tanoue, W. Suda, H. Morita, M. Hattori, K. Honda, M. Mori, Y. Doki, S. Sakaguchi, Two FOXP3(+)/CD4(+) T cell subpopulations distinctly control the prognosis of colorectal cancers. *Nat. Med.* **22**, 679–684 (2016).
19. M. Ahmadzadeh, S. A. Rosenberg, IL-2 administration increases CD4+ CD25(hi) Foxp3+ regulatory T cells in cancer patients. *Blood.* **107**, 2409–2414 (2006).
20. K. Staveley-O’Carroll, E. Sotomayor, J. Montgomery, I. Borrello, L. Hwang, S. Fein, D. Pardoll, H. Levitsky, Induction of antigen-specific T cell anergy: An early

- event in the course of tumor progression. *Proc. Natl. Acad. Sci. U. S. A.* **95**, 1178–1183 (1998).
21. A. M. Levin, D. L. Bates, A. M. Ring, C. Krieg, J. T. Lin, L. Su, I. L. Moraga, M. E. Raeber, G. R. Bowman, P. Novick, V. S. Pande, C. G. Fathman, O. Boyman, K. C. Garcia, Exploiting a natural conformational switch to engineer an Interleukin-2 superkine. *Nature*. **484**, 529–533 (2012).
22. D. L. Wallace, M. Bérard, M. V. D. Soares, J. Oldham, J. E. Cook, A. N. Akbar, D. F. Tough, P. C. L. Beverley, Prolonged exposure of naïve CD8+ T cells to interleukin-7 or interleukin-15 stimulates proliferation without differentiation or loss of telomere length. *Immunology*. **119**, 243–253 (2006).
23. L. V. Hurton, H. Singh, A. M. Najjar, K. C. Switzer, T. Mi, S. Maiti, S. Olivares, B. Rabinovich, H. Huls, M.-A. Forget, V. Datar, P. Kebriaei, D. A. Lee, R. E. Champlin, L. J. N. Cooper, Tethered IL-15 augments antitumor activity and promotes a stem-cell memory subset in tumor-specific T cells. *Proc. Natl. Acad. Sci.* **113**, E7788–E7797 (2016).
24. P. F. Robbins, Y. F. Li, M. El-Gamil, Y. Zhao, J. A. Wargo, Z. Zheng, H. Xu, R. A. Morgan, S. A. Feldman, L. A. Johnson, A. D. Bennett, S. M. Dunn, T. M. Mahon, B. K. Jakobsen, S. A. Rosenberg, Single and Dual Amino Acid Substitutions in TCR CDRs Can Enhance Antigen-Specific T Cell Functions. *J. Immunol. Baltim. Md 1950*. **180**, 6116–6131 (2008).

25. P. F. Robbins, S. H. Kassim, T. L. N. Tran, J. S. Crystal, R. A. Morgan, S. A. Feldman, J. C. Yang, M. E. Dudley, J. R. Wunderlich, R. M. Sherry, U. S. Kammula, M. S. Hughes, N. P. Restifo, M. Raffeld, C.-C. R. Lee, Y. F. Li, M. El-Gamil, S. A. Rosenberg, A pilot trial using lymphocytes genetically engineered with an NY-ESO-1-reactive T-cell receptor: long-term follow-up and correlates with response. *Clin. Cancer Res. Off. J. Am. Assoc. Cancer Res.* **21**, 1019–1027 (2015).
26. J. Z. Williams, G. M. Allen, D. Shah, I. S. Sterin, K. H. Kim, V. P. Garcia, G. E. Shavey, W. Yu, C. Puig-Saus, J. Tsoi, A. Ribas, K. T. Roybal, W. A. Lim, Precise T cell recognition programs designed by transcriptionally linking multiple receptors. *Science.* **370**, 1099–1104 (2020).
27. C. C. Kloss, M. Condomines, M. Cartellieri, M. Bachmann, M. Sadelain, Combinatorial antigen recognition with balanced signaling promotes selective tumor eradication by engineered T cells. *Nat. Biotechnol.* **31**, 71–75 (2013).
28. G. P. Mognol, R. Spreafico, V. Wong, J. P. Scott-Browne, S. Togher, A. Hoffmann, P. G. Hogan, A. Rao, S. Trifari, Exhaustion-associated regulatory regions in CD8+ tumor-infiltrating T cells. *Proc. Natl. Acad. Sci. U. S. A.* **114**, E2776–E2785 (2017).
29. T. Chinen, A. K. Kannan, A. G. Levine, X. Fan, U. Klein, Y. Zheng, G. Gasteiger, Y. Feng, J. D. Fontenot, A. Y. Rudensky, An essential role for the IL-2 receptor in Treg cell function. *Nat. Immunol.* **17**, 1322–1333 (2016).

30. G. Oliveira, K. Stromhaug, S. Klaeger, T. Kula, D. T. Frederick, P. M. Le, J. Forman, T. Huang, S. Li, W. Zhang, Q. Xu, N. Cieri, K. R. Clauser, S. A. Shukla, D. Neuberg, S. Justesen, G. MacBeath, S. A. Carr, E. F. Fritsch, N. Hacohen, M. Sade-Feldman, K. J. Livak, G. M. Boland, P. A. Ott, D. B. Keskin, C. J. Wu, Phenotype, specificity and avidity of antitumour CD8⁺ T cells in melanoma. *Nature*. **596**, 119–125 (2021).
31. J. Li, K. T. Byrne, F. Yan, T. Yamazoe, Z. Chen, T. Baslan, L. P. Richman, J. H. Lin, Y. H. Sun, A. J. Rech, D. Balli, C. A. Hay, Y. Sela, A. J. Merrell, S. M. Liudahl, N. Gordon, R. J. Norgard, S. Yuan, S. Yu, T. Chao, S. Ye, T. S. K. Eisinger-Mathason, R. B. Faryabi, J. W. Tobias, S. W. Lowe, L. M. Coussens, E. J. Wherry, R. H. Vonderheide, B. Z. Stanger, Tumor Cell-Intrinsic Factors Underlie Heterogeneity of Immune Cell Infiltration and Response to Immunotherapy. *Immunity*. **49**, 178-193.e7 (2018).
32. S. R. Hingorani, L. Wang, A. S. Multani, C. Combs, T. B. Deramaudt, R. H. Hruban, A. K. Rustgi, S. Chang, D. A. Tuveson, Trp53R172H and KrasG12D cooperate to promote chromosomal instability and widely metastatic pancreatic ductal adenocarcinoma in mice. *Cancer Cell*. **7**, 469–483 (2005).
33. T. N. D. Pham, M. A. Shields, C. Spaulding, D. R. Principe, B. Li, P. W. Underwood, J. G. Trevino, D. J. Bentrem, H. G. Munshi, Preclinical Models of Pancreatic Ductal Adenocarcinoma and Their Utility in Immunotherapy Studies. *Cancers*. **13**, 440 (2021).

34. I. M. Stromnes, T. M. Schmitt, A. Hulbert, J. S. Brockenbrough, H. Nguyen, C. Cuevas, A. M. Dotson, X. Tan, J. L. Hotes, P. D. Greenberg, S. R. Hingorani, T. Cells Engineered against a Native Antigen Can Surmount Immunologic and Physical Barriers to Treat Pancreatic Ductal Adenocarcinoma. *Cancer Cell*. **28**, 638–652 (2015).
35. M. K. Gately, T. D. Anderson, T. J. Hayes, Role of asialo-GM1-positive lymphoid cells in mediating the toxic effects of recombinant IL-2 in mice. *J. Immunol. Baltim. Md 1950*. **141**, 189–200 (1988).
36. E. Hooijberg, A. Q. Bakker, J. J. Ruizendaal, H. Spits, NFAT-controlled expression of GFP permits visualization and isolation of antigen-stimulated primary human T cells. *Blood*. **96**, 459–466 (2000).
37. H. Yamaue, S. V. Kashmiri, R. De Filippi, C. Nieroda, J. R. Yannelli, K. Y. Tsang, J. Schlom, Enhanced interleukin-2 production in human tumor-infiltrating lymphocytes engineered by 3'-truncated interleukin-2 gene. *J. Immunother. Emphas. Tumor Immunol. Off. J. Soc. Biol. Ther.* **16**, 262–274 (1994).
38. Y. Hart, S. Reich-Zeliger, Y. E. Antebi, I. Zaretsky, A. E. Mayo, U. Alon, N. Friedman, Paradoxical Signaling by a Secreted Molecule Leads to Homeostasis of Cell Levels. *Cell*. **158**, 1022–1032 (2014).
39. Y. Refaeli, L. Van Parijs, C. A. London, J. Tschopp, A. K. Abbas, Biochemical mechanisms of IL-2-regulated Fas-mediated T cell apoptosis. *Immunity*. **8**, 615–623 (1998).

40. M. E. Pipkin, J. A. Sacks, F. Cruz-Guilloty, M. G. Lichtenheld, M. J. Bevan, A. Rao, Interleukin-2 and Inflammation Induce Distinct Transcriptional Programs that Promote the Differentiation of Effector Cytolytic T Cells. *Immunity*. **32**, 79–90 (2010).
41. J. H. Levine, E. F. Simonds, S. C. Bendall, K. L. Davis, E. D. Amir, M. D. Tadmor, O. Litvin, H. G. Fienberg, A. Jager, E. R. Zunder, R. Finck, A. L. Gedman, I. Radtke, J. R. Downing, D. Pe'er, G. P. Nolan, Data-Driven Phenotypic Dissection of AML Reveals Progenitor-like Cells that Correlate with Prognosis. *Cell*. **162**, 184–197 (2015).
42. M. T. Saung, S. Muth, D. Ding, D. L. Thomas, A. B. Blair, T. Tsujikawa, L. Coussens, E. M. Jaffee, L. Zheng, Targeting myeloid-inflamed tumor with anti-CSF-1R antibody expands CD137+ effector T-cells in the murine model of pancreatic cancer. *J. Immunother. Cancer*. **6**, 118 (2018).
43. Y. Liu, N. Zhou, L. Zhou, J. Wang, Y. Zhou, T. Zhang, Y. Fang, J. Deng, Y. Gao, X. Liang, J. Lv, Z. Wang, J. Xie, Y. Xue, H. Zhang, J. Ma, K. Tang, Y. Fang, F. Cheng, C. Zhang, B. Dong, Y. Zhao, P. Yuan, Q. Gao, H. Zhang, F. Xiao-Feng Qin, B. Huang, IL-2 regulates tumor-reactive CD8+ T cell exhaustion by activating the aryl hydrocarbon receptor. *Nat. Immunol.* **22**, 358–369 (2021).
44. S. A. Rosenberg, IL-2: The First Effective Immunotherapy for Human Cancer. *J. Immunol. Baltim. Md 1950*. **192**, 5451–5458 (2014).
45. C. Rs, P. Js, G. Ma, S. Ta, W. Ea, G. Aa, R. Sa, L. Mt, Endothelial activation during interleukin 2 immunotherapy. A possible mechanism for the vascular leak

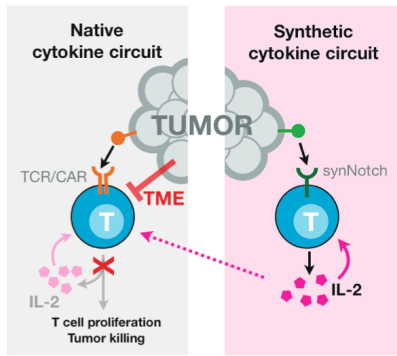
syndrome. *J. Immunol. Baltim. Md 1950.* **140** (1988) (available at <https://pubmed.ncbi.nlm.nih.gov/3279124/>).

46. A. Oyler-Yaniv, J. Oyler-Yaniv, B. M. Whitlock, Z. Liu, R. N. Germain, M. Huse, G. Altan-Bonnet, O. Krichevsky, A Tunable Diffusion-Consumption Mechanism of Cytokine Propagation Enables Plasticity in Cell-to-Cell Communication in the Immune System. *Immunity.* **46**, 609–620 (2017).
47. K. Thurley, D. Gerecht, E. Friedmann, T. Höfer, Three-Dimensional Gradients of Cytokine Signaling between T Cells. *PLOS Comput. Biol.* **11**, e1004206 (2015).
48. H. S. Wong, K. Park, A. Gola, A. P. Baptista, C. H. Miller, D. Deep, M. Lou, L. F. Boyd, A. Y. Rudensky, P. A. Savage, G. Altan-Bonnet, J. S. Tsang, R. N. Germain, A local regulatory T cell feedback circuit maintains immune homeostasis by pruning self-activated T cells. *Cell.* **184**, 3981 (2021).
49. W. N. D'Souza, L. Lefrançois, IL-2 is not required for the initiation of CD8 T cell cycling but sustains expansion. *J. Immunol. Baltim. Md 1950.* **171**, 5727–5735 (2003).
50. D. Busse, M. de la Rosa, K. Hobiger, K. Thurley, M. Flossdorf, A. Scheffold, T. Höfer, Competing feedback loops shape IL-2 signaling between helper and regulatory T lymphocytes in cellular microenvironments. *Proc. Natl. Acad. Sci. U. S. A.* **107**, 3058–3063 (2010).
51. F. Fuhrmann, T. Lischke, F. Gross, T. Scheel, L. Bauer, K. W. Kalim, A. Radbruch, H. Herzog, A. Hutloff, R. Baumgrass, Adequate immune response

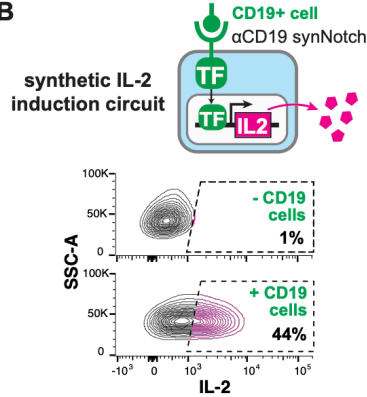
ensured by binary IL-2 and graded CD25 expression in a murine transfer model. *eLife*. **5**, e20616 (2016).

52. T. Höfer, O. Krichevsky, G. Altan-Bonnet, Competition for IL-2 between Regulatory and Effector T Cells to Chisel Immune Responses. *Front. Immunol.* **3**, 268 (2012).
53. B. M. Allen, K. J. Hiam, C. E. Burnett, A. Venida, R. DeBarge, I. TenVooren, D. M. Marquez, N. W. Cho, Y. Carmi, M. H. Spitzer, Systemic dysfunction and plasticity of the immune macroenvironment in cancer models. *Nat. Med.* **26**, 1125–1134 (2020).

A

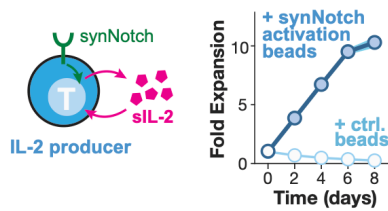


B



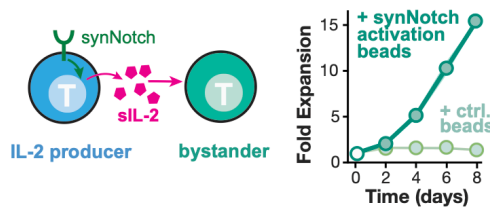
C

autocrine T cell expansion (*in vitro*)



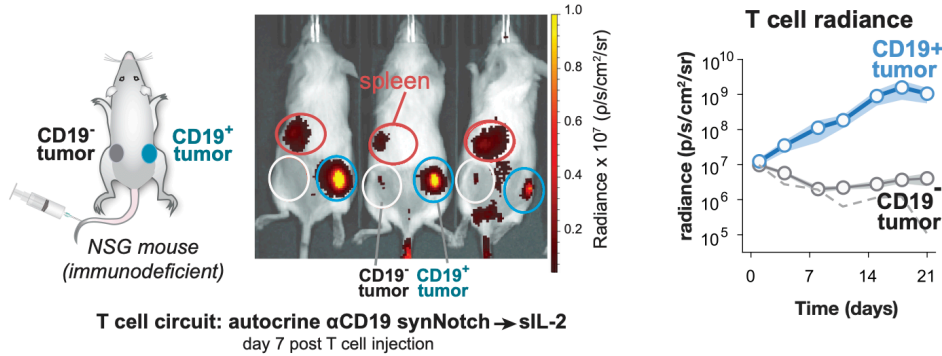
D

paracrine T cell expansion (*in vitro*)



E

Local T cell expansion *in vivo* (TCR/CAR independent) in subcutaneous dual flank model



F

Enhancement of targeted TCR killing in immunodeficient mouse model

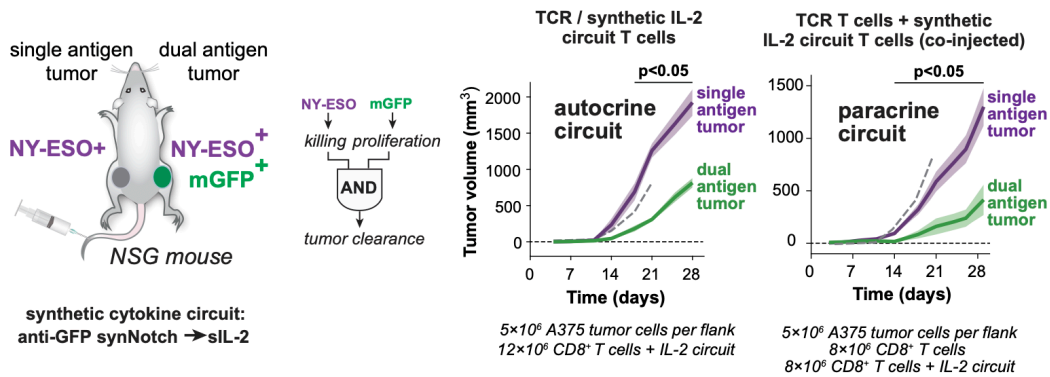


Fig. 2.1. Synthetic synNotch→IL-2 circuits can drive local T cell proliferation independent of TCR activation or cooperatively with T cell killing.

(A) The tumor microenvironment (TME) acts to suppress T cell activation, including inflammatory cytokine (e.g. IL-2) production. To bypass suppression, we propose to engineer synthetic IL-2 circuits triggered by tumor antigens in a manner independent from TCR/CAR activation.

(B) Synthetic IL-2 circuits were created in human primary T cells using anti-CD19 synNotch receptors to drive production of an inflammatory cytokine (super IL-2/sIL-2). IL-2 is produced only when stimulated by A375 tumor cells bearing the cognate CD19 antigen. Compare to **Figure 2.S1A**.

(C) Synthetic IL-2 circuit drives autocrine proliferation of primary human T cells *in vitro*, only when the circuit is triggered (here myc-tagged synNotch is activated by anti-myc antibody coated beads).

(D) Synthetic IL-2 circuit signals in a paracrine fashion to stimulate proliferation of a bystander population of human T cells that lack a synthetic circuit *in vitro*. For C and D, median is plotted; shading shows S.E.M., n=3 and filled markers indicate significant expansion > 1, right-tailed students t-test, p <0.05. Additional replicates of autocrine and paracrine proliferation are in **Figure 2.S1B**.

(E) Dual flank tumor model in NSG mice to monitor T cell trafficking *in vivo*. Primary human T cells were engineered with synthetic anti-CD19→sIL-2 circuit and eff-luc (to track cells) and administered to mice engrafted with CD19⁺ (right) and CD19⁻ (left) K562 tumors. Example bioluminescence imaging shown 7 days after T cell injection. Circles indicate tumors (blue, white) and spleen (red). Plot shows quantification of T cell luminescence over time for CD19⁺ and CD19⁻ tumors. Dashed line shows T cells in CD19⁺ tumor with no circuit added; shading shows S.E.M.

(F) Tumor reactive T cells, such as ones bearing an anti-NY-ESO TCR, fail to produce effective cytokine and killing responses against antigen positive tumors. We hypothesize that simultaneously engaging the TCR and a synthetic IL-2 circuit could enhance a local T cell response. In this case T cells bearing an anti-NY-ESO TCR and an anti-membrane-bound GFP (mGFP) synNotch→sIL-2 circuit could function as an AND gate that requires two antigen inputs to stimulate tumor killing allowing more precise recognition strategies. Here a two-flank A375 tumor model in NSG mice, with NY-ESO only on left and NY-ESO/GFP on right was generated. Plots show tumor growth over time. Both autocrine and paracrine forms of the TCR + anti-GFP synNotch→sIL-2 cells show significantly enhanced control of only the dual antigen tumor. Error shading: S.E.M. Dashed line indicates dual antigen tumor growth curve with no T cell treatment. NY-ESO TCR only control and individual tumor growth curves available in **Figure 2.S4**.

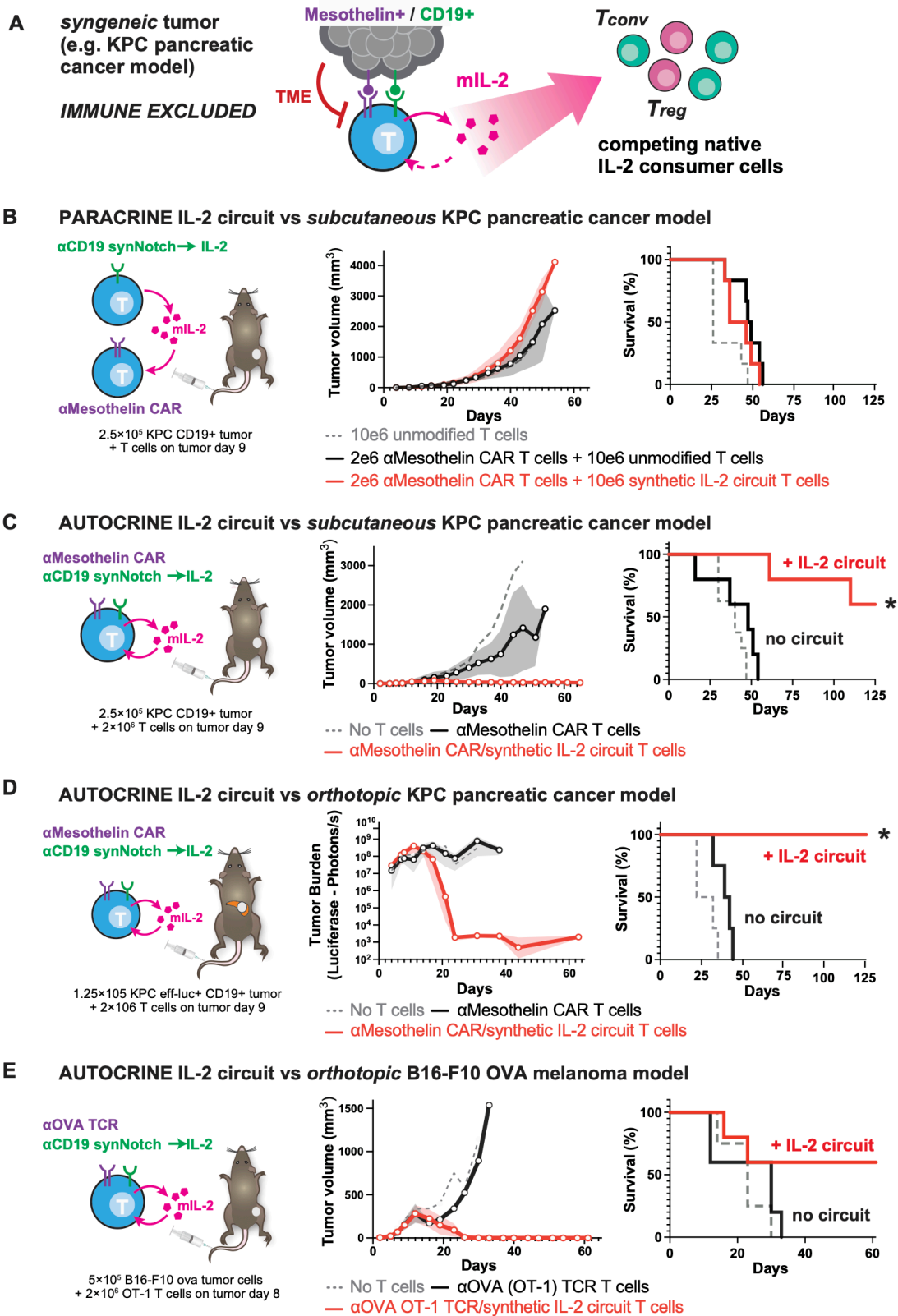


Fig. 2.2 Autocrine synthetic IL-2 circuits strongly improve T cell cytotoxicity against multiple models of immune-excluded syngeneic tumors.

(A) The synthetic IL-2 circuit was recapitulated in mouse T cells producing mouse IL-2 (mIL-2) to test circuits in presence of an intact immune system, suppressive TME and native IL-2 consumer cells.

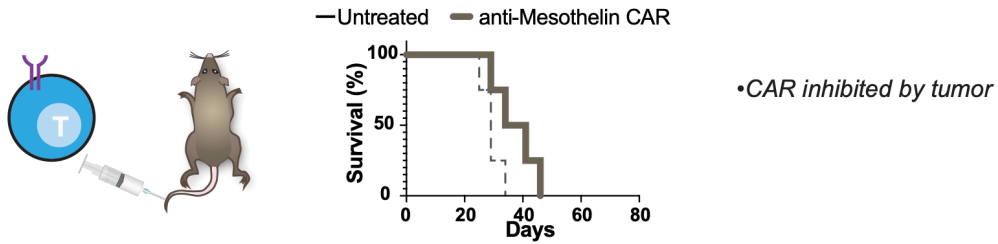
(B) KPC CD19⁺ pancreatic tumors were engrafted subcutaneously into immunocompetent C57/B16 mice and treated 9 days later with synthetic IL-2 circuit T cells and anti-Mesothelin CAR T cells as a two-cell paracrine system. No tumor control was observed in this paracrine configuration, even though KPC tumors express mesothelin.

(C) KPC CD19⁺ pancreatic tumors were engrafted as in B and treated 9 days later with T cells engineered with both a synthetic IL-2 circuit and an anti-Mesothelin CAR (autocrine configuration). Significant improvement in tumor control was observed (*red lines*) compared to anti-Mesothelin CAR T cells combined with dummy synthetic cytokine circuit (synNotch only produces BFP, black lines).

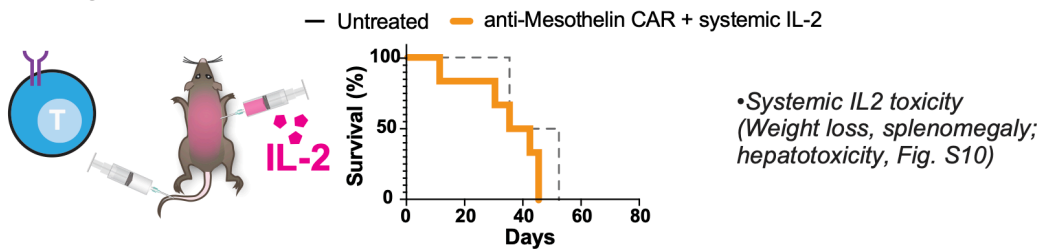
(D) KPC CD19⁺ pancreatic tumors were engrafted orthotopically in the pancreas tail and treated 9 days later with engineered T cells. 100% survival was observed only with the addition of the IL-2 circuit out to 120 days (duration of study).

(E) B16F10 OVA CD19⁺ melanoma tumors were engrafted orthotopically into immunocompetent C57/B16 mice and treated 8 days later with 2e6 engineered mouse CD8⁺ OT-1 (anti-OVA) T cells. Tumor control was only observed in mice treated with T cells expressing the IL-2 circuit. For B-E All plots show tumor burden measured by average +/- S.E.M. of caliper or bioluminescence measurements and overall survival (n=4-5 per group, * = significant difference in survival with addition of IL-2 circuit using log-rank test, p < 0.05). See **Fig. 2.S7 and 2.S8** for individual growth curves data.

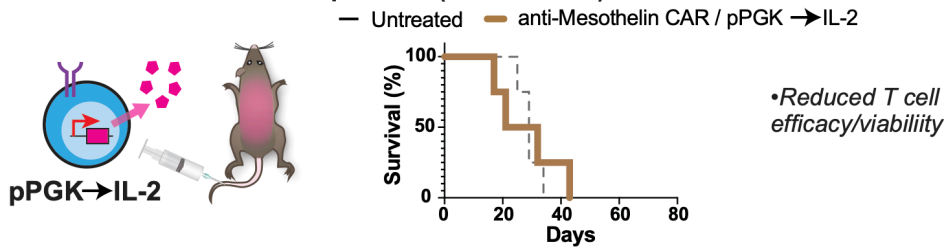
A. CAR T cell without additional IL2



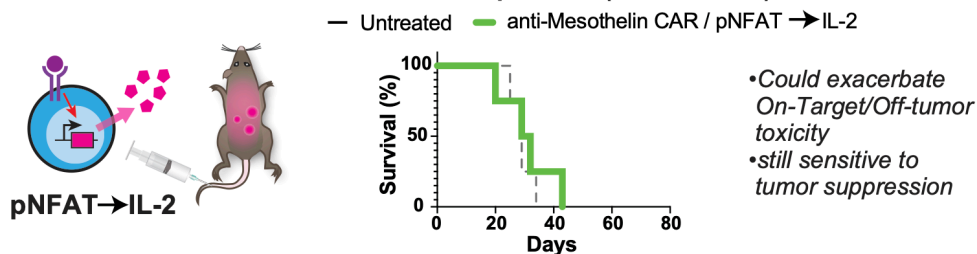
B. CAR T + Systemic IL-2 administration



C. CAR T + Constitutive IL-2 expression (cell delivered)



D. CAR T + TCR/CAR activation induced IL-2 expression (cell delivered)



E. CAR T + synNotch induced IL-2 expression (cell delivered)

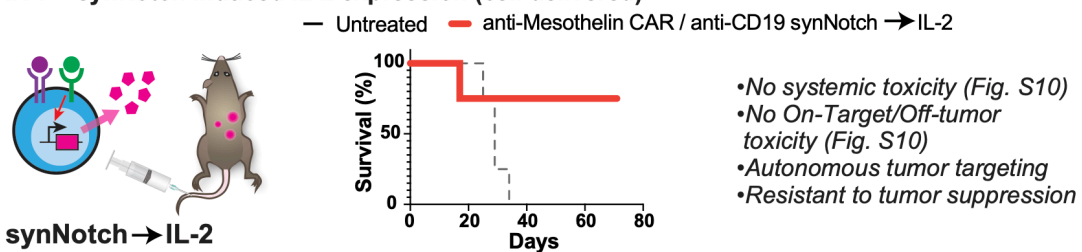


Fig. 2.3. Synthetic Notch based cytokine delivery is required for effective control of KPC tumors.

KPC CD19+ pancreatic tumors were engrafted subcutaneously into immunocompetent C57/Bl6 mice and treated 9 days later with T cells as labeled. Plotted is schematic for IL-2 production as well as overall survival for each cell design compared to matched untreated mice. n=4,5 per group. Tumor measurements for each condition are plotted in **Figure 2.S9**.

(A) 1e6 anti-Mesothelin CAR T cells with no additional IL-2.

(B) 2e6 anti-Mesothelin CAR T cells with systemic IL-2 administered at high dose (250,000 to 750,000 IU/mL) twice daily intraperitoneally for 7 days.

(C) 1e6 anti-Mesothelin CAR T cells engineered to constitutively express mIL-2 using a PGK promoter.

(D) 1e6 anti-Mesothelin CAR T cells engineered to inducibly express mIL-2 under the control of a NFAT promoter.

(E) 1e6 anti-Mesothelin CAR T cells engineered to inducibly express mIL-2 under the control of an anti-CD19 synNotch.

T cell infiltration of tumors (anti-CD3 staining)

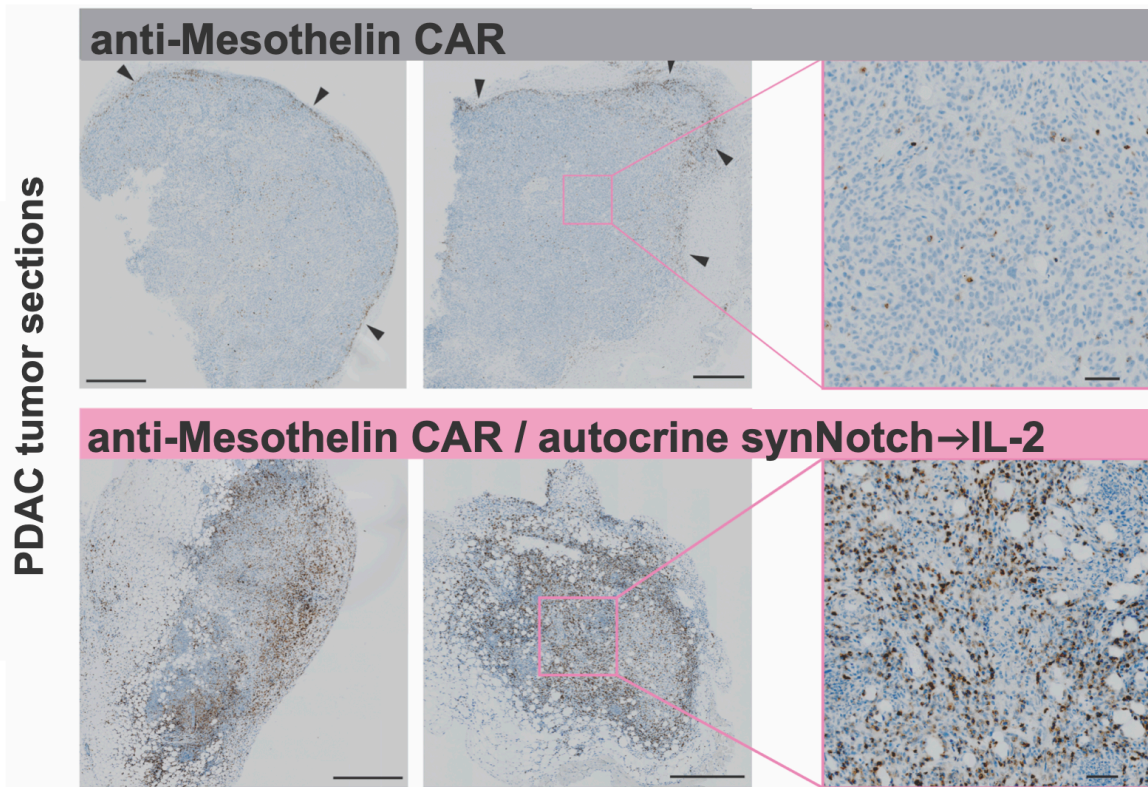


Fig. 2.4. Synthetic IL-2 circuit enables T cell infiltration into immune excluded tumors.

KPC CD19⁺ tumors were engrafted subcutaneously, treated with engineered T cells, and analyzed by IHC for T cell infiltration (anti-CD3 stain). Anti-mesothelin CAR T cells (*top*) failed to penetrate into the tumor, infiltrating the tumor edges (*black arrows*). Addition of synthetic autocrine IL-2 circuit (*bottom*) resulted in dramatically increased T cell infiltration into tumor core. Tumors were collected 23 days (*left*) and 8 days (*center*) after T cell injection. Zoomed out scale bars are 500 microns, zoomed in are 50 microns.

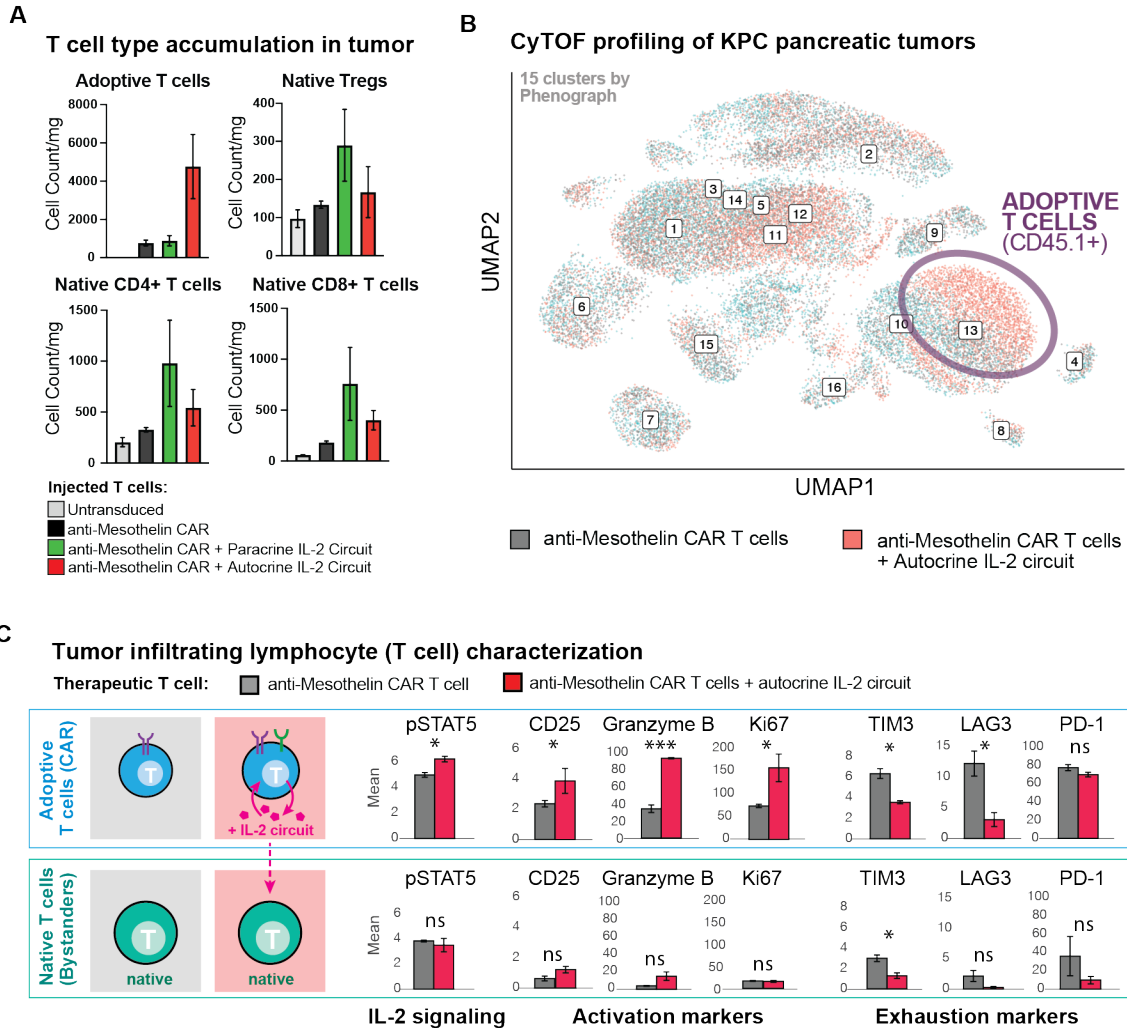


Fig. 2.5. Profiling of tumor micro-environment shows expansion and activation of CAR T cells with autocrine IL-2 circuit.

(A) Treated KPC CD19⁺ tumors were collected as in (A) after 9 days for analysis by CyTOF using CD45.1 as a marker of adoptively transferred T cells and CD45.2 as marker of native T cells. Native T cells and Regulatory T cells (Tregs) showed expansion in tumors treated with anti-mesothelin CAR + synthetic IL-2 circuit in autocrine or paracrine conFig.uration, while adoptive (CAR) T cells showed far more dramatic expansion only with anti-mesothelin CAR + synthetic IL-2 circuit in autocrine conFig.uration. n=3 samples per treatment, no p value calculated. Counts are normalized to tumor weight.

(B) Unsupervised analysis of CyTOF data. UMAP shown for KPC tumors treated by anti-mesothelin CAR +/- IL-2 circuit (autocrine). Labelled numbers indicate clusters by

Phenograph. Enrichment was only seen in adoptively transferred CAR T cells when the synthetic IL-2 circuit was engaged, see **Fig. 2.S13** for mean marker expression for each Phenograph cluster, and measure of cluster enrichment.

(C) Analysis of tumor infiltrating lymphocytes in markers in CAR T cells (CD45.1) from CyTOF data shows that CAR T cells with the synthetic IL-2 circuits in autocrine show higher expression of markers of IL-2 signaling (pSTAT5), activation (CD25), effector function (Granzyme B) and proliferation (Ki67), while showing decreased expression of markers of exhaustion (Tim3, Lag3, PD1). Matched analysis of native T cells (CD45.2) shows limited IL-2 signaling, activation, effector responses, proliferation, or exhaustion markers, with or without addition of synthetic IL-2 circuit. Mean +/- S.D. is plotted. See **Fig. 2.S13-S15**, for additional data including repeat CyTOF run. Statistical significance was tested using a two-tailed Student's t test [not significant (ns) > 0.05, *P < 0.05, *** P < 0.001].

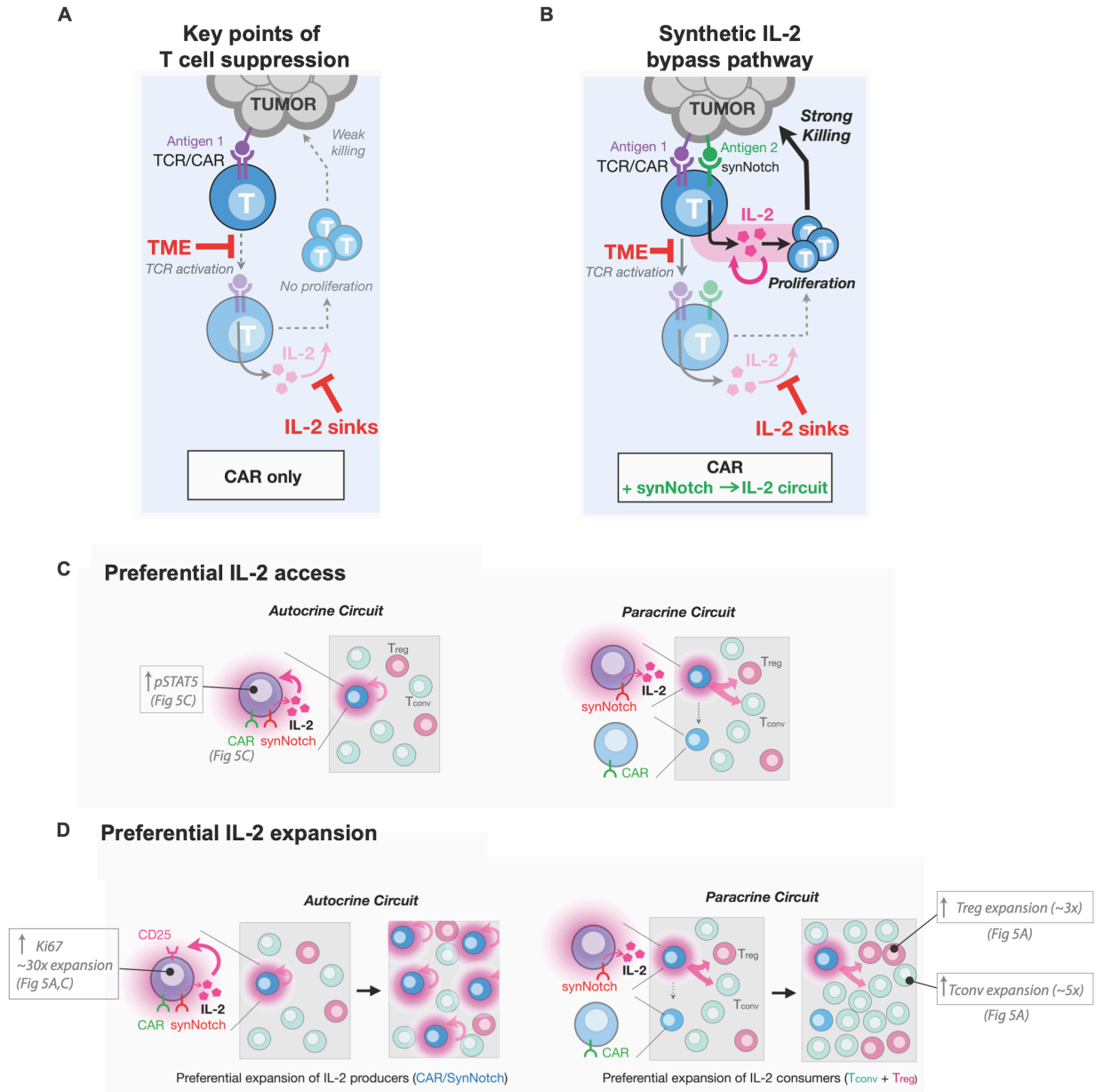


Fig. 2.6. Bypassing tumor immune suppression mechanisms with a synthetic IL-2 delivery circuit

(A) Standard CAR/TCR T cell activity in suppressive microenvironments is limited by inhibition of T cell activation, minimal production of IL-2, and consumption of IL-2 by competing native cells (sinks). Activation of both TCR and cytokine signaling, required for the full T cell response (AND gate), is blocked at these steps.

(B) Creating a bypass channel for IL-2 production that is independent of CAR/TCR activation can overcome key suppressive steps. New circuits allow initiation of T cell activation via synergistic TCR/cytokine stimulation, leading to positive feedback, T cell activation, proliferation, and efficient killing of tumor cells. The synthetic circuit

reconstitutes the key requirements for a strong T cell response in a manner that bypasses key suppressive bottlenecks.

(C) Schematic differences between autocrine and paracrine IL-2 signaling in the presence of IL-2 consumers. An autocrine IL-2 circuit provides preferential spatial access to self-made IL-2 in comparison to a paracrine IL-2 circuit, where CAR T cells must compete with other IL-2 consumers (Tregs or T-naive cells).

(D) An autocrine IL-2 leads to preferential expansion of IL-2 producers (through T cell activation and upregulation of CD25) in contrast in a paracrine circuit IL-2 producers compete on equal or lesser footing with IL-2 consumers and are not selectively enriched limiting total IL-2 produced and failing to accumulate enough IL-2 to overcome thresholds required for T cell activation.

Materials and Methods

Viral DNA constructs

Primary human T cells were engineered with constructs cloned into a second generation 5' self-inactivating lentiviral backbone (pHR). All lentiviral constructs and sequences are detailed in Tables S1 and S2. Lentiviral synthetic cytokine circuits cells were made by transducing human T cells with a synNotch component and a response element component. SynNotch genes were expressed constitutively from mouse PGK promoters whereas response elements were controlled by a 5xGAL4 repeat with a minimal CMV promoter. The payloads controlled by synNotch were either expressed as “cytokine IRES mCherry” or “BFP P2A cytokine,” where the cytokine was super-2 (sIL-2), human IL-2, IL-7, or IL-15. For in vitro experiments, bystander T cells were transduced with an SFFV eGFP vector. For in vivo experiments, the autocrine circuit was generated by placing the synNotch and response element in one lentiviral vector and either a SFFV effluc P2A mCherry or PGK BFP P2A anti-NY-ESO-1 TCR in the other vector. Paracrine circuits were created by placing the synNotch and response element in one cell and the effluc or NY-ESO-1 TCR in the other cell. Primary mouse T cells were engineered with constructs cloned into pMIG2 alternatively known as pMSCV or the self-inactivating pRetroX plasmid (Takara Bio). All retroviral constructs and sequences are detailed in Tables S3 – S6.

Primary immune cell culture

Primary human CD8⁺ and CD4⁺ T cells and NK cells were isolated from leukapheresis packs using EasySep kits (Stemcell Technologies), following which they were frozen in

RPMI with 20% human AB serum and 10% DMSO. For assays, frozen T cells were thawed in human T cell media (hTCM; X-VIVO media [Lonza], 5% human AB serum, 10 mM n-acetyl cysteine, 55 μ M β mercaptoethanol) with IL-2 (always 30 U/mL unless otherwise specified) and resuspended at 1e6 cells/mL. One day after thawing T cells were activated with 25 μ L anti-CD3/anti-CD28 coated beads (Dynabeads Human T-Activator CD3/CD28 [Gibco]) per 1e6 T cells. 24 hours after activation T cells were infected by incubating 1e6 activated T cells with 1 to 1.5 mL of lentivirus for 24 hours. Following infection viral supernatant was removed from cells which were resuspended in media with IL-2. Cells were sorted for positive transduction on a FACSAria Fusion 5 days after activation based on expression of a fluorescent protein marker or for positive staining of a Myc-tag (anti-Myc-tag antibody, 9B11, Alexa Fluor 647 conjugate, Cell Signaling Technology, Cat# 2233) on synNotch, or both. Cells were then expanded by counting daily and diluting with hTCM with IL-2 to a cell concentration of 5e5 cells/mL for an additional week to allow cells to rest from initial activation prior to in vitro analysis or in vivo use. Frozen NK cells were thawed and resuspended in hTCM 24 hours prior to use.

Mouse T cells were isolated from spleens and lymph nodes of female C57/Bl6 or OT-1 mice, which were mechanically dissociated over a 40 micron filter. RBCs were lysed using RBC lysis buffer (Biolegend) prior to negative selection for CD3⁺ or CD8⁺ T cells (StemCell) with purity confirmed post-sort by surface staining. Mouse T cells were grown in RPMI supplemented with 10% fetal bovine serum, 2 mM Glutamax, 20 mM HEPES, 1% pen/strep, 1 mM sodium pyruvate, 0.05 mM beta-mercaptoethanol, and 50

IU/mL human IL-2. Mouse T cells were activated on day of isolation with either anti-mouse CD3/CD28 dynabeads (ThermoFisher) or OVA peptide (GenScript). 24 hours after activation 1e6 mouse T cells were spininfected at 2000g for 2 hours at 32C on retronectin coated (15 ug/mL, Takara Bio) non-TC coated 24 well plates with 1 to 1.5 mL of retrovirus and 4 ng/mL polybrene (Sigma-Aldrich). Retrovirus was removed after 4 hours and mouse T cells expanded until 3 days after activation when they were sorted on a FACSaria as above. Mouse T cells were then expanded daily by counting and diluting with mTCM + IL-2 to maintain a concentration of 1e6 cells/mL for 9 days after activation prior to use with in vitro or in vivo assays.

Virus Production

Lentivirus was produced using Lx293t lentiviral packaging cells (Takara bio, Cat# 632180) that were seeded in 6-well plates at 7e5 cells/well and 24 hours later transfected with pHR constructs and pCMV and pMD2.g packaging plasmids using FuGene HD (Promega) following manufacturer's protocol. 48 hours after transfection viral supernatant was collected and filtered prior to use with human T cell cultures.

Retrovirus was producing using Plat-E retroviral packaging cells (Cell Biolabs, Cat# RV-101) that were seeded in 6 well plates at 9e5 cells/well and 24 hours later transfected with pMIG2 or pRetroX constructs using FuGene HD (Promega) following manufacturer's protocol. 48 hours after transfection viral supernatant was collected and filtered prior to use with mouse T cell cultures.

Tumor Cell Culture

Human K562 cells were purchased from the ATCC (CCL-243) and were cultured in Iscove Modified Dulbecco's Modified Eagle Medium with 10% FBS and split to 2.5×10^5 cells/mL every 3 days or 3.5×10^5 cells/mL every 2 days. Human A375 cells were purchased from the ATCC (CRL-1619) and cultured in DMEM with 10% FBS and split 1:6 every 2 days or 1:10 every 3 days. K562 lines were transduced to constitutively expressed mCherry and/or CD19 ligand (membrane-tethered CD19 extracellular domain). A375 lines endogenously present NY-ESO-1 antigen and were transduced to express GFP ligand (membrane-tethered GFP), or not. Murine C57/Bl6 KPC (Kras^{LSL.G12D/+}; p53^{R172H/+}; PdxCre^{tg/+}) cells were a kind gift of the Stanger Lab (25) and were cultured in Dulbecco's Modified Eagle Medium with 10% FBS and split 1:5 every 2 days or 1:10 every 3 days. Murine C57/Bl6 B16F10 OVA cells were a kind gift of the Krummel Lab and were cultured in Dulbecco's Modified Eagle Medium with 10% FBS and split 1:5 every 2 days or 1:10 every 3 days.

In-Vitro Assays

T cells and target cells were washed of residual media and cytokines by two rounds of centrifugations at 400xg for 4 minutes followed by resuspension in hTCM without IL-2. In some cases, T cells were stained with 1:5000 CellTrace CFSE proliferation stain (Molecular Probes) following manufacturer's protocol. Magnetic anti-HA or anti-Myc-tag antibody-coated beads (Pierce) were washed 3 times with hTCM using a magnet before using. Immune cells were seeded at 2.5×10^5 cells/mL and K562 cells at 1.25×10^5 cells/mL. IL-2 was added as indicated. For beads, 2.5 μ L (in terms of original suspension before

washing) per well was used. Every 2 days, wells were trituated and 50 μ L cell suspension was taken to analyze by flow cytometry. A 96-well magnet array was used to retain magnetic beads. The media was then replenished: cells were pelleted, 100 μ L of old media was removed, then 150 μ L fresh hTCM was added to restore the volume to 200 μ L.

Mouse Experiments

Prior to injection into mice, T cells were washed in PBS, resuspended at 10 times the injection amount per mL, and 100 μ L was injected via the tail vein on day 0. Mouse T cells were administered to female 6 to 12 week old C57/Bl6 mice (Jackson Labs Strain #000664) and human T cells were administered to female 6 to 12 week old NSG (NOD-*scid* IL2R γ ^{null}) mice. Heterotopic K562, A375 and KPC tumors were prepared by washing cells in PBS three times, resuspending at 10 times the injection amount per mL, and injecting 100 μ L subcutaneously in each flank on day 0 (K562 tumors), day -4 (A375 tumors) or day -7 to -9 (KPC tumors). Orthotopic B16-F10 tumors were prepared as before but resuspended at 25 times the injection amount per mL, and 25 μ L was injected intradermally on day -7 to -9. Orthotopic KPC tumors were prepared as before with 125,000 cells implanted into the tail of the pancreas in 25 μ L in a 1:1 mix with Matrigel (Fisher Scientific). Sub-cutaneous and intra-dermal tumor size was measured by caliper while orthotopic tumor size was measured by luciferase signal.

Bioluminescence imaging was performed using an IVIS Spectrum (Perkin Elmer). Mice were injected intraperitoneally with 200 μ L of 15 mg/mL d-luciferin (Goldbio) and imaged 15 minutes later. Typical sample size per group was 5 mice with randomization at time

of tumor implantation. Tumor measurements were performed by staff blinded to treatment groups, only mice that were engrafted tumors were included in analysis. All animal studies were performed under the UCSF Office of Research Institutional Animal Care and Use Program approval number AN183960-02N.

In-Vitro Immune Cell Assays

Flow cytometry was performed either on a BD LSRii or BD Fortessa X-20 with high-throughput system. Analysis of flow data was performed in FlowJo (FlowJo, LLC). For counting, constant volumes were taken from each well and all events were counted within those volumes. IL-2 production in primary human T cells was measured in 96 well flat bottom plates with A375 cells in co-culture with T cells. After 24 hours T cells were exposed to golgi-plug/stop (BD Biosciences) for four hours and then fixed and stained with PE-Texas Red anti-CD4 (Biolegend, Cat# 317448, AB_2565847) and BUV-737 conjugated anti-human IL-2 (BD Bioscience, Cat# 564446) before flowing. ELISA measurements of IL-2 production from mouse T cells were performed using a human or mouse IL-2 quantikine ELISA kit (R&D systems, Cat# M2000). Absolute T Cell proliferation was measured by adding 2 uL of anti-myc Tag beads to T cells in a 200 uL volume on Day 0 and sampling 50 uL of cells with replacement of media every 2 days. Viable T Cell counts were quantified using 1:500 Sytox (Molecular Probes) in PBS and accounting for dilution of wells. T cell proliferation was also analyzed by dilution of CFSE cell trace dye (Thermo Fisher). NK cell expansion was measured in co-culture of T cells, NK cells and K562 cells. Cells were stained with 1:100 anti-CD3 and 1:100 anti-CD8 fluorescent conjugated antibodies in flow buffer (PBS, 5% FBS) for 30 minutes at

4°C followed by 1:500 DRAQ7 (Molecular Probes) in flow buffer. Mouse T cell cytotoxicity was tested against GFP labeled target cells that were plated at indicated count in 100 uL in 96 well flat bottom plates and placed in an Incucyte Live-Cell Imaging System (Sartorius). T cells were added at indicated count in 100 uL of mTCM without IL2 and survival of GFP labeled target cells was recorded by imaging. Mouse T cell differentiation measured with BV605 anti-PD-1 (Biolegend, Cat# 135220, AB_2562616) and PE Lag3 (Biolegend, Cat #125208, AB_2133343). Human T cell differentiation measured with FITC anti-CD45RO (Biolegend, Cat #304242, AB_314420) and AF647 anti-CCR7 (Biolegend, Cat #353217, AB_10913812). Cytokine receptor expression measured with BV-421 anti-IL7R (Biolegend, Cat# 351309, AB_10898326), APC anti-IL15Ra (Biolegend, Cat #330209, AB_2561439), PE-TR anti-CD25 (Biolegend, Cat # 302645, AB_2734259).

Analysis of tumor specimens: IHC

Tumors samples were collected for IHC and fixed in 10% formalin for 24 to 48 hours prior to preservation in 70% ETOH. Tissue was embedded in paraffin, sectioned and mounted for staining with single chromogenic anti-CD3 (clone SP7) antibody at the UCSF Biorepository core facility.

Analysis of tumor specimens: Flow cytometry

Tumor samples for flow cytometry were collected and immediately processed. Tumors were finely minced, digested in a mixture of 1 mg/mL collagenase IV, 20 U/mL DNase IV, and 0.1 mg/mL hyaluronidase V for 30 min at 37°C with shaking, passed through 70

µm cell strainers, washed twice with PBS + 0.04% EDTA, and aliquoted in 96 well plates for high-throughput flow cytometry. Cells were stained with 1:500 Live/Dead (Molecular Probes) in flow buffer for 15 minutes, followed by additional surface staining. Antibodies used to profile murine tumors included an AF700 anti-CD45 (Biolegend, Cat# 103127, AB_493714), PE-594 anti-CD3 (Biolegend, Cat# 100245, AB_2565882), APC anti-CD4 (Biolegend, Cat# 100411, AB_312696), BV711 anti-CD8 (Biolegend, Cat# 100747, AB_11219594), and APC-Cy7 anti-Thy1.1 (Biolegend, Cat# 202519, AB_2201418). Flow cytometry was performed on a BD Fortessa X-20 with high-throughput system and analysis of flow data was performed in FlowJo (FlowJo, LLC), compensation was performed with Ultracomp eBeads (ThermoFisher).

Analysis of tumor specimens: CyTOF (Cytometry by time of flight)

Tumor samples for CyTOF were processed immediately after collection. Tumor samples were minced and digested in RPMI 1640 with 1 mg/ml collagenase IV and 0.1 mg/ml DNase I for 30 min at 37°C with shaking. Digested tumor samples were filtered with a 70 µm cell strainer and washed with PBS + 5mM EDTA at 4°C. Cells were resuspended 1:1 with PBS + 5mM EDTA + 50µM Cisplatin (Sigma) for exactly 60s prior to quenching 1:1 with PBS + 5mM EDTA + 0.5% BSA to determine viability. Tumor sample was fixed for 10 min at room temperature using 1.6% PFA and frozen at -80°C. Mass-tag cellular barcoding and antibody staining of samples for CyTOF were performed as previously described (2). A summary of all antibodies used for CyTOF are detailed in Tables S7. All antibodies were conjugated at the UCSF Parnassus Flow Cytometry Core. Each antibody clone and lot was titrated to optimal staining concentration using primary

murine samples. CyTOF was performed on a Helios mass cytometer (Fluidigm) with data analysis performed in CellEngine and R.

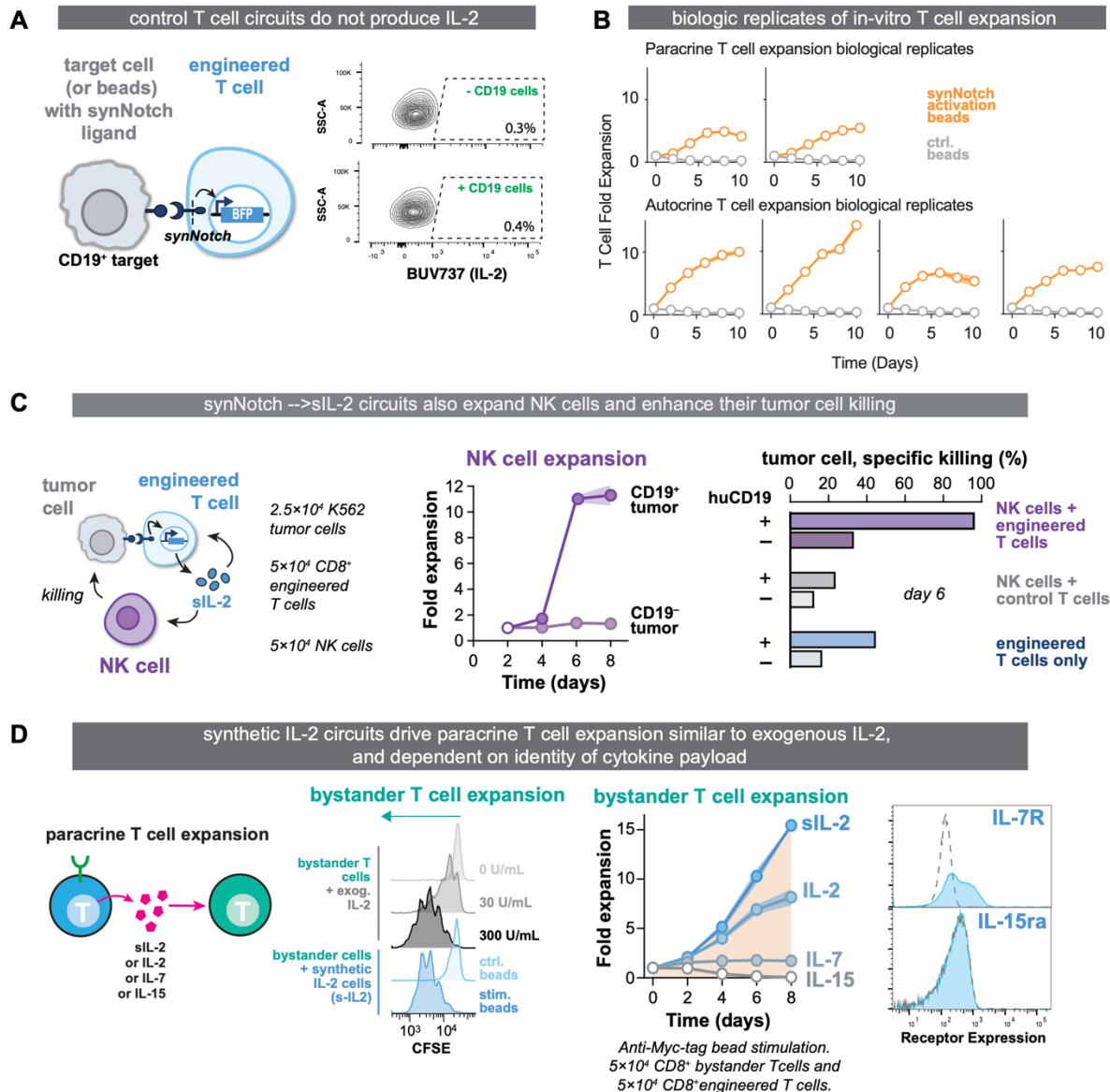


Fig. 2.S1. Driving immune cell expansion with synNotch \rightarrow IL-2 circuits.

(A) Control Human T cells engineered with an anti-CD19 synNotch driving production of a dummy payload (blue fluorescent protein) do not produce IL-2 (as measured by intracellular flow) when co-cultured with CD19+ or CD19- A375 tumor cells, compare to Figure 2.1B.

(B) Additional biologic replicates of human T cell expansion when engineered with an anti-CD19 SynNotch \rightarrow sIL-2 circuit in paracrine (top) or autocrine (bottom) from different donor, compare to Figure 2.1C and 2.1D.

(C) (left) Synthetic IL-2 circuit T cells stimulate expansion and cytotoxicity of NK cells in a paracrine fashion. (middle) tumor antigen-specific NK cell expansion by synthetic IL-2 circuit T cells. (right) Specific killing of tumor cells by NK cells when co-cultured with synthetic IL-2 circuit (engineered) T cells is antigen-specific and exceeds killing with control T cells or synthetic IL-2 circuit (engineered) cells alone.

(D) Synthetic IL-2 circuit T cells delivering different cytokines to expand bystander T cells. (center) Shown here is bystander cell CFSE dye proliferation assay; cell division creates peaks of successively lower fluorescence. Bystander cells co-cultured with synthetic IL-2 circuit cells and anti-Myc-tag beads (blue histograms) proliferated similarly to those treated with high doses of exogenous IL-2 (grey histograms). (right) Measurements of bystander T cell proliferation when synthetic synNotch->IL-2 circuit T cells producing labeled cytokine were activated. Filled markers: significant expansion >1, right-tailed Student's t-test, $p < 0.05$. Error shading in: S.E.M. (far right) Expression of IL-7R and IL-15R alpha in primary human CD8+ T cells used in proliferation assay. Dash grey line indicates isotype control, filled blue line cell staining.

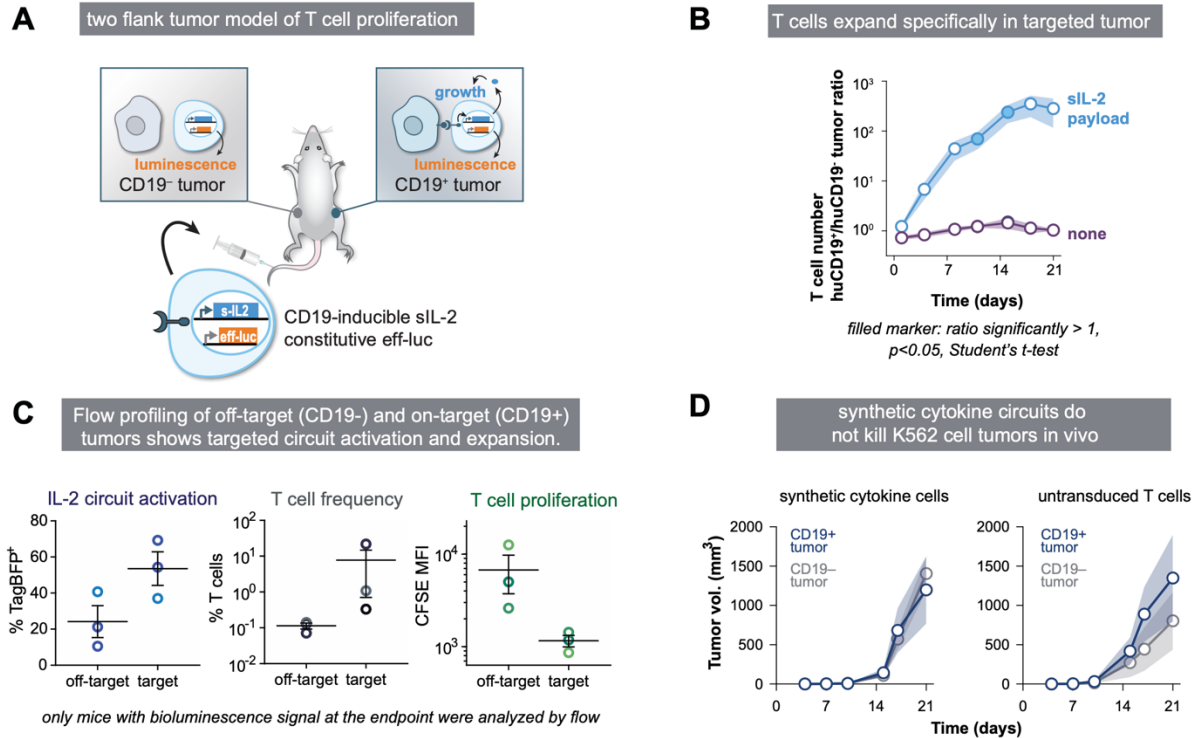


Fig. 2.S2. Local autocrine proliferation in vivo driven by synthetic IL-2 circuit

(A) Bilateral tumor model for local proliferation as shown in Figure 2.1. Right and left flank tumors: CD19+ and CD19- K562 cells, respectively. Human T cells expressing anti-CD19 synNotch driving sIL-2 and constitutively expressing eff-luc were injected intravenously and T cell localization monitored by serial bioluminescence.

(B) Ratio of bioluminescence signal from on-target tumor (CD19+) to off-target tumor (CD19-) shows selective T cell expansion in the targeted CD19+ tumor for cells engineered with a cytokine circuit producing sIL-2 (blue) but not in cells that don't express a cytokine payload (violet). Filled markers: significant ratio > 1, right-tailed Student's t-test, $p < 0.05$.

(C) In the CD19+ compared to CD19- tumor, T cells were more likely to have the synthetic IL-2 circuit activated as measured by co-produced BFP marker (left) and were more frequent as a proportion of live cells in the tumor (middle) with evidence for more T cell proliferation as measured by dilution of CFSE membrane dye that T cells were stained with prior to injection (right).

(D) Tumor volume of mice given CD19 targeted synthetic IL-2 circuit expressing T cells (left) or untransduced T cells (right), comparing CD19+ (dark blue) to CD19- (gray) tumors. The synthetic IL-2 circuit alone in NSG mice had no effect on tumor growth. Error shading: S.E.M. Open markers indicate no significant difference between tumors, Student's t-test, $p > 0.05$.

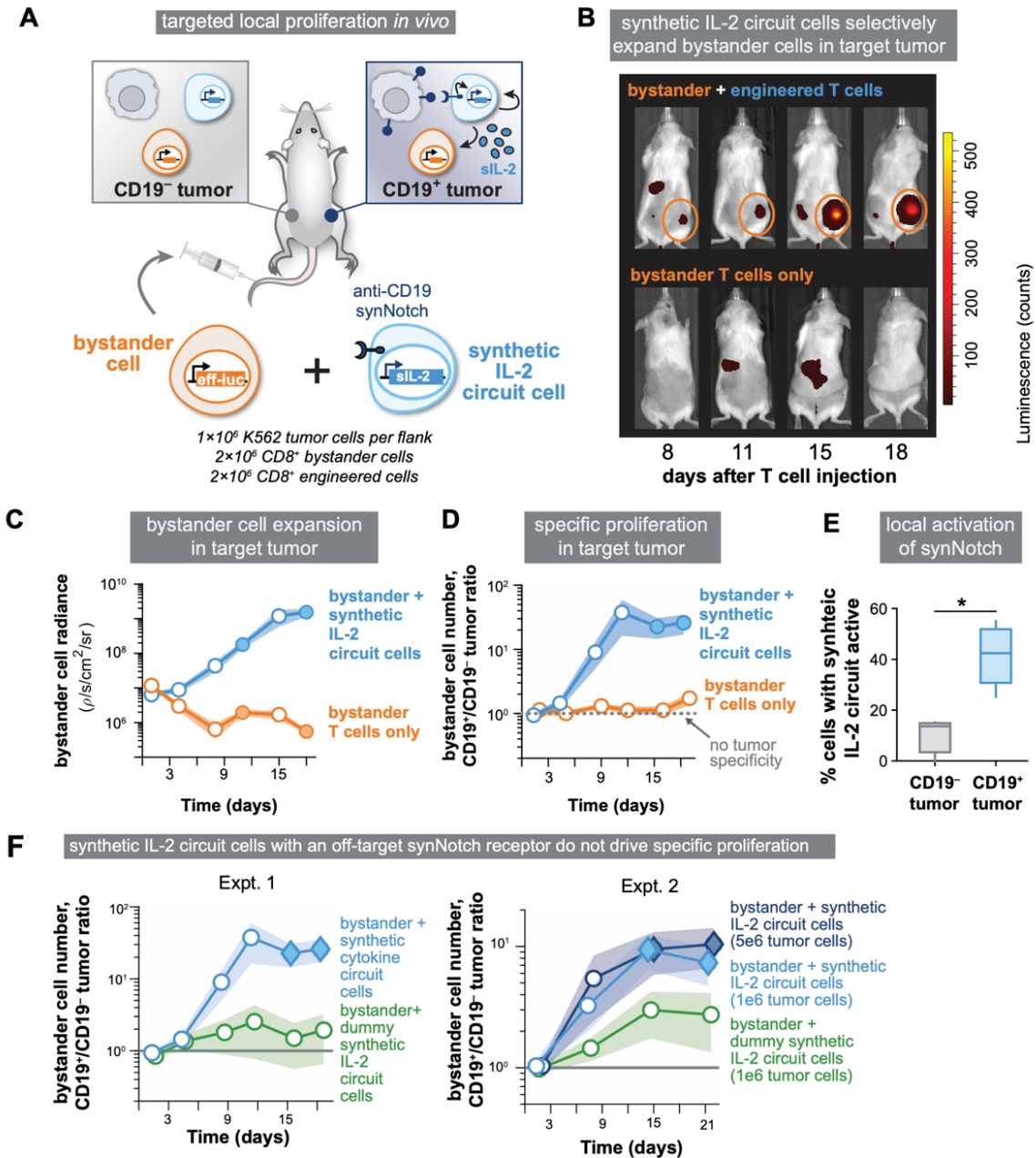
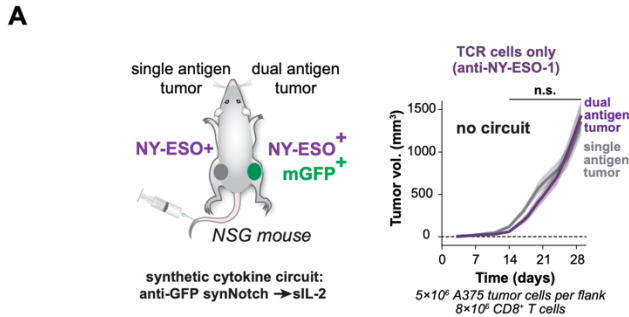


Fig. 2.S3. Local paracrine proliferation *in vivo* driven by synthetic IL-2 circuit. (A) Bilateral tumor model for local proliferation. Right and left flank tumors: CD19+ and CD19-K562 cells, respectively. Bystander T cells expressing eff-luc were co-injected with synthetic IL-2 circuit T cells (anti-CD19 synNotch => SIL-2). (B) Bioluminescence imaging of eff-luc-expressing bystander T cells. Circles highlight proliferation in the CD19+ tumor in mice that also received synthetic IL-2 circuit T cells. One mouse per group is shown. (C) Bystander cell radiance in CD19+ tumor rose in mice receiving both cell types (blue), but fell with bystander cells only (orange). Filled marker: significant difference between groups, Student's t-test, $p < 0.05$. Error shading in C, D: S.E.M.

(D) Tumor specificity: ratio of bystander cell radiance in CD19* to CD19 tumor. Bystander cell proliferation was specific for the CD19+ tumor only with co-injection of CD19 targeted synthetic IL-2 circuit cells. (Filled markers: significant ratio>1, right-tailed Student's t-test, $p<0.05$).

(E) The Synthetic IL-2 circuit was only activated in the targeted (CD19+) tumor. Activation measured by expression of mCherry (co-expressed with s-IL2). * indicates significant difference by Student's t-test, $p<0.05$, and boxplot shows, median, quartiles, and extent of data.

(F) Antigen specificity of bystander cell proliferation, determined by the ratio of bystander cell bioluminescence in the CD19+ to CD19- tumor. Comparison between groups of mice given bystander cells with synthetic IL-2 circuit cells (blue or dark blue for 1e6 or 5e6 tumor cells implanted) or "dummy" synthetic IL-2 circuit expressing a synNotch for an irrelevant antigen (anti-mGFP; green), across two experimental replicates (left and right). Error shading: S.E.M. Filled markers: ratio>1, right-tailed Student's t-test, $p<0.05$.



Individual growth curves for tumor volumes in Figure 2.

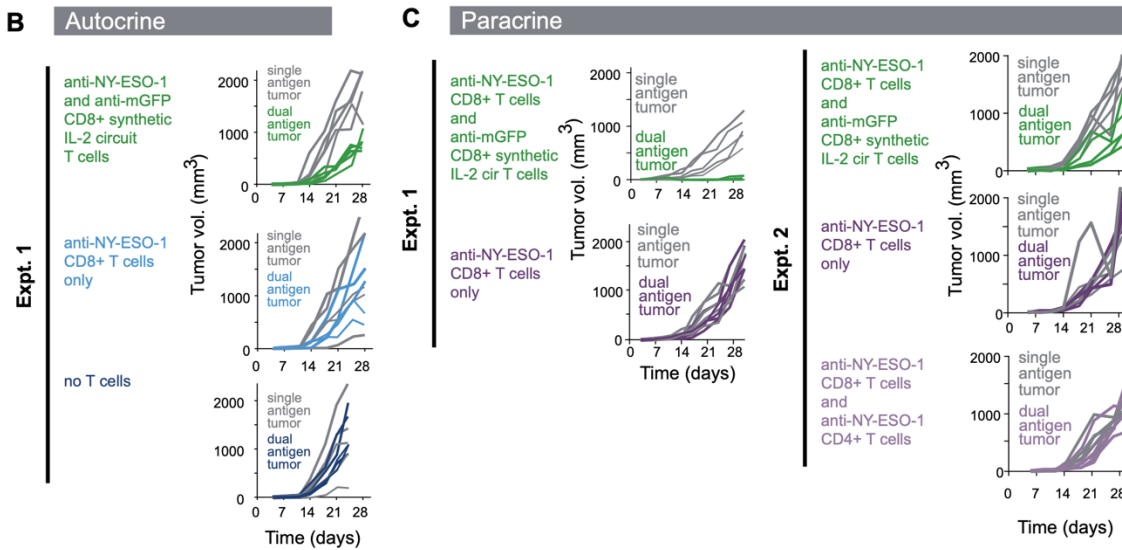


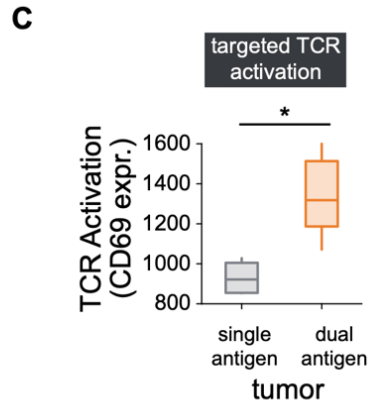
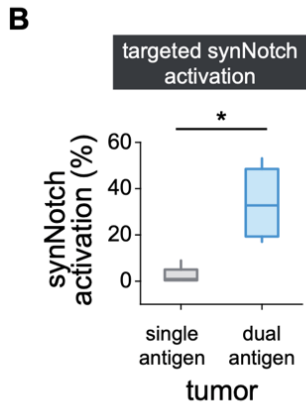
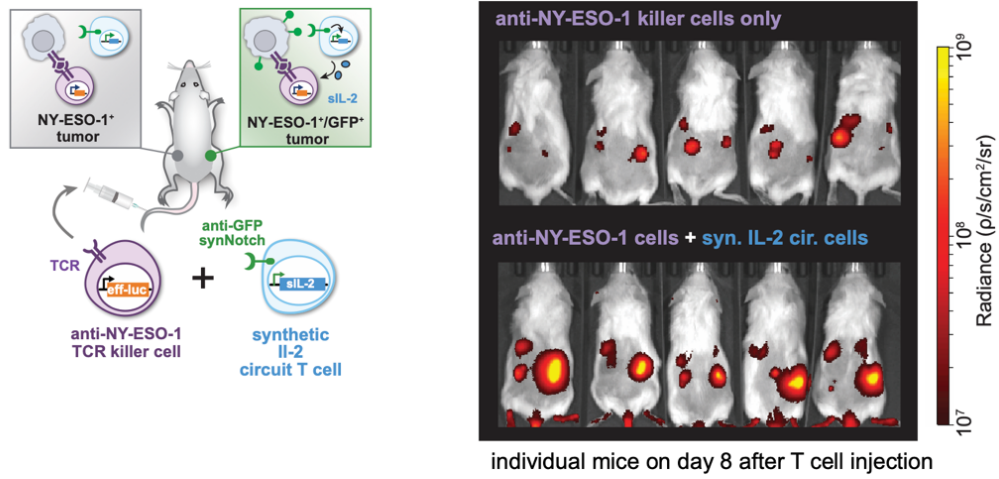
Fig. 2.S4. Tumor killing enhanced by synthetic IL-2 circuits in individual mice.

(A) Two-flank A375 tumor model in NSG mice, with NY-ESO only on left and NY-ESO/GFP on right. Plots show tumor growth over time. T cells with only anti-NY-ESO TCR do not clear either tumor. Error shading: S.E.M.

(B) Individual mouse tumor volume trajectories given anti-NY-ESO-1 TCR CD8⁺ T cells engineered with a synthetic IL-2 circuit (green), anti-NY-ESO-1 TCR only CD8⁺ T cells (light blue), or no T cells (dark blue).

(C) Individual mouse tumor volume trajectories given anti-NY-ESO-1 TCR cells with (green) or without (violet) synthetic cytokine cells, or with anti-NY-ESO-1 CD4⁺ T cells (light violet) instead of synthetic IL-2 cells, across two experimental replicates. For A,B: dual antigen tumor (colored line) compared to single antigen tumor (gray line) volume.

A local expansion of eff-Luc+ anti-NY-ESO-1 TCR T cells



D synthetic IL-2 circuit alone does not kill A375 tumors *in vivo*

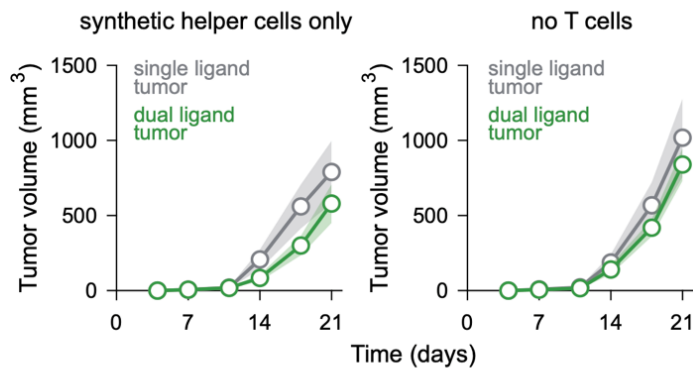


Fig. 2.S5. Enhanced local proliferation of tumor-reactive TCR T cells when co-delivered with synthetic IL-2 circuit T cells.

(A) Bilateral tumor model to test local killing enhancement by synthetic IL-2 circuit cells. Left tumor (single antigen): A375 malignant melanoma cells natively presenting NY-ESO-1 antigen. Right tumor (dual antigen): mGFP+ A375 cells. Killer T cells expressing anti-NY-ESO-1 TCR and eff-luc were co-injected with synthetic IL-2 circuit T cells expressing anti-mGFP synNotch driving sIL-2. Bioluminescence of killer cells at day 8 shows specific proliferation in the dual antigen tumor only with synthetic IL-2 circuit T cells.

(B) Flow cytometry analysis of treated tumors show specific activation of the synthetic IL-2 circuit only in the dual antigen tumor. Activation measured by expression of mCherry (co-expressed with sIL-2).

(C) Flow cytometry analysis of treated tumors show increased markers of T cell activation (CD69) only in the dual antigen tumor. In E,F: difference between dual antigen/single antigen tumors by Student's t-test, $p < 0.05$. Boxplot shows, median, quartiles, and extent of data.

(D) Tumor volume of mice given synthetic IL-2 circuit cells only (left) or no T cells (right), comparing dual (green) and single (gray) antigen tumors. Error shading: S.E.M. Open markers represent no significant difference between tumors, Student's t-test, $p > 0.05$.

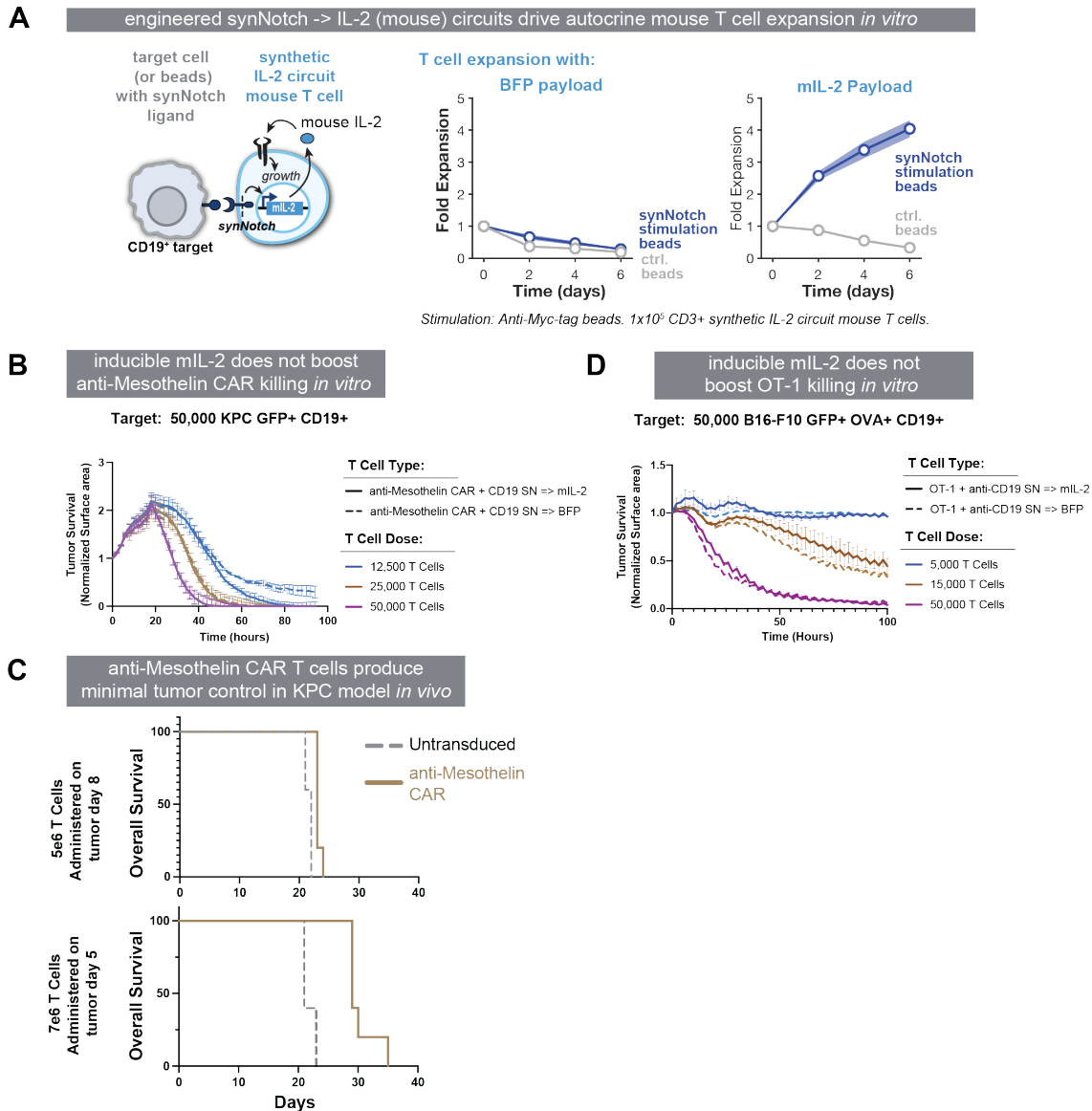


Fig. 2.S6. In-vitro characterization of engineered mouse T cells used in syngeneic tumor model experiments.

(A) Primary mouse CD3+ T cells were engineered with a single retroviral vector encoding an inducible BFP or an inducible mL-2 payload driven by an anti-CD19 SynNotch. After resting from initial CD3/CD28 expansion, IL-2 was removed from the media and synNotch receptor activated using anti-Myc beads (receptor is myc tagged). T cells were seen to proliferate specifically with synNotch activation only. (B) Primary mouse mouse CD3+ T cells were engineered with an anti-Mesothelin CART and either an anti-CD19 SynNotch inducible BFP or anti-CD19 SynNotch inducible mL-2. The indicated number of T cells were incubated with 50,000 GFP+ KPC CD19* target cells and tumor cell survival was measured in real time with an Incucyte Live Cell Imaging system. There was no apparent difference in tumor survival when tumor cells were co-cultured with cytotoxic T cells engineered to make mL-2.

(C) Survival of mice after eff-luc+ CD19- KPC tumors were implanted in the tail of the pancreas and treated with labeled number of sorted anti-Mesothelin CD3+ CAR T cells on the indicated number of days after tumor implantation. CAR treatment alone provided minimal tumor control even at high T cell doses given at early time points with no mice surviving.

(D) As in (B) cytotoxicity of mouse OT-1 CD8+ T cells engineered to express either an anti-CD19 synNotch inducible BFP or anti-CD19 synNotch inducible mIL-2 targeting 50,000 B16-F10 GFP+ OVA+ CD19+ tumor cells.

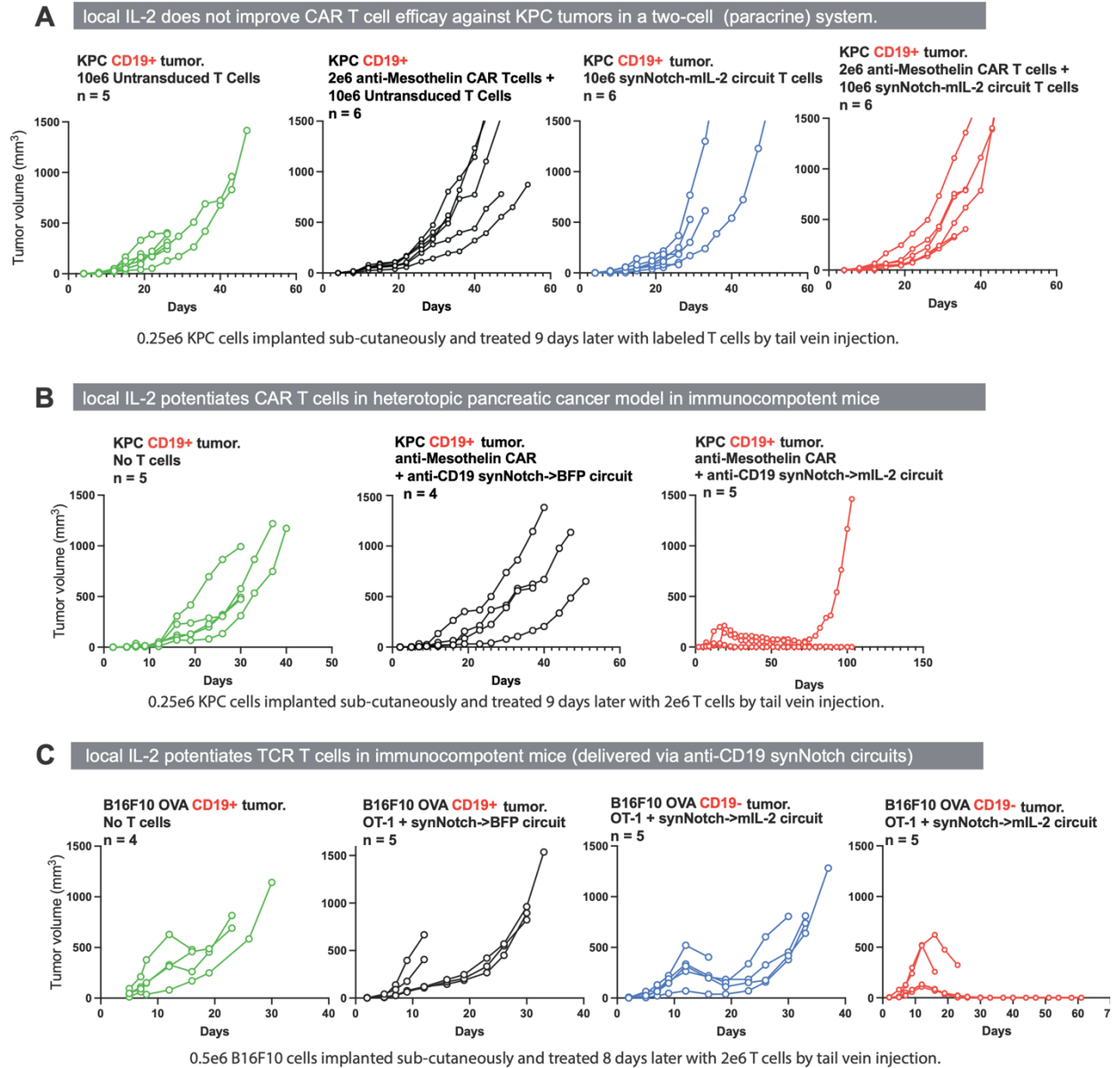


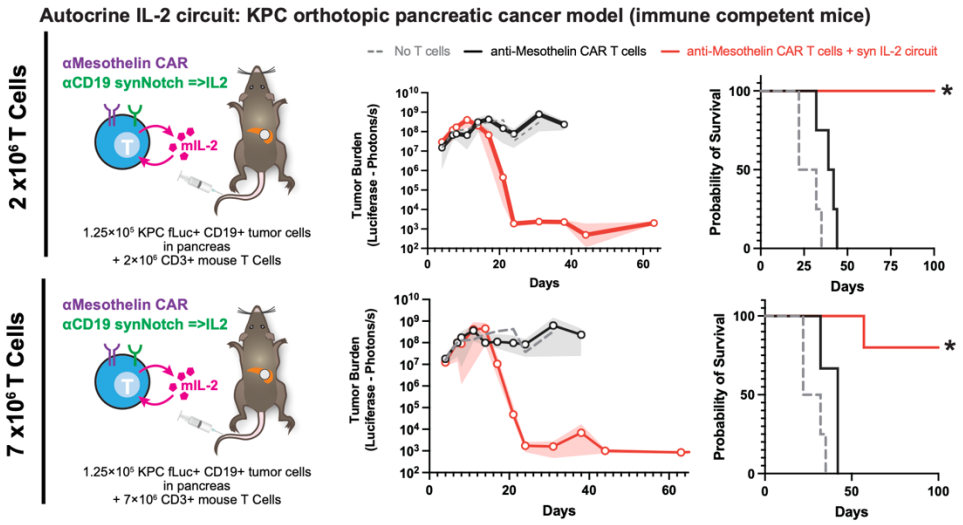
Fig. 2.S7. Individual mouse tumor volume data for experiments showing that syngeneic tumor killing is enhanced by synthetic IL-2 circuits (synNotch=>mIL-2). Plots of individual growth curves from tumors in specified mice.

(A) 250,000 sub-cutaneously implanted KPC CD19* tumor cells treated with T cell doses as labeled, matching Figure 3B.

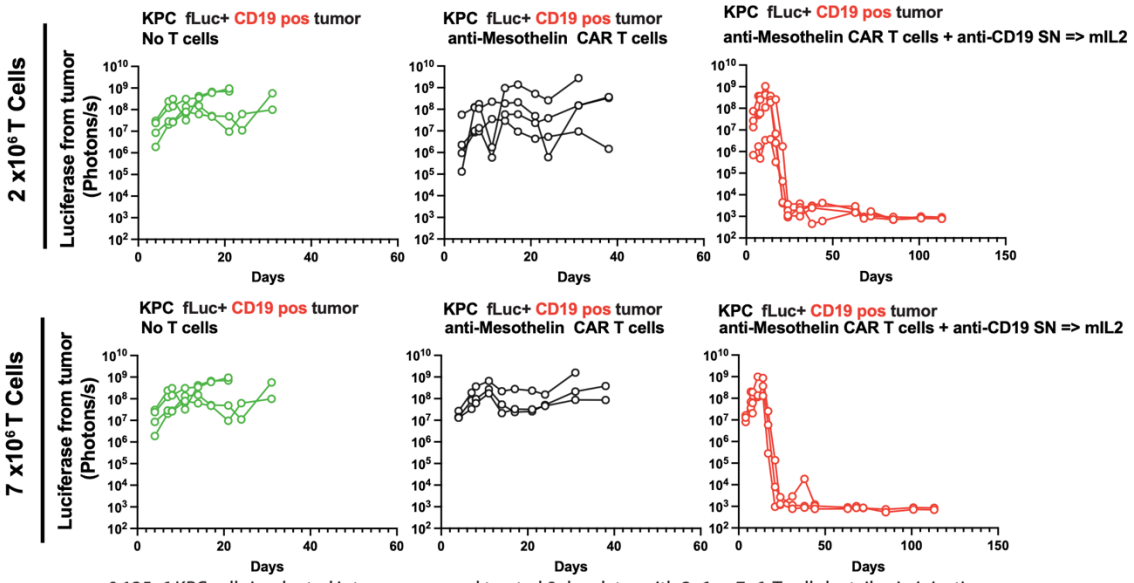
(B) 250,000 sub-cutaneously implanted KPC CD19+ tumors cells treated with 2e6 mouse T cells engineered as labeled, matching Figure 3C.

(C) 500,000 sub-cutaneously implanted B16F10 OVA tumor cells (+/- CD19 as labeled) treated with 2e6 mouse T cells engineered as labeled, matching Figure 3E.

A synthetic IL-2 circuit potentiates CAR T cell activity across a large dose range



B Individual mouse tumor burdens from panel A (above)



0.125e6 KPC cells implanted into pancreas and treated 9 days later with 2e6 or 7e6 T cells by tail vein injection.

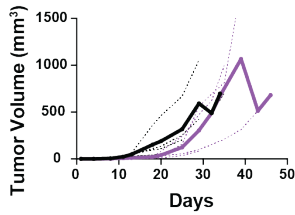
Fig. 2.S8 Orthotopic syngeneic tumor killing enhanced by synthetic cytokine circuits

(A) KPC CD19+ fLuc* pancreatic tumors were engrafted orthotopically into tail of the pancreas into immunocompetent C57/B16 mice and treated 9 days later with 2e6 or 7e6 engineered mouse CD3+ T cells by tail vein injection. Tumor control was only seen with anti-Mesothelin CAR T cells engineered with a synthetic IL-2 circuit. Plots show tumor burden as measured by average +/- S.E.M. of luciferase signal from abdominal cavity and overall survival (n=4-5 per group, * = significant difference in survival with addition of IL-2 circuit using log-rank test, p < 0.05).

(B) Plots of individual growth curves from tumors in specified mice in panel A.

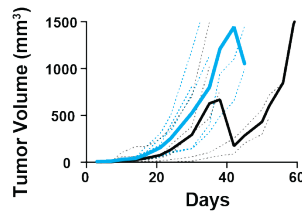
A. CAR T cell without additional IL-2

— Untreated — anti-Mesothelin CAR



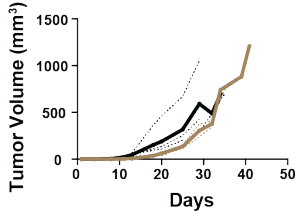
B. CAR T cell + Systemic IL-2 administration

— Untreated — anti-Mesothelin CAR



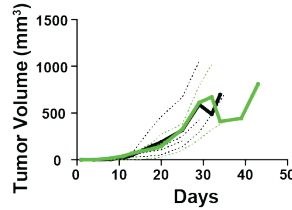
C. CAR T cell + Constitutive IL-2 expression

— Untreated — anti-Mesothelin CAR + pPGK => mIL-2



D. CAR T + TCR/CAR activation induced IL-2 expression

— Untreated — anti-Mesothelin CAR + pNFAT=> mIL-2



E. CAR T cell + synNotch induced tumor-targeted IL-2 expression (T cell)

— Untreated — anti-Mesothelin CAR + anti-CD19 synNotch => mIL-2

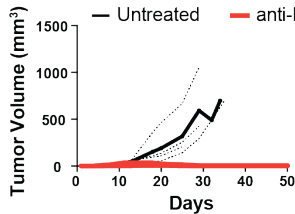


Fig. 2.S9. Comparison of alternative strategies to deliver IL-2 to enhance T cell cytotoxicity against tumors.

Tumor growth curves corresponding to Figure 3. KPC CD19+ pancreatic tumors were engrafted subcutaneously into immunocompetent C57/B16 mice and treated 9 days later with T cells as labeled. Plotted is individual (dash line) and mean (solid line) growth curves for each cell design compared to matched untreated mice. n=4,5 per group.

(A) 1e6 anti-Mesothelin CAR T cells with no additional IL-2.

(B) 2e6 anti-Mesothelin CAR T cells with systemic IL-2 administered at high dose (250,000 to 750,000 IU/mL) twice daily intraperitoneally for 7 days.

(C) 1e6 anti-Mesothelin CAR T cells engineered to constitutively express mIL-2 using a PGK promoter.

(D) 1e6 anti-Mesothelin CAR T cells engineered to inducibly express mIL-2 under the control of a NFAT promoter.

(E) 1e6 anti-Mesothelin CAR T cells engineered to inducibly express mIL-2 under the control of an anti-CD19 synNotch.

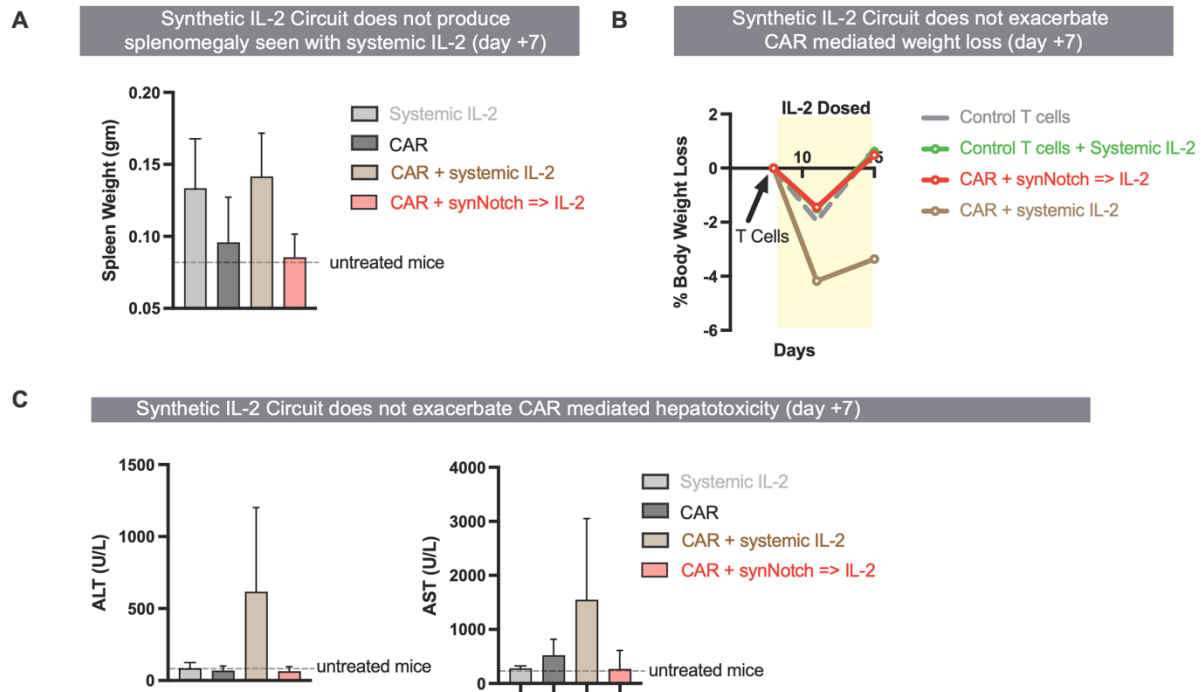


Fig. 2.S10. Evaluating toxicity: SynNotch-->IL-2 circuit does not produce systemic toxicity or worsen CAR toxicities.

To assess potential toxicity of a synthetic IL-2 circuit, C57/B16 mice were engrafted with KPC CD19+ tumors sub-cutaneously and given either 2e6 control untransduced T cells +/- systemic IL-2, 2e6 anti-Mesothelin CAR T cells +/- IL-2, or 2e6 anti-Mesothelin CAR T cells with an anti-CD19 SynNotch => IL-2 circuit. Systemic human IL-2 was given at high dose (250,000 to 750,000 IU/mL) twice daily intraperitoneally for 7 days. 7 days after T cell treatment, 3-5 mice per group were sacrificed for analysis of toxicity measurements and the remaining mice were monitored for survival.

(A) Systemic IL-2 caused splenomegaly in all mice, but no splenomegaly was seen with the synthetic cytokine circuit. This IL-2 mediated toxicity was seen in presence or absence of anti-Mesothelin CAR T cells.

(B) Systemic IL-2 combined with the anti-mesothelin CAR also induced a more profound weight loss in mice when compared with CAR T cells combined with a synthetic IL-2 circuit or systemic IL-2 only, again suggesting that systemic IL-2 can exacerbate CAR T cell toxicities.

(C) Systemic IL-2 combined with CAR T cell therapy produced significant hepatotoxicity (as measured by ALT and AST) in mice that received CAR and systemic cytokine. No similar toxicity was seen with systemic IL-2 only or when CAR was combined with a synthetic IL-2 circuit. This suggests that systemic IL-2 can exacerbate CAR T cell toxicities, which may include on-tumor/off-target CAR t cell reactions against normal tissue (liver).

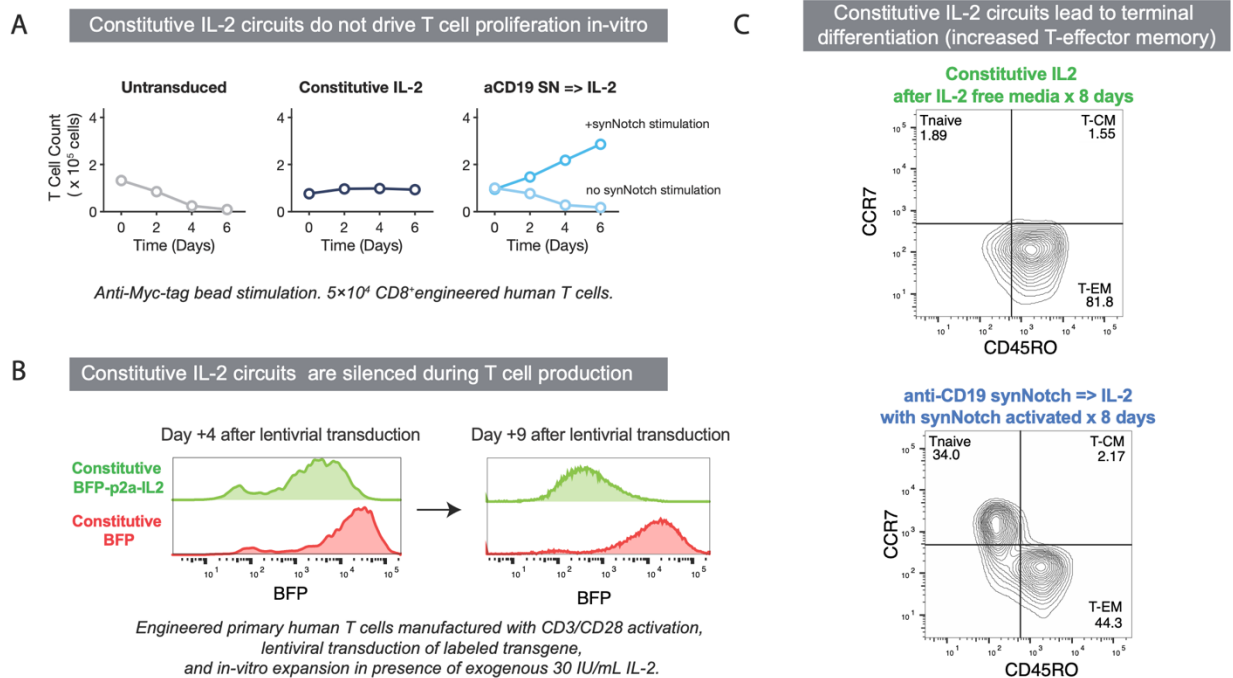


Fig. 2.S11. Comparison of effect of constitutive vs inducible IL-2 on T cell behavior.

(A) Primary human T cells that were either unmodified, engineered to express a constitutive sIL-2 payload (PGK promoter) or an anti-CD19 synNotch inducible sIL-2 were assessed for their ability to autonomously proliferate in IL-2 free media as in Figure 2.1. Constitutive IL 2 production led to cell survival but not expansion, when compared to synNotch inducible IL-2 production.

(B) sIL-2 expression from human T cells was approximated by use of co-expressed BFP marker (using a 2a element with a PGK promoter). During 5 days of in-vitro culture significant silencing of BFP marker was seen for the BFP-p2a-IL2 plasmid but not for a BFP only plasmid expressed in matched T cells, suggesting constitutive IL-2 circuits are selected against.

(C) Primary human T cell differentiation was approximated using surface marker staining for CCR7 and CD45RO. Constitutive IL-2 production led to almost all cells being in a CD45RO⁺CCR7⁻ effector memory state. In comparison matched T cells expressing an anti-CD19 synNotch => IL-2 circuit that was triggered using anti-myc beads (synNotch receptor is myc tagged) show far less terminal differentiation and maintenance of a CD45RO⁺CCR7⁺ naive population.

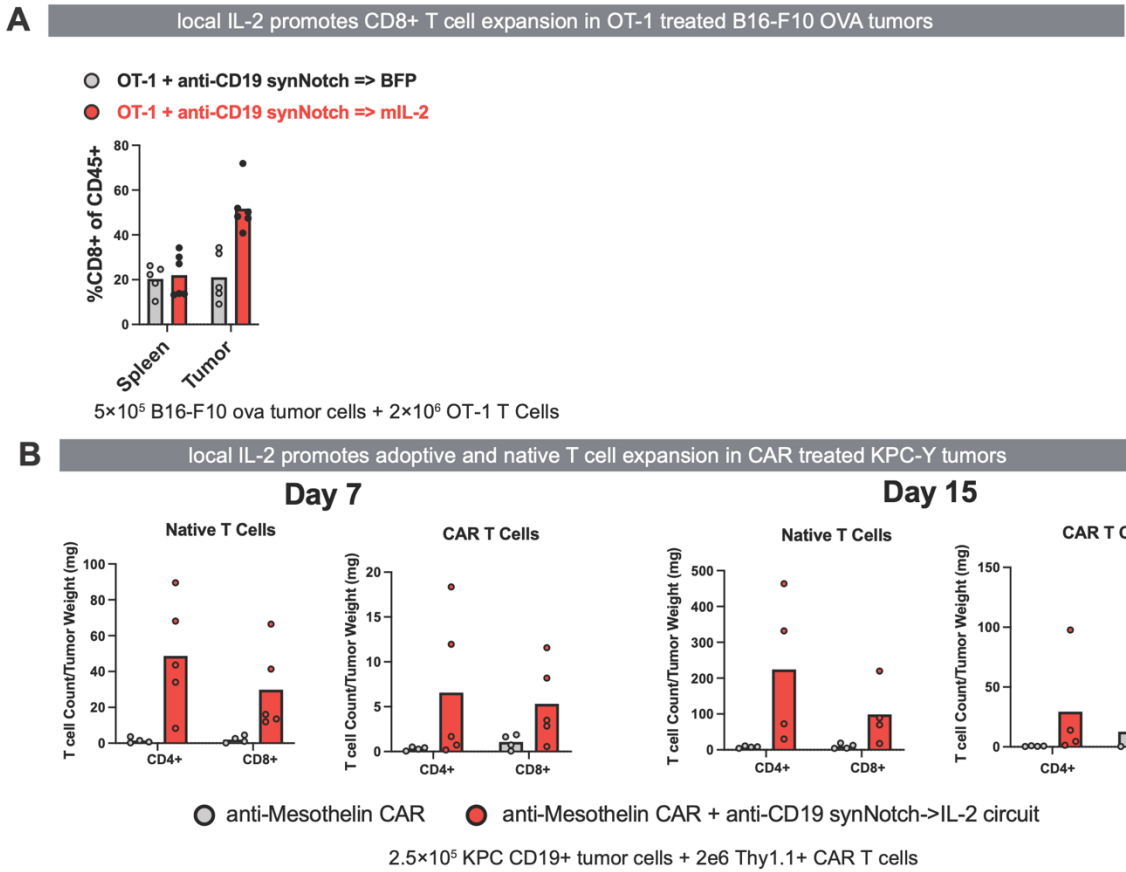


Fig. 2.S12. Enhanced local infiltration of T cells in immunocompetent melanoma and pancreatic tumors.

(A) B16-F10 OVA tumors expressing the synNotch target ligand CD19 were treated with 2e6 dose of OT-1 T cells 8 days after tumor implantation. T cells were engineered with anti-huCD19 SynNotch expressing either mIL2 (synthetic cytokine circuit) or irrelevant payload (effLuc or BFP). Tumor size was monitored, and tumors and spleens were collected at indicated endpoint and fraction of CD45+ cells expressing CD8 were calculated.

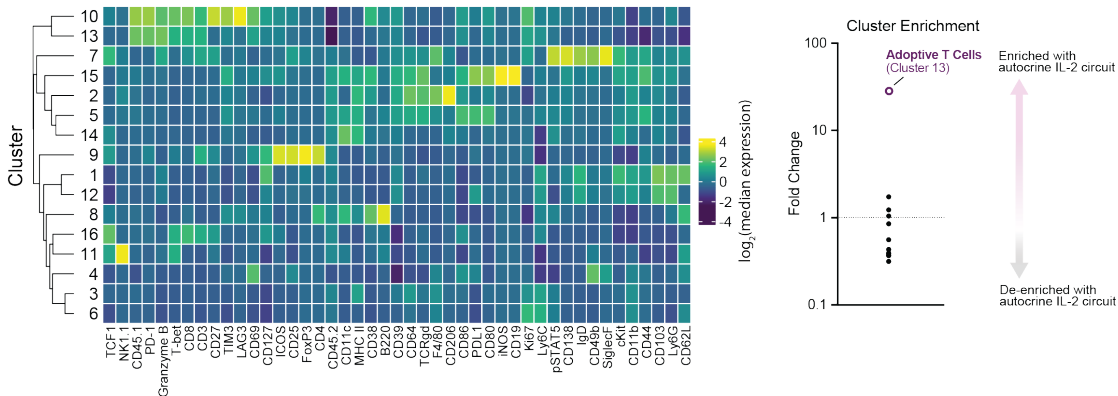
(B) KPC tumors were engrafted sub-cutaneously and treated on tumor day 9 with 2e6 engineered CD3+ mouse T cells. Tumors were collected 7 days and 15 days after T cell treatment and analyzed by flow cytometry for T cell infiltration (CD4 and CD8) from either native (Thy1.2) or adoptive/CAR (Thy1.1) origin. Data is plotted as T cell count per milligram of tumor analyzed.

A

mean marker expression for clusters used in phenograph plots in Figure 5

CyTOF PROFILING OF KPC PANCREATIC TUMORS

Unsupervised clustering, Day 9 after treatment, Mean marker expression for each Phenograph cluster Matching Figure 4C.

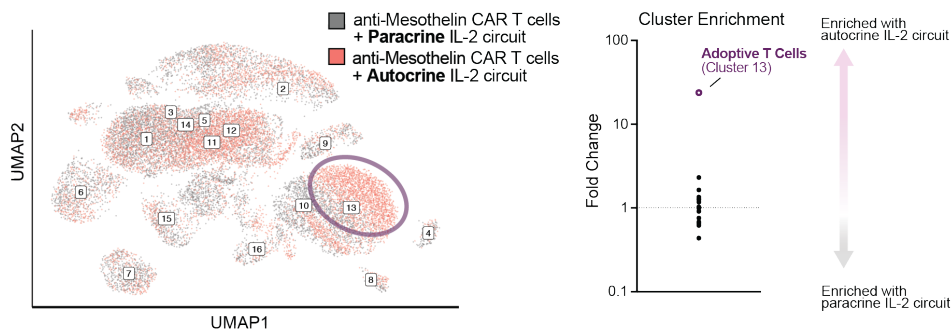
**B**

Autocrine IL-2 circuit shows enrichment of activated CAR T cells not seen with paracrine circuit.

CyTOF PROFILING OF KPC PANCREATIC TUMORS (AUTOCRINE VS PARACRINE SYNNOTCH-IL-2 CIRCUITS)

Unsupervised clustering, Day 9 after treatment

Paracrine IL-2 circuit vs Autocrine IL-2 circuit (mean marker expression as above)

**Fig. 2.S13. CyTOF analysis of autocrine and paracrine IL-2 circuits in KPC tumors.**

(A) As in Figure 2.4, KPC CD19* tumors were engrafted sub-cutaneously and treated on tumor day 9 with 2e6 engineered CD3+ T cells as labelled. Tumors were collected 9 days after T cell treatment and analyzed by CyTOF. Shown is a heatmap with marker expression for individual unsupervised clusters by Phenograph of CD45+ cells collected from the tumors (see Figure 5B). Marker expression is shown as the log₂ of median expression (normalized to the median of each marker). Enrichment was only seen in adoptively transferred CAR T cells when the synthetic IL-2 circuit was engaged (purple circles, $P < 0.0001$ one-way ANOVA).

(B) Here a UMAP spatial projection is shown comparing anti-Mesothelin CAR T cells with a paracrine IL-2 circuit (a second cell is engineered with the synNotch => mIL-2 circuit) to the autocrine circuit (the same cell expresses both synNotch and CAR receptors). The autocrine circuit shows enrichment of the adoptive T cells only (see panel A for mean marker expression of each phenograph cluster).

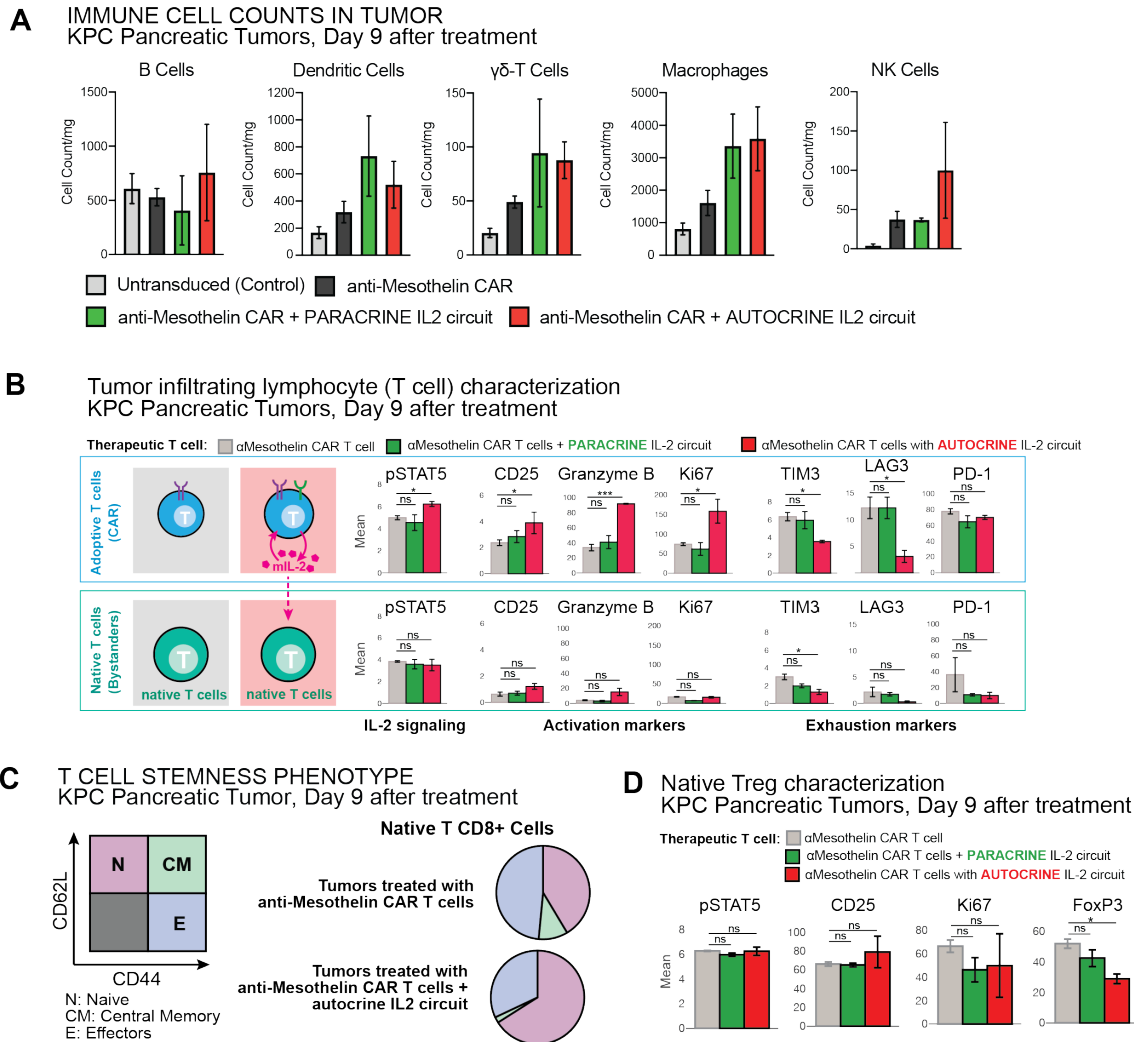


Fig. 2.S14. CyTOF analysis of treated KPC pancreatic tumors

(A) As in Figure 2.4, KPC CD19* tumors were engrafted sub-cutaneously and treated on tumor day 9 with 2e6 engineered CD3+ T cells as labelled. Tumors were collected 8 days after T cell treatment and analyzed by CyTOF. Shown is cell counts as determined by manual gating (n=3). All counts are normalized by tumor weight, compare to Figure 2.5A.

(B) KPC CD19* tumors were analyzed by CyTOF as in (A). IL-2 signaling markers (pSTAT5), activation markers (CD25, Granzyme B, Ki67) and exhaustion markers (CD39, Tim3, Lag3, PD-1) in adoptive/CAR T cells (CD45.1) compared to native/endogenous T cells (CD45.2). Adoptive T cells show increased IL-2 signaling, activation, and reduced exhaustion when combined with a synthetic IL-2 circuit in autocrine but not paracrine. Native T cells shows minimal activation or exhaustion in all circuits. Statistical significance was tested using a two-tailed Student's t test [not significant (ns) > 0.05, *P < 0.05, ***P < 0.001] comparing to αMesothelin CAR T cell only.

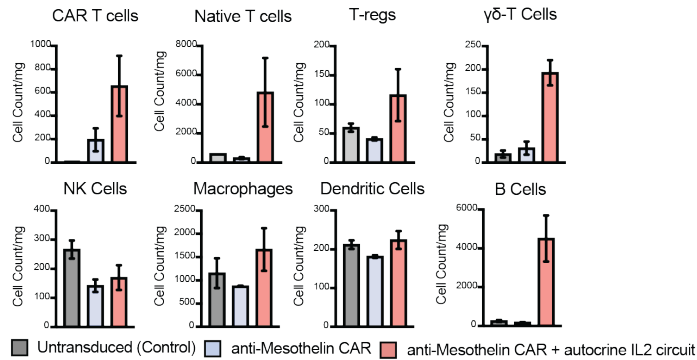
(C) KPC CD19⁺ tumors were analyzed by CyTOF as in (4). Native T cell phenotype was analyzed and showed that the majority of native T cells are in a naive (non-antigen experienced phenotype) state when a synthetic IL-2 circuit was administered.

(D) KPC CD19⁺ tumors were analyzed by CyTOF as in (A). Markers (pSTAT5, CD25, Ki67, FoxP3) in native Tregs are shown. Statistical significance was tested using a two-tailed Student's t test [not significant (ns) > 0.05, *P<0.05]

A

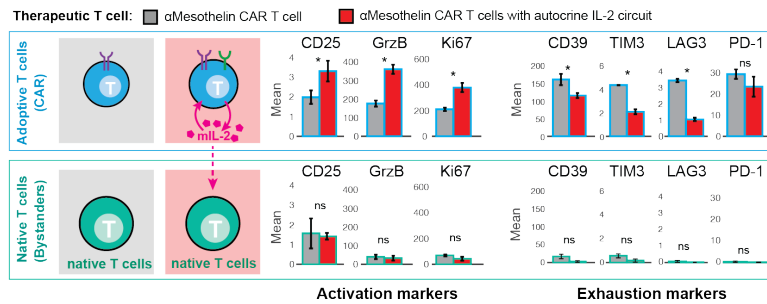
Establishing reproducibility of CyTOF data with repeat run.

Repeat CYTOF run, similar to Figure S13, IMMUNE CELL COUNTS IN TUMOR KPC Pancreatic Tumors, Day 8 after treatment



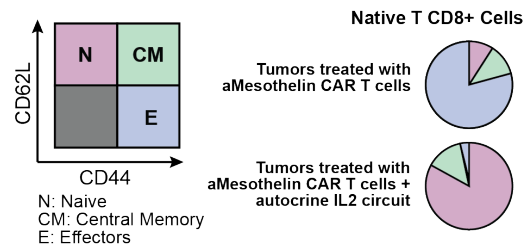
B

Tumor infiltrating lymphocyte (T cell) characterization KPC Pancreatic Tumors, Day 8 after treatment



C

T CELL STEMNESS PHENOTYPE Repeat CYTOF run KPC Pancreatic Tumor, Day 8 after treatment



D

Native Treg characterization KPC Pancreatic Tumors, Day 8 after treatment

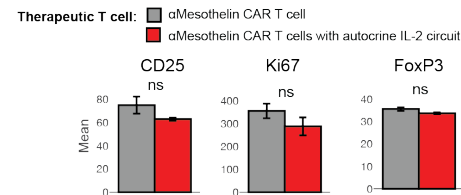


Fig. 2.S15. Repeat CyTOF analysis of treated KPC pancreatic tumors

(A) As in Sup Fig 2.14, KPC CD19+ tumors were engrafted sub-cutaneously and treated on tumor day 9 with 2e6 engineered CD3+ T cells as labelled. On this repeat experiment tumors were collected 8 days after T cell treatment and analyzed by CyTOF. Shown are cell counts that were determined by manual gating (n=2). All counts are normalized by tumor weight.

(B) KPC CD19+ tumors were analyzed by CyTOF as in (A). Exhaustion markers (CD39, Tim3, Lag3, PD-1) showed low expression on endogenous CD8+ T cells. Statistical significance was tested using a two-tailed Student's t test [not significant (ns) > 0.05, *P < 0.05, ***P < 0.001].

(C) KPC CD19⁺ tumors were analyzed by CyTOF as in (4). Native T cell phenotype was analyzed and showed that the majority of native T cells are in a naive (non-antigen experienced phenotype) state when a synthetic IL-2 circuit was administered.

(D) KPC CD19⁺ tumors were analyzed by CyTOF as in (A). Markers (pSTAT5, CD25, Ki67, FoxP3) in native Tregs are shown. Statistical significance was tested using a two-tailed Student's t test [not significant (ns) > 0.05, *P<0.05]

A CyTOF PROFILING OF **SPLEENS**
Unsupervised clustering, Day 9 after treatment
CAR only vs Autocrine IL-2 circuits

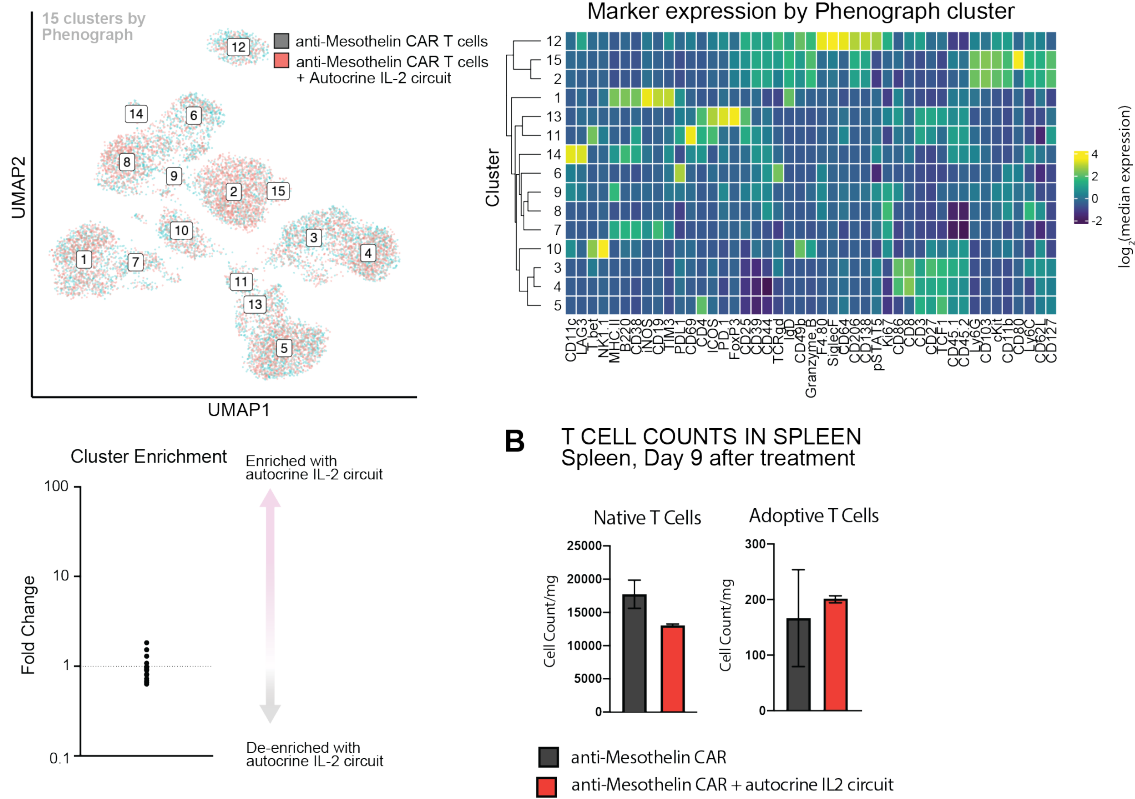
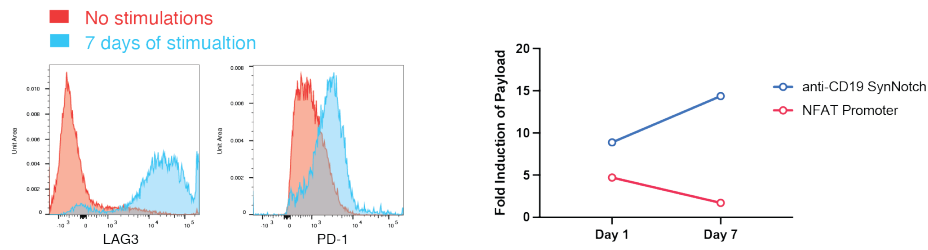


Fig. 2.S16. CyTOF analysis of spleens in mice treated.

(A) As in Figure 2.5, KPC CD19+ tumors were engrafted sub-cutaneously and treated on tumor day 9 with 2e6 engineered CD3+ T cells as labelled. Spleens were collected 9 days after T cell treatment and analyzed by CyTOF. Shown is unsupervised analysis of CyTOF data from the spleens. UMAP shown for spleens in mice treated by anti-Mesothelin CAR +/- IL-2 circuit (autocrine). Labelled numbers indicate clusters by Phenograph. a heatmap with marker express for individual unsupervised clusters by Phenograph of CD45+ cells collected from the spleens is on the right. Marker expression is shown as the log 2 of median expression (normalized to the median of each marker).

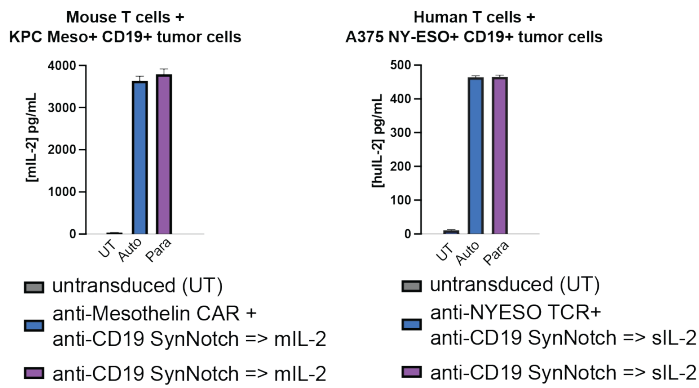
(B) CyTOF counts of native (CD45.2)+ and adoptive/CAR (CD45.1)+ T cells in the spleens of mice as in (panel A) shows no proliferation of T cells outside the tumor micro-environment.

A Synthetic Cytokine Circuits are Resistant to Exhaustion

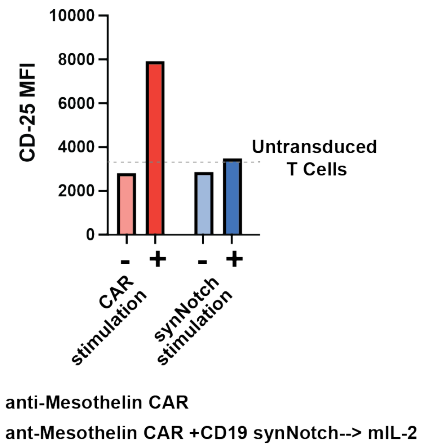


OT-1 T cells were serially exposed to B16F10 OVA tumor cells over 7 days, and ability to induce a reporter (BFP) payload measured before and after stimulation.

B Autocrine and paracrine circuits produce similar amounts of IL-2



C CAR but not SynNotch activation upregulates CD25



D synNotch => mIL-7 or mIL-15 circuits are not active in syngeneic tumor models

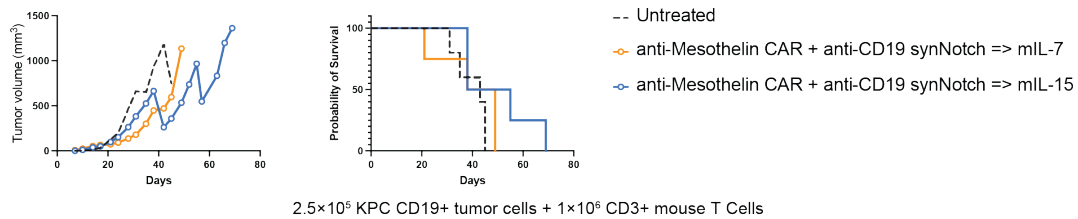


Fig. 2.S17. Estimation of synthetic cytokine circuit strength and induction of CD25

(A) OT-1 T cells with either an anti-CD19 SynNotch => BFP or PNFAT => BFP circuit were co-cultured with B16F10 OVA CD19+ tumor cells for 7 days at a 1:1 ratio. Every 2 days T cells were collected, counted, and re-challenged with fresh B16-F10 OVA CD19+ tumor cells to induce T cell exhaustion. After 7 days exhaustion was measured by cell surface staining for Lag3 and PD1 (as shown) and ability of inducible promoters to drive targeted payload (BFP) measured by flow cytometry.

(B) 50,000 mouse T cells as indicated were co-cultured with 50,000 CD19+ KPC tumor cells and supernatant collected and analyzed by ELISA for expression of mouse IL-2. For human T cells experiments: 50,000 human T cells as indicated were co-cultured with 50,000 CD19+ A375 tumor cells and supernatant collected and analyzed by ELISA for expression of human IL-2.

(C) 50,000 mouse T cells as indicated were cultured with or without stimulation for 48 hours and CD25 expression measured by flow cytometry. CAR T cells were stimulated with 50,000 CD19+ KPC tumor cells; myc-tagged SynNotch T cells were stimulated with anti-myc beads. CD25 was only upregulated when CAR was activated.

(D) Mouse T cells were engineered with an anti-CD19 SynNotch => mIL-7 or anti-CD19 SynNotch => mIL-15 circuit as labelled and used to treat sub-cutaneously engrafted KPC CD19+ tumors (as in Figure 2.2). On left tumor growth curves are shown and on the right mouse survival is plotted.

Chapter 3 – Engineering synthetic suppressor T cells capable of locally targeted immune suppression

Authors: Nishith R. Reddy¹⁻², Hasna Maachi³, Yini Xiao³, Milos S. Simic¹⁻², Wei Yu¹⁻², Daniela A. Cabanillas¹⁻², Yurie Tonai¹⁻², Audrey V. Parent³, Matthias Hebrok³, Wendell A. Lim¹⁻²

Affiliations:

¹ UCSF Cell Design Institute; University of California San Francisco, San Francisco, CA 94158, United States.

² Department of Cellular and Molecular Pharmacology, University of California San Francisco; San Francisco, CA 94158, United States

³ Diabetes Center, University of California San Francisco, San Francisco, CA, USA.

Abstract:

The immune system achieves homeostasis through the interplay of inflammatory and tolerance responses. Recent advances in cell therapy have demonstrated the ability to engineer user-targeted inflammatory or cytotoxic responses, as in the case of CAR T cells engineered to kill tumors. Here we attempt the converse: engineering user-targeted suppressor cells that can protect specific tissues from immune attack. We show that CD4⁺ T cells can be engineered to be effective suppressors by using synNotch receptors to drive expression of diverse anti-inflammatory cytokines (e.g. IL-10 or TGFβ1), inhibitory factors (e.g. PD-L1), as well as inflammatory cytokine sinks

(e.g. high affinity IL-2 receptor, CD25). These designer suppressor cells are activated by a synNotch-recognized antigen, and thus block CAR T killing in a localized manner, without causing systemic suppression. We show that synthetic suppressor cells can be used in conjunction with CAR T cells to create robust NOT-gate tumor killing circuits. The suppressor cells can also protect transplanted beta-cell organoids from cytotoxic T cell attack. Engineered suppressor cells are a complementary set of tools for sculpting local immune microenvironments in ways that could be applied to treat autoimmunity, prevent organ rejection, or block off-target CAR T toxicity.

Contributions to This Chapter: My contribution to this work was in all experiments, analysis, and writing other than those indicated. Other contributions: Wei Yu and Yurie Tonai contributed to tumor measurements, T cell I.V. injections in mice, and glucose challenge experiments in Fig. 3.3, 3.S3, 3.5. Hasna Maachi, Yini Xiao, and Audrey V. Parent contributed to all hPSC-derived islet differentiation and transplantation in Fig. 3.4, 3.5, 3.S4, 3.S5. Daniela A. Cabanillas contributed to ELISA experiments in Fig. 3.2, 3.S1, and 3.S2. Wendell A. Lim, Matthias Hebrok, and Milos Simic were involved in the conceptualization of the project.

INTRODUCTION

Immune homeostasis requires a complex balance between inflammation and tolerance signals within tissues. In recent years, there have been advances in cell therapies capable of driving user-directed inflammation or cytotoxic activity, such as with chimeric antigen receptor (CAR) T cells directed against cancer [1]. The converse, suppressors cells capable of locally targeted immune suppression, has the potential to downregulate improper immune activation and maintain tolerance within inflamed tissues. This cellular toolkit for targeted immune suppression could remodel immune microenvironments in many inflammatory or autoimmune disorders without the toxicities associated with systemic immune suppression.

What are minimal requirements for making immune suppressor cells? Synthetic reconstitution of immune suppressive signals allowed us to identify features that are sufficient for effective immune suppression. Here, we engineer synthetic suppressor T cells by using synthetic Notch (synNotch) induction circuits to reconstitute immune suppressive functions in human CD4⁺ T cells. SynNotch receptors are chimeric receptors that consist of an extracellular recognition domain, cleavable transmembrane Notch-based domain, and intracellular transcription factor. Binding to cognate antigen induces intramembrane receptor cleavage that releases a synthetic transcription factor domain capable of inducing transcription of a target transgene [2-4]. Since these engineered T cells require a synNotch antigen to trigger production of suppressive payloads, they can act in a locally targeted manner. These synthetic suppressor T cells could be programmed to target immune suppression in diverse contexts and have the potential to be highly customized for particular therapeutic applications.

By exploring a diverse library of synNotch-induced payloads and combinations thereof, we designed suppressor T cell circuit capable of locally blocking strong cytotoxic T cell responses, such as those induced by CAR T cells, both in vitro and in vivo. Importantly, these synthetic suppressor T cells can block CAR T cells locally in two tumor models without causing systemic suppression. The most effective synthetic suppressor T cell circuits recapitulated key features of other immune suppressor cells such as regulatory T cells (Tregs) by acting as both a sink for pro-inflammatory cytokine IL-2 and a source of suppressive cytokines like IL-10 or TGF β 1.

Combining synthetic suppressor T cells with CAR T cells enables the design of effective multicellular NOT-gate tumor killing circuits for specific targeting of tumors. These circuits are capable of blocking off-target CAR T cell toxicity without compromising on-target tumor killing. In addition, we explored whether these suppressor cells could protect transplanted organs, such as human pluripotent stem cell (hPSC)-derived islet-like organoids, from cytotoxic T cell killing. We found that these T cell circuits could protect islet-like organoid transplants in an antigen-specific manner and also maintain endocrine signaling by the transplanted organoid in vivo. These results demonstrate the potential of synthetic suppressor T cells as a therapeutic platform for locally target immune suppression that could be applied to treat allogeneic transplant rejection, autoimmunity, or block off-target CAR T cell toxicity.

RESULTS

Engineering synthetic suppressor T cells that inducibly produce suppressive payloads

To design T cells capable of antigen-induced production of suppressive payloads, we used a synthetic Notch (synNotch) receptor to induce transcription of a custom transgene. Here, we built a circuit in primary human CD4⁺ T cells using an anti-CD19 synNotch receptor to induce the production of a custom immune suppressive payload upon recognition of model antigen, CD19. Engineered CD4⁺ T cells - *synthetic suppressor T cells* - can induce a diverse library of suppressive payloads including suppressive cytokines (e.g. IL-10, TGF β 1, IL-35), inflammatory cytokine sinks (e.g. CD25, sTNF α R), inhibitory receptors (e.g. PD-L1, CTLA4, CD39), and proliferative cytokines (e.g. IL2). CD4⁺ T cells with synNotch induction circuits produce suppressive payloads at high levels, comparable to those produced by stimulated FoxP3⁺ polyclonal regulatory T cells in vitro (Fig. 3.S1A).

We screened the ability of these synthetic suppressor T cells producing various payloads to suppress CD4⁺ and CD8⁺ CAR T cell proliferation and killing of target cells in vitro (Fig. 3.1A). Synthetic suppressor cells were co-cultured with anti-Her2 CAR T cells and target cells (K562) that express both a model CAR antigen (Her2) and synNotch antigen (CD19). Suppressor cells producing either IL-10, TGF β 1, or PD-L1 suppressed the expansion of CD4⁺ CAR T cells, while induced production of TGF β 1 or PD-L1 suppressed the expansion of CD8⁺ CAR T cells in vitro (Fig. 3.1B). Other SynNotch-induced payloads failed to show significant changes in the expansion of CAR

T cells in vitro. Particular suppressive cytokines such as IL-10 only impact CD4+ CAR T cells, but not CD8+ CAR T cells, whereas other cytokines such as TGF β 1 suppresses both CD4+ T cells and CD8+ CAR T cells (Fig. 3.S1C).

Combination suppressor payloads yield strongest CAR T suppression

Synthetic suppressor cells can be engineered to induce the production of combinations of payloads. We engineered human primary CD4+ T cells using dual lentiviral transduction, where each lentivirus introduces one synNotch-induced custom transgene. We engineered suppressor cells that produce all 55 unique pairwise combinations of suppressive payloads from the payload library. The ability of suppressor cells to block CD4+ CAR T cell or CD8+ CAR T cell expansion and cytotoxicity was evaluated in vitro in a co-culture with target cells. The most effective circuits for suppression of CD4+ CAR T cells induced both an IL-2 sink (CD25) and an inhibitory cytokine (TGF β 1 or IL-10) or inhibitory receptor (PD-L1). The most effective circuit for suppression of CD8+ CAR T cells induced both TGF β 1 + CD25. Induction of each payload alone failed to drive strong suppression (Fig. 3.1C).

These synNotch circuits reconstitute minimal features for strong CAR T suppression in vitro, particularly the combination of an inhibitory cytokine (*source*) with CD25 (*sink*). The combined induction of TGF β 1 and CD25 outperforms each payload alone at suppressing CD8+ CAR T cells in vitro (Fig. 3.2A). This circuit also significantly reduces the accumulation of IL-2 produced by stimulated CD4+ T cells (Fig. 3.2B; Fig S2B). We tested different initial doses of suppressor cells in the in vitro co-cultured and assessed suppression of CD8+ CAR T cell expansion and cytotoxicity on target cells.

Circuits that make a combination of TGF β 1 and CD25 increase the amplitude and reduced the EC50 of suppression required for suppression of CD8+ CAR T cell expansion and target cell protection compared to each individual payload (Fig. 3.2C). The combined induction of IL-10 and CD25 was also effective at suppressing the expansion and cytotoxicity of CD4+ CAR T cells (Fig. 3.2A).

Separation of these functions into a two-cell system, where one suppressor cell produces CD25 and another produces TGF β 1, fails to drive the same level of CAR T cell suppression as a one-cell system, where a single suppressor cell produces both TGF β 1 and CD25 (Fig. 3.2C). CD25 acts both as a sink for IL2 and drives proliferation when overexpressed in CD4+ T cells (Fig. 3.S1B). The addition of CD25 also drives higher levels of TGF β 1 than circuits that only induce TGF β 1 in vitro (Fig. 3.2D). CD25 can contribute to enhanced suppression by two mechanisms, both enhancing the consumption of IL-2 and driving proliferation of suppressor cells that increases TGF β 1 levels (Fig. 3.2E).

Synthetic suppressor cells locally inhibit T cell killing in vivo without systemic suppression in vivo

We tested the ability of synthetic suppressor cells to locally suppress immune responses in a two-tumor mouse model. In this model, we implanted K562 tumors into two flanks of immunocompromised non-obese diabetic *scid* gamma (NSG) mice. Both tumors express a model antigen Her2 recognized by CAR T cells that kill the tumors, but only one tumor expressed the synNotch target antigen, CD19, recognized by the synthetic suppressor T cells (Fig. 3.3A). CAR T cells injected i.v. alone clear both

tumors. When synthetic suppressor T cells with synNotch \rightarrow TGF β 1+CD25 were co-injected with CAR T cells, we observed local, antigen-specific suppression of CAR T cell killing of the dual antigen tumor, without effecting clearance of the single antigen tumor. The individual payloads TGF β 1 or CD25 alone fail to protect the dual antigen tumor from CAR T cell killing in this model. These circuits show reduced expansion of both CD4+ and CD8+ CAR T cells as well as increased synthetic suppressor T cells in the dual antigen tumor (Fig. 3.3C).

Synthetic suppressor cell circuits with the synNotch \rightarrow TGF β 1 + CD25 circuit rely on paracrine signals for suppression. Therefore, we hypothesized that these circuits could overcome heterogeneity in synNotch priming antigen expression and protect bystander target cells by remodeling the local immune microenvironment. To assess whether these circuits could function with heterogeneous synNotch priming antigen, we mixed dual antigen (Her2+ CD19+) and single antigen (Her2+) target cells in vitro. When target cells are mixed such that 50% of the cells are dual antigen target cells and 50% are single antigen target cells, we observe that both types of target cells were able to expand in vitro at similar rates, suggesting that these circuits exhibit trans-protection of bystander target cells that do not express the synNotch antigen.

In the two-tumor mouse model in vivo, we assessed suppression with a varied percent of dual antigen target cells in an implanted tumor with a mix of different ratios of dual antigen and single antigen target cells. All mice were also injected subcutaneously with a single antigen tumor that lacked a synNotch priming antigen in the alternate flank. This single antigen tumor, which lacked the synNotch priming antigen, was cleared by CAR T cells in vivo in all cases. We observed effective local suppression of CAR T cell

killing of the tumor containing only 25% dual antigen target cells at the time of engraftment, while still observing clearance of the single antigen tumors in the opposing flank (Fig. 3.S3B).

Suppressor cells can yield NOT-gate tumor killing circuits

Off-target toxicity of CAR T cells that can recognize and attack healthy tissues expressing antigens similar to the target tumor antigen, remains a significant challenge. Boolean logic gates using synthetic molecular switches can be introduced into CAR T cells to increase their specificity and limit off-target toxicity. One example is inhibitory CAR (iCAR) receptors, which have been developed to block CAR T cell killing in an antigen-dependent manner. Unlike conventional CARs that only have activating domains, iCARs incorporate an inhibitory domain that is capable of blocking the intracellular signaling pathways that activates conventional CAR T cells [5]. However, in the two-tumor mouse model, CD8⁺ T cells engineered to co-expressing an anti-Her2 CAR and anti-CD19 PD-1 iCAR fail to block CAR T cell killing of the dual antigen tumor at the administered dose (Fig. 3.3D).

We propose the use of a multicellular NOT gate consisting of two cells: one CD8⁺ T cell expresses an anti-Her2 and a second synthetic suppressor T cell expressed an anti-CD19 synNotch→TGFβ1 + CD25 circuit. These multicellular NOT gates lead to more consistent suppression of the dual antigen tumor without blocking CAR T cell killing of the single antigen tumor. Synthetic suppressor cells can be directed to healthy tissue to block off-target CAR T cell toxicity without impacting the on-target

tumor killing. By minimizing the risk of off-target toxicity, synthetic suppressor T cell circuits could expand the repertoire of possible tumor antigens to target [6].

Synthetic suppressor cells can prevent T cell killing of islet-like organoids

We wanted to assess whether synthetic suppressor T cells could protect transplanted organs from T cell rejection. Transplantation of human pluripotent stem cells (hPSC)-derived islet-like organoids is an emerging therapy to replace dysfunctional or damaged islets in type 1 diabetes. However, these therapies often fail from immune rejection of the transplant [7].

We tested whether islet-like organoids could be protected from cytotoxic T cell attack using synthetic suppressor T cells. We differentiated enriched beta cell clusters (eBCs) from hPSCs [8] and engineered them to express a model antigen, CD19 (Fig. 3.4A). eBCs express GFP from the insulin promoter and are HLA-A2+ (Fig. 3.S4A, 3.S4B). Human CD8+ T cells expressing an anti-HLA-A2 CAR [9] can kill eBCs in vitro (Fig. 3.4B), while anti-PPI TCR was unable to kill eBCs (Fig. 3.S4C). The introduction of suppressor cells with an anti-CD19 synNotch → TGFβ1 + CD25 circuit protect CD19+ eBCs from CAR T cell killing and reduce caspase 3/7 reporter signal, while a control synNotch circuit inducing no payload fails to block CAR T cells of the eBCs (Fig. 3.4C).

We observed that suppressors with synNotch → TGFβ1 + CD25 circuits self-organized around CAR T cells during suppression in vitro. Single CAR T cells in contact with the eBCs can be surrounded by synthetic suppressor T cells (Fig. 3.4D). Recent studies have shown similar spatial organization of Tregs around effector T cells within lymphoid tissues plays a key role in their function. Within lymph nodes, Tregs are often

found in close proximity to effector T cells, forming microdomains that sets the threshold for inducing strong T cell activation to antigen [10-12]. This organization of suppressor cells could limit transmission of pro-inflammatory signals of between effector T cells such as IL-2 required to mount a strong immune response.

Synthetic suppressor cells can protect organoid transplants from cytotoxic T cell killing in vivo

To evaluate the potential of synthetic suppressor T cells to protect organoid transplants from cytotoxic T cell killing in vivo, beta cell organoids were transplanted into the kidney capsules of immunodeficient NSG mice (Fig. 3.5A). To mimic a transplant rejection scenario in which organoid transplants may be targeted by host cytotoxic T cells, anti-HLA-A2 CD4⁺ and CD8⁺ CAR T cells were injected i.v. to attack the transplanted beta cell organoids. The survival of the effLuc⁺ transplants was tracked by luciferase signaling in the presence or absence of suppressor cells with an anti-CD19 synNotch → TGFβ1 + CD25 circuit (Fig. 3.5B).

CAR T cells alone drove clearance of the CD19⁺ eBC transplant within 12 days in all cases (Fig. 3.5C). When synthetic suppressor T cells were co-injected i.v. with CAR T cells, CD19⁺ eBCs were protected from T cell killing in vivo (suppression observed in 6 of 8 replicates). To test antigen-specific suppression of cytotoxic T cell killing by synthetic suppressor cells, experiments were conducted with transplanted eBCs lacking the synNotch antigen, CD19 (Fig. 3.5D). We observed that suppression of T cell killing was dependent on the presence of the synNotch antigen, CD19⁺, on the

transplanted cells. No protect of CD19- eBC transplants was observed in the presence of CAR T cells and suppressor cells in all cases.

The functionality of the transplanted beta cell organoids protected by synthetic suppressor T cells was assessed following CAR T cell attack. Glucose challenge experiments were conducted to test the endocrine function of the transplanted beta cells at the endpoint 35 days after transplantation (Fig. 3.5E). Mice were fasted overnight prior to glucose injection. The blood c-peptide secretion under fasting conditions and 30 minutes post-glucose injection was measured to assess transplant function. Transplanted organoids were cleared by CAR T cells in the absence of synthetic suppressor cells and therefore had minimal c-peptide secretion in response to glucose. In the presence of synthetic suppressor T cells, transplants remained intact (Fig. 3.S4B) and functional despite CAR T cell attack. Synthetic suppressor T cells were able to both protect the beta cell organoids from cytotoxic T cell killing and maintain their endocrine function in vivo.

DISCUSSION

Diverse suppressive payloads can generate targeted suppressor T cell

We have developed a novel approach to generating synthetic suppressor T cells capable of locally targeted immune suppression. By engineering CD4+ T cells with synNotch induction circuits producing a diverse library of payloads, we identified minimal circuits inducing both CD25 and an inhibitory cytokine, either IL-10 or TGF β 1, were sufficient to drive strong local suppression of cytotoxic T cell killing in vitro and in

vivo. By requiring a synNotch antigen to trigger payload production, these T cell circuits enabled targeted immune suppression without systemic suppression.

The most effective circuits induced both TGF β 1 and CD25, which mimic key features of other suppressor cells like Tregs and could reflect critical signals they are required to achieve suppression. We found that circuit must produce both TGF β 1 and CD25 from the same cell for effective suppression. CD25 both contributes to increased local IL-2 consumption and drives more proliferation of suppressor cells, consequently driving more TGF β 1 accumulation locally. Separation of these functions into two cells could limit autocrine proliferation of suppressor cells required to drive increased TGF β 1.

Advantages to Tregs

Strategies for redirecting Treg to treat inflammatory disease face major challenges in their stability, ex vivo expansion, and targeting [13]. Synthetic suppressor T cells have several advantages to Treg therapies, as they are derived from human CD4⁺ T cells, making them easier to work with and target. By using synNotch circuits to induce suppressive responses, synthetic suppressor T cells are potentially more stable as they act independent of the Treg fate and bypass requirements of TCR signaling to induce immune suppressive responses. Additionally, these circuits are highly customizable. SynNotch receptor can be programmed to induce diverse payloads relevant for specific applications or disease indications, such as non-native or engineered suppressive cytokines or antibodies.

Synthetic suppressor cells as a general tool for targeted immune suppression

Synthetic suppressor T cells could be applied to sculpt immune environments in various contexts, including cancer NOT gates, transplant rejection, and autoimmune disease. For CAR T cell therapies against cancer, synthetic suppressor T cell NOT gates could be directed to healthy tissue, blocking off-target toxicity without compromising on-target tumor killing (Fig. 3.6A). Suppressor NOT gate circuits could enhance tumor recognition, expanding the set of possible antigen targets. In the context of allogeneic organ transplantation, synthetic suppressor T cells have the potential to locally protect transplants from host immune rejection (Fig. 3.6B). Synthetic suppressor T cells could be targeted to native or engineered transplant antigens to locally promote immune tolerance. Finally, these synthetic suppressor T cells could be used to block autoimmune diseases or acute inflammation. In autoimmune diseases such as type 1 diabetes or multiple sclerosis, synthetic suppressor T cells could be directed to damaged tissue such as the pancreatic islets or the central nervous system to suppress destruction by autoreactive host immune cells (Fig. 3.6C).

In summary, we reconstituted immune suppressive responses using synNotch circuits to generate designer suppressor cells, a therapeutic platform for targeting immune suppression. We demonstrated proof-of-principle that these synthetic suppressor cells can be applied with CAR T cells to design effective anti-tumor NOT gates and protect transplanted organs from T cell killing in vitro. Our findings suggest that synthetic suppressor cells may be extended to target immune suppression in a variety of contexts. Synthetic reconstitution offers a powerful approach to dissect

minimal requirements for immune suppression and to design effective therapeutic immune suppressor cells.

REFERENCES

1. Lim, W. A., June, C. H., The Principles of Engineering Immune Cells to Treat Cancer. *Cell*. **168**(4), 724-740 (2017).
2. L. Morsut, K. T. Roybal, X. Xiong, R. M. Gordley, S. M. Coyle, M. Thomson, W. A. Lim, Engineering Customized Cell Sensing and Response Behaviors Using Synthetic Notch Receptors. *Cell*. **164**, 780–791 (2016).
3. K. T. Roybal, L. J. Rupp, L. Morsut, W. J. Walker, K. A. McNally, J. S. Park, W. A. Lim, Precision Tumor Recognition by T Cells With Combinatorial Antigen-Sensing Circuits. *Cell*. **164**, 770–779 (2016).
4. Allen, G. M., Frankel, N.W., Reddy, N.R., Bhargava, H. K., Yoshida, M.A., Stark, S.R., Purl, M., Lee, J., Yee, J. L., Yu, W., Li, A.W., Garcia, K.C., El-Samad, H., Roybal, K.T., Spitzer, M.H., Lim, W.A, Synthetic cytokine circuits that drive T cells into immune-excluded tumors. *Science*, **378**, eaba1624 (2022).
5. Fedorov, V.D., Themeli, M., Sadelain, M., PD-1– and CTLA-4–Based Inhibitory Chimeric Antigen Receptors (iCARs) Divert Off-Target Immunotherapy Responses. *Sci. Trans. Med.* **5**(215), 215ra172 (2013).
6. Nair, G. G., Tzanakakis, E.S., Hebrok, M. Emerging routes to the generation of functional β -cells for diabetes mellitus cell therapy. *Nat. Rev. Endocrinol.*, **16**(9), 506–518 (2020).
7. Dannenfelser, R., Allen. G. M., VanderSluis, B., Koegel, A. K., Levinson, S., Stark, S. R., Yao, V., Tadych, A., Troyanskaya, O. G., Lim, W. A. Discriminatory Power of Combinatorial Antigen Recognition in Cancer T Cell Therapies. *Cell Systems*, **11**(3), p215-228.e5 (2020).

8. Nair, G.G., Liu, J.S., Russ, H. A., Tran, S., Saxton, M. S., Chen, R., Juang, C., Li, M., Nguyen, V. Q., Giacometti, S., Puri, S., Xing, Y., Wang, Y., Szot, G. L., Oberholzer, J., Bhushan, A., Hebrok, M. Recapitulating endocrine cell clustering in culture promotes maturation of human stem-cell-derived β cells. *Nat Cell Biol*, **21**(2), 263-274 (2019).
9. Muller, Y. D., Ferreira, L. M. R., Ronin, E., Ho, P., Nguyen, V., Faleo, G., Zhou, Y., Lee, K., Leung, K. K., Skartsis, N., Kaul, A. M., Mulder, A., Frans, H. J. C., Wells, J.A., Bluestone, J. A., Tang, Q. Precision Engineering of an Anti-HLA-A2 Chimeric Antigen Receptor in Regulatory T Cells for Transplant Immune Tolerance. *Front Immunol*, **12**, 686439 (2021).
10. A. Oyler-Yaniv, J. Oyler-Yaniv, B. M. Whitlock, Z. Liu, R. N. Germain, M. Huse, G. Altan-Bonnet, O. Krichevsky, A Tunable Diffusion-Consumption Mechanism of Cytokine Propagation Enables Plasticity in Cell-to-Cell Communication in the Immune System. *Immunity*, **46**, 609–620 (2017).
11. H. S. Wong, K. Park, A. Gola, A. P. Baptista, C. H. Miller, D. Deep, M. Lou, L. F. Boyd, A. Y. Rudensky, P. A. Savage, G. Altan-Bonnet, J. S. Tsang, R. N. Germain, A local regulatory T cell feedback circuit maintains immune homeostasis by pruning self-activated T cells. *Cell*. **184**, 3981 (2021).
12. T. Höfer, O. Krichevsky, G. Altan-Bonnet, Competition for IL-2 between Regulatory and Effector T Cells to Chisel Immune Responses. *Front. Immunol*, **3**, 268 (2012).
13. Raffin, C., Vo, L. T., Bluestone, J. A. Treg cell-based therapies: challenges and perspectives. *Nat Rev Immunol*, **20**, 158-172 (2020).

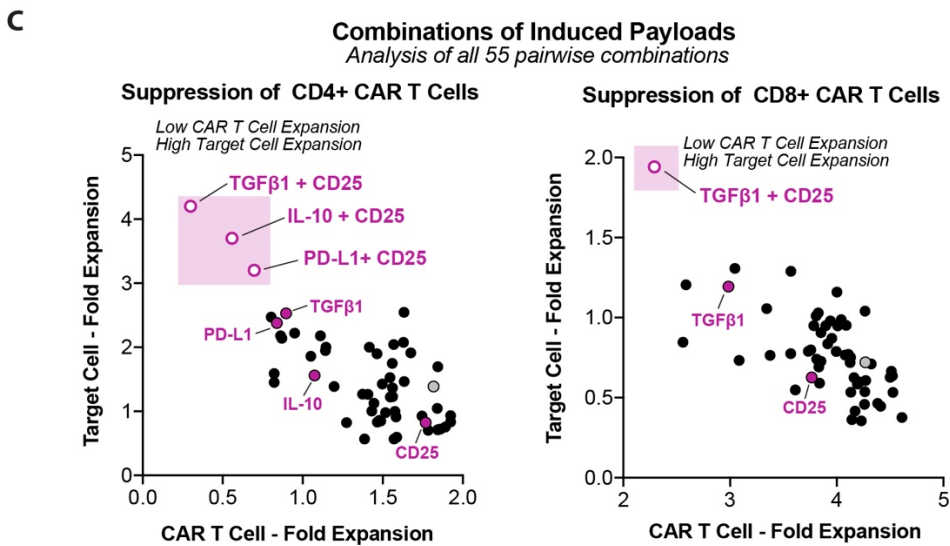
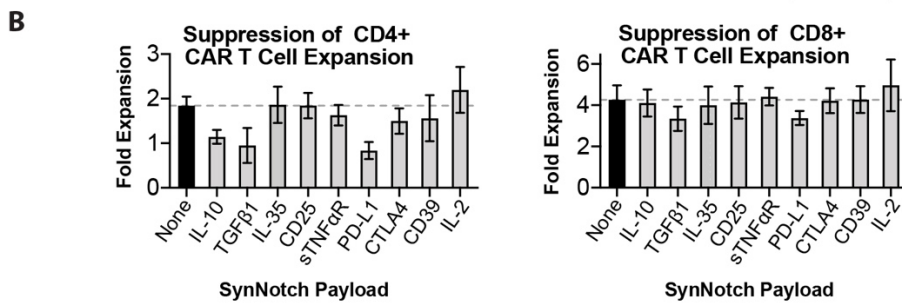
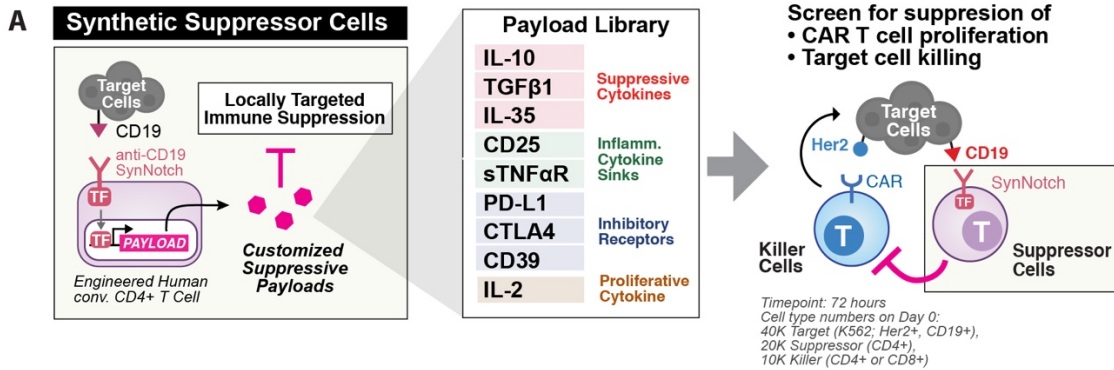


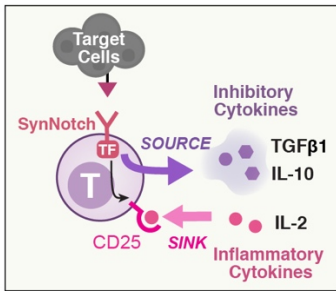
Figure 3.1. Engineering synthetic suppressor T cells that drive antigen-induced expression of immune suppressive payloads.

(A) Design of synthetic suppressor T cells that inducibly express suppressive payloads. These are human conventional CD4⁺ cells engineered to express synthetic Notch receptor that recognizes target cell antigen, and in response, induces expression of diverse payloads. Co-culture assay with CAR T cells and target cells was used to assess engineered cells ability to block CAR T cell proliferation and target cell killing.

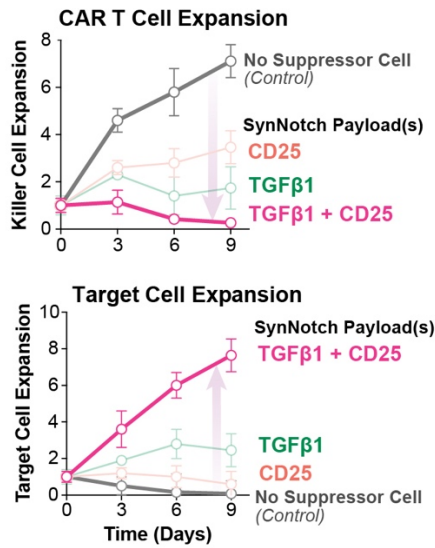
(B) As described in (A), suppression of expansion of CD4⁺ and CD8⁺ CAR T expansion over 72 hours by synthetic suppressor T cells inducing different synNotch payloads. Fold change normalized to the 0 hour timepoint.

(C) The expansion of K562 target cells (Her2⁺, CD19⁺) and CAR T cells is shown for both co-cultures of suppressor T cells and target cells with CD4⁺ and CD8⁺ CAR T cells. Each point indices a pairwise combination of payloads from the library in (A) induced by anti-CD19 SynNotch suppressor cell. Gray point is the no payload control.

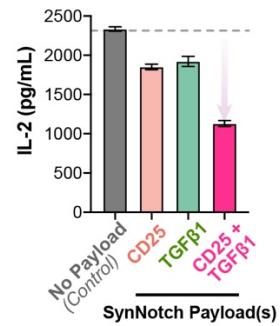
A Combination source & sink synthetic suppressor cell



Cell type numbers on Day 0:
40K Target (K562, Her2+, CD19+),
20K Suppressor (CD4+), 10K Killer (CD8+)

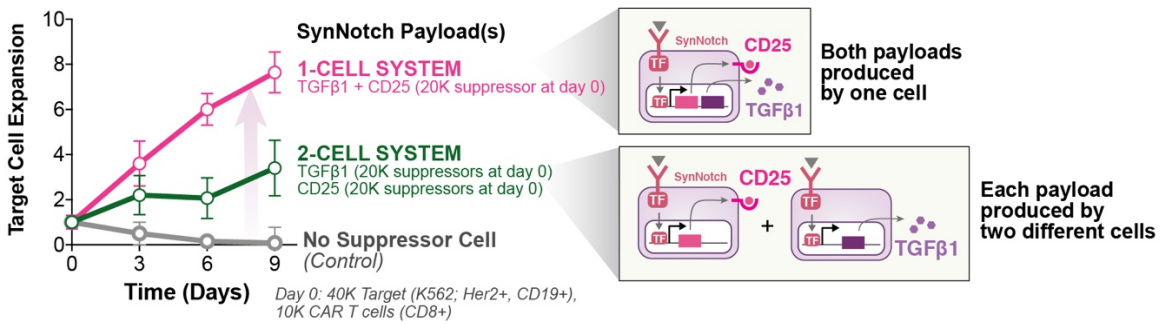


B Secreted IL-2 Levels (t = 48h)

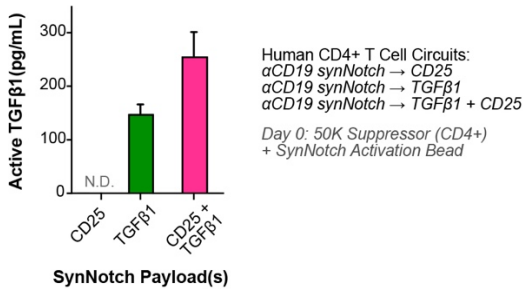


Cell type numbers on Day 0:
50K Suppressor (CD4+),
50K T Cells activated with
anti-CD3/CD28 beads (CD4+)

C Target cell expansion in the presence of CAR T cells



D TGFβ1 Secretion (t = 72h)



E Two mechanisms by which CD25 can contribute to synthetic suppressor cell activity

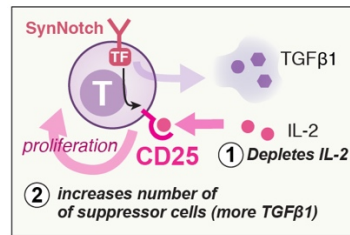


Figure 3.2. Combinatorial induction of both CD25 and TGFβ1 by the same suppressor cell leads to more effective suppression of CAR T cells in vitro.

(A) Synthetic suppressor T cells with synNotch circuits that induce a combination of TGFβ1 and CD25 are more potent at suppression of CD8+ CAR T cell activity to compared to each individual payload alone. CAR T cell and target cell expansion measured by flow cytometry.

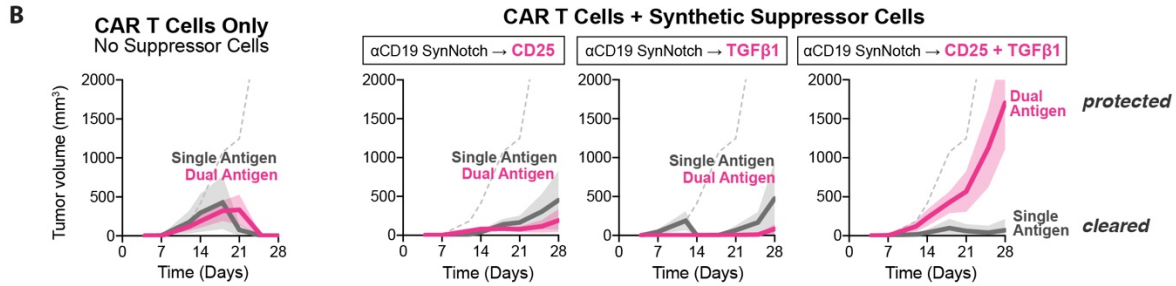
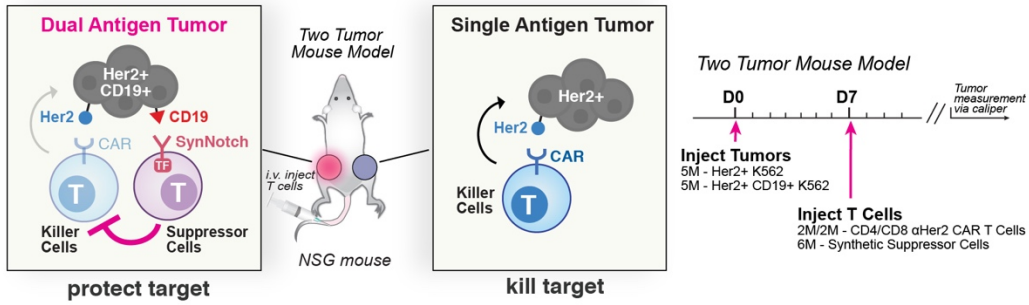
(B) Synthetic suppressor T cells block IL-2 accumulation produced by CD4+ T cells. Human CD4+ T cells activated anti-CD3/CD28 dynabeads for 24 hours were co-cultured with synthetic suppressor T cells activated with anti-myc dynabeads. The IL2 levels in the media supernatant was measured by ELISA (t = 48 hours).

(C) Separation of TGFβ1 and CD25 into two separate cells leads to less effective suppression of CD8+ CAR T cell killing than a one-cell system where both payloads are produced by the same suppressor T cell in vitro. The expansion of target cells was measured by flow cytometry.

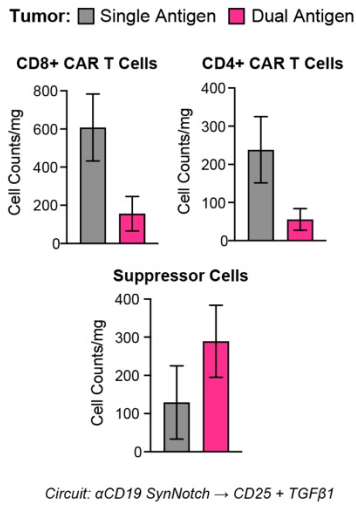
(D) Synthetic suppressor cells that induce a combination of TGFβ1 and CD25 leads to more TGFβ1 secretion than suppressor cells inducing TGFβ1 alone. TGFβ1 measured by ELISA of media supernatant (t = 72 hours).

(E) CD25 can enhance suppressor cell activity by two mechanisms: depleting IL2 and proliferation that increases suppressor cell number.

A Local Immune Suppression by Synthetic Suppressors



C T Cell Counts in Tumors (Day 14)



D NOT Gate Circuits (CAR Override)

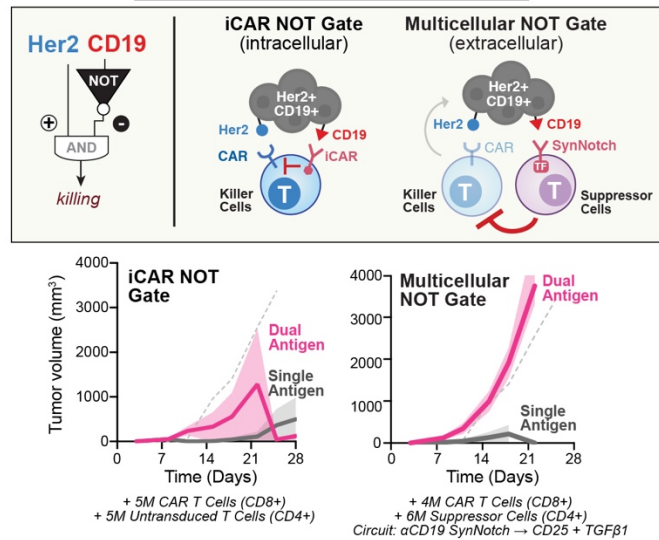


Figure 3.3. Synthetic suppressor cells block CAR T cell killing in vivo in locally targeted manner.

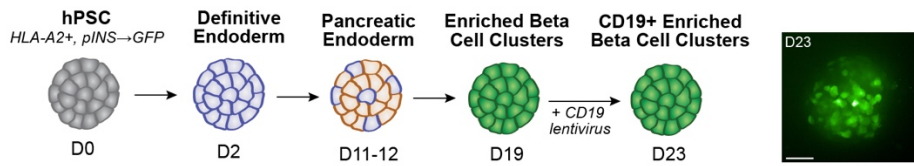
(A) Two tumor mouse model in NSG mice, where the right flank has a dual antigen tumor (Her2+ CD19+ K562 tumor) and the left flank has a single antigen tumor (Her2+ K562 tumor). Her2 is CAR target antigen, CD19 is synNotch target antigen. Human anti-Her2 CAR T cells can kill both tumors, while synthetic suppressor cells will only induce suppressive payloads in the CD19+ dual antigen tumor.

(B) Synthetic suppressors with anti-CD19 SynNotch circuits inducing both CD25 and TGF β 1 are effective at suppressing CAR T cell killing of the dual antigen tumor. Each individual payload was not sufficient for suppression in this model. Tumor measurements show as time after T cell injection.

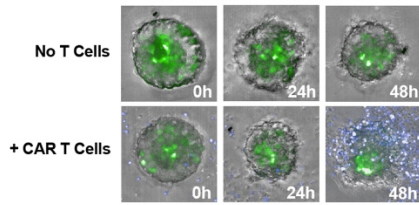
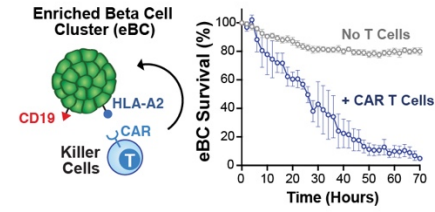
(C) Flow analysis of isolated tumors shows reduced expansion of both CD4+ and CD8+ CAR T cells and an increase in suppressor cells in the dual antigen tumor at day 14 after T cell injection.

(D) Multicellular NOT gate combining CAR T cells and synthetic suppressor T cells with differential recognition leads to stronger specific suppression than iCAR NOT circuit [5]. CAR T cells recognize and kill both tumors while synthetic suppressor T cells block killing in the dual antigen tumor.

A hPSC-derived Enriched Beta Cell Clusters

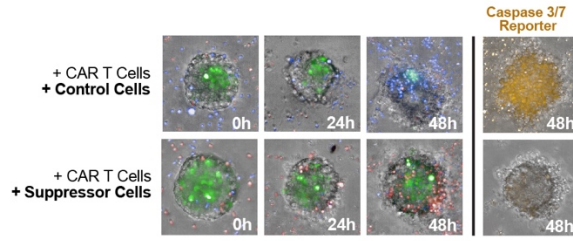
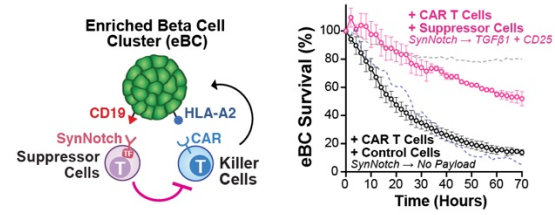


B T Cell Killing of Beta Cells *in vitro*



Cell type numbers at 0h: eBCs: 50 clusters;
CAR T cells (CD8+): 10K

C Suppressor Cell Protection of Beta Cells *in vitro*



Cell type numbers at 0h: eBCs: 50 clusters;
CAR T cells (CD8+): 10K; Suppressor cell (CD4+): 20K

D Spatial Organization of CAR and Suppressor T Cells

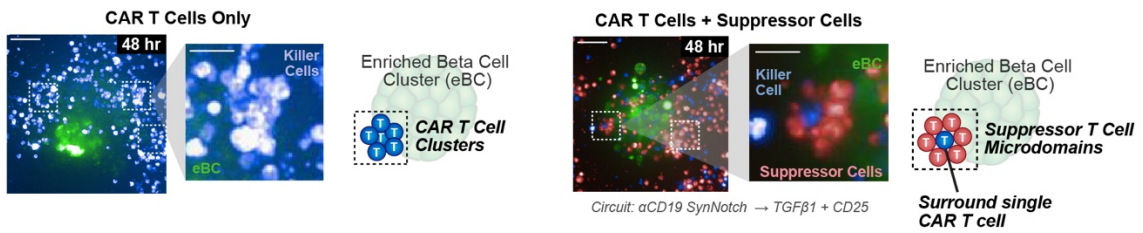


Figure 3.4. Synthetic suppressor cells protect beta cells from T cell-mediated destruction in vitro.

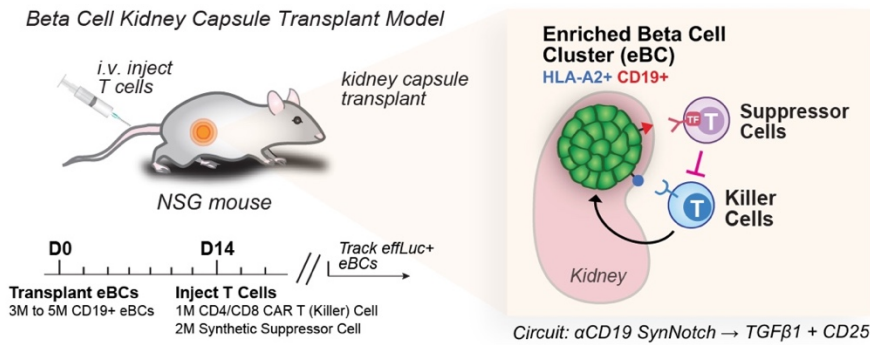
(A) Human enriched beta cell clusters (eBCs) are differentiated from human pluripotent stem cell (hPSC). eBCs can be engineered to express model antigen CD19 by lentiviral transduction. eBCs are HLA-A2⁺ and express GFP label from the insulin promoter.

(B) anti-HLA-A2 CAR T cells kill HLA-A2⁺ hPSC-derived beta cell (enriched beta cell clusters). Confocal microscopy (maximum projection images) shows that eBCs are destroyed with CAR T cells in vitro.

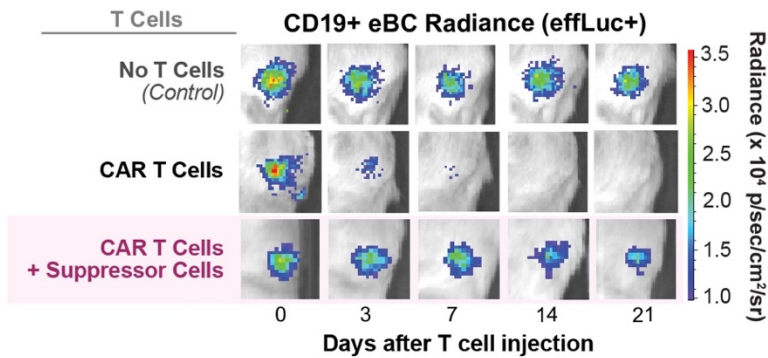
(C) As in (B), anti-HLA-A2 CAR T cell killing of eBCs can be blocked by synthetic suppressor T cells activated by anti-CD19 synNotch to induce TGF β 1 and CD25, but not a no payload control.

(D) Spatial analysis shows that synthetic suppressor cells expressing spatially self-organize around individual activated CAR T cells during suppression, blocking the CAR T cell clustering that is normally observed in target killing.

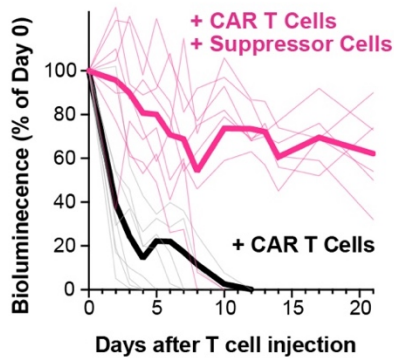
A Protection of Beta Cell Transplants from T Cell-Mediated Destruction



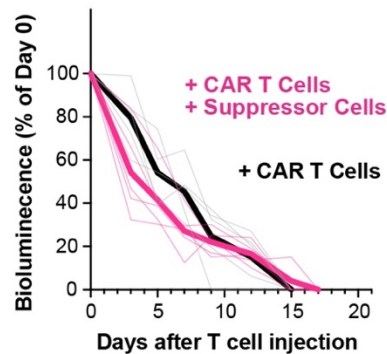
B



C CD19+ eBC Transplant Survival



D CD19- eBC Transplant Survival



E Glucose Challenge Test

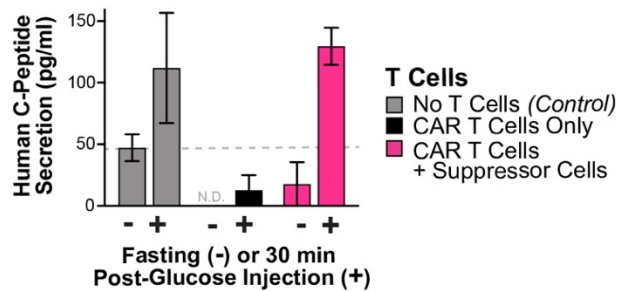
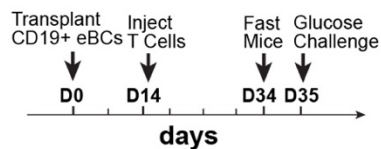


Figure 3.5. Synthetic suppressor cells locally protect hPSC-derived beta cell transplants from T cell-mediated killing in vivo.

(A) Enriched beta cell clusters (eBCs) can be transplanted into the kidney capsule of N.S.G. mice. After 14 days post-transplantation, human CAR T cells and synthetic suppressor T cells are injected i.v.

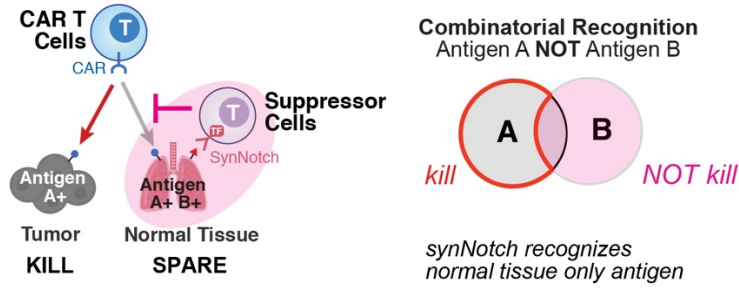
(B) Luciferase imaging of eBC transplants in N.S.G. mice over time after different T cell injections i.v.

(C) Survival of CD19⁺ eBC transplants is assessed by non-invasive imaging of effLuc⁺ eBCs. There is increased survival of eBC transplants with synthetic suppressor T cells, but all eBCs were cleared with CAR T cells only.

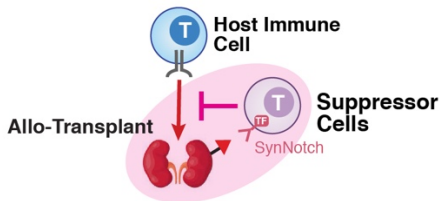
(D) Survival of CD19⁻ eBC transplants is assessed by non-invasive imaging of effLuc⁺ eBCs as in panel B.

(E) Glucose challenge test was performed on N.S.G. mice with eBC transplants 21 days post-injection of T cells. The blood serum was collected and c-peptide levels were measured by ELISA during fasting conditions and 30 minutes after IP glucose injection. Glucose challenge showed that eBCs in mice injected with synthetic suppressor cells remain functional and can secrete c-peptide post-glucose injection, while mice injected with CAR T cells alone were no longer able to produce human c-peptide.

A Enhance tumor recognition with anti-cancer NOT gates



B Protect transplants from allo-rejection



C Suppress autoimmune disease or acute inflammation

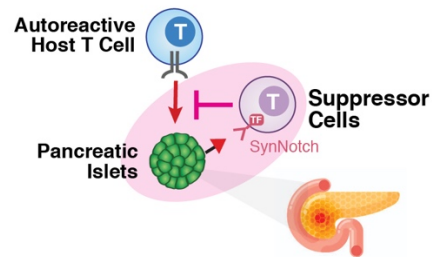


Figure 3.6. Potential application of synthetic suppressor cells for local immune tolerance.

(A) Synthetic suppressor cells can act as NOT gates to block off-target CAR T cell toxicity without blocking on-target killing.

(B) Synthetic suppressor cells can recognize allogeneic transplants and locally suppress rejection by host immune cells.

(C) Synthetic suppressor cells can block autoimmune destruction of tissues locally (e.g. Type 1 Diabetes, Multiple Sclerosis)

MATERIALS AND METHODS

Primary Human T Cell Isolation and Culturing

Human leukapheresis packs were obtained from anonymous donors with approval by the University Institutional Review Board. Primary human CD4⁺ and CD8⁺ T cells were isolated from leukapheresis packs using EasySep kits (Stem Cell Technologies) and frozen in RPMI with 20% human AB serum and 10% DMSO. Human T cells were thawed and cultured in human T cell media (X-VIVO media [Lonza], 5% human AB serum, 10 mM n-acetyl cysteine, 55 μ M β mercaptoethanol, 30 U/mL IL-2). T cells are activated one day after thawing with 25 μ L anti-CD3/CD28 coated beads (Dynabeads Human T-Activator CD3/CD28 [Gibco]) per 1e6 T cells. T cells were infected with lentivirus the day after (2 days after thawing) and the virus was removed from the T cells the following day (3 days after thawing) by centrifugation of T cells at 400xG for 4 minutes and removal of lentivirus-containing supernatant and resuspending in human T cell media. T cells were sorted 5 days after thawing for expression of synNotch or CAR by positive staining of a Myc-tag (anti-Myc-tag antibody, 9B11, Alexa Fluor 647 conjugate, Cell Signaling Technology, Cat# 2233) or fluorescent protein expression. T cells were expanded at 1e6 cells/mL every day until 10 days post-sort prior to starting in vitro or in vivo assays.

Lentivirus Production

Lentivirus was produced using Lx293t lentiviral packaging cells (Takara bio, Cat# 632180) that were seeded in 6-well plates at 7e5 cells/well and 24 hours later

transfected with pHR constructs and pCMV and pMD2.g packaging plasmids using FuGene HD (Promega) following manufacturer's protocol. 48 hours after transfection viral supernatant was collected, filtered, and concentrated with LentiX concentrator (Takara bio, Cat# 631231) prior to use with human T cell cultures.

Tumor Cell Culture

Human K562 cells were purchased from ATCC (CCL-243) and cultured in Iscove Modified Dulbecco's Modified Eagle Medium with 10% FBS and split to 3×10^5 cells/mL every 2 days. Human K562s were engineered to express antigens by lentiviral transduction. Lentivirus was added to the K562 media, removed after 24 hours, and cells were sorted by positive staining 48 hours after removing virus.

Stem Cell-Derived Beta Cells Enriched Beta Cell Clusters (eBC) Differentiation

Mell $INS^{GFP/wt}$ human embryonic stem cells, obtained from S.J. Micallef and E.G. Stanley (Monash Immunology and Stem cell laboratories, Australia) were cultured on embryonic fibroblast (MEFs) in hESC media and passaged using enzymatic digestion. At the beginning of the differentiation, confluent hESC were digested into single cell suspension using TrypLE and seeded at 5.5×10^6 cell/well in a 6 well suspension plates in 5.5 ml hPSC media supplemented with 10 ng/ml Activin A (R&D Systems) and 10 ng/ml HeregulinB (Peprotech). The plates were incubated at 37°C and 5% CO₂ on an orbital shaker at 100 rpm to induce 3D sphere formation. After 24 hours, the spheres were collected in a 50 ml falcon then washed with RPMI media (Gipco) and resuspended in day 1 media in a new 6 well suspension plates. Thereafter media was changed every day

at the same time until day 19 as previously described (Nair et al; doi:10.1038/s41556-018-0271-4) with the exception that all media were enriched with 5 ug/ml Aphidicolin (Cayman Chemical) starting at day 12. On day 19, the spheres were collected and dissociated in a single cell suspension using Accumax (Sigma-Aldrich) then filtered with a 40-um cell Strainer (falcon) to ensure the removal of debris or non-digested spheres. The cells were seeded at 4×10^6 cell/well in a new 6 well suspension plates in the presence or absence of the lentivirus containing CD19 antigen and then placed in orbital shaker at 100 rpm to induce 3D sphere aggregation. The media was changed the following day, then every other day until d27-29.

eBC Transplantation Experiments

NOD-*scid* IL2Rgamma^{null} (NSG) mice were obtained from Jackson Laboratories and bred in our facility. Male and female mice between the age group of 12–16 weeks were used in this study and were maintained according to protocols approved by the University of California, San Francisco, Institutional Animal Care and Use Committee. This study follows all relevant ethical regulations regarding animal research. Mice were Anesthetized with isoflurane and transplanted with ~4000 eBC ($\sim 4 \times 10^6$ cells) under the kidney capsule. Two weeks after the surgery, the mice were injected intravenously either with ($\sim 1 \times 10^6$ cells) CD4/CD8 HLA-A2 CAR T cells alone or in combination with ($\sim 2 \times 10^6$ cells) anti-CD19 synNotch suppressor cells. To assess xenograft luciferase expression, mice were injected intraperitoneally with 15 mg/ml D-luciferin solution (Goldbio Biotechnology) and then imaged using the Xenogen IVIS 200 imaging system (Perkin

Elmer). Same size regions of interest were manually plotted for analysis of all data points to ensure signal consistency within the same experiment.

For the in vivo glucose challenge experiments, five weeks after the surgeries, male transplanted mice were fasted overnight, and the serum was collected by sub-mandibular bleeding at t0 (before) and t30 (30 min) following intraperitoneal D-Glucose injection (1.8 g kg⁻¹). Circulating C-peptide was measured using STELLUX® Chemic Human C-peptide ELISA kit (Alpco)

In-Vitro Assays

T cells were labeled with 1:5000 CellTrace CFSE proliferation stain (Molecular Probes) or 1:5000 CellTrace FarRed proliferation stain (Molecular Probes). T cells and target cells were diluted in their respective media to the appropriate density without IL-2 and combined at a 1:1 ratio with equal media of each type. For activation by synNotch activation beads, T cells were mixed with anti-Myc-tag antibody-coated beads (Pierce) were washed 3 times with hTCM using a magnet before using. For assays longer than 3 days, 100 uL of cells and media were diluted in 100 uL of fresh media for a total volume of 200 uL. For measurement of secreted cytokines, supernatant was measured by ELISA (R&D systems). For measurement of intracellular cytokine production, T cells were mixed with target cells and then exposed to golgi-plugin/stop (BD biosciences) then fixed prior to staining. All flow cytometry analysis was performed on a BD Fortessa X-20 and analyzed using FlowJo (FlowJo, LLC). All cell counts were measured by flow cytometry analysis of a fixed volume of the in vitro culture.

In-Vitro Microscopy Assays

In vitro assays for suppression of T cell killing of enriched beta cell clusters was performed on an Incucyte Live-Cell Analysis System (Sartorius) or Opera Phenix Plus High-Content Screening System. Enriched beta cell survival was quantified as the integrated GFP signal normalized to the 0 hour timepoint. Caspase 3/7 reporter (Incucyte, Cat# 4704) was added at the 0 hour timepoint at 0.2 μ M.

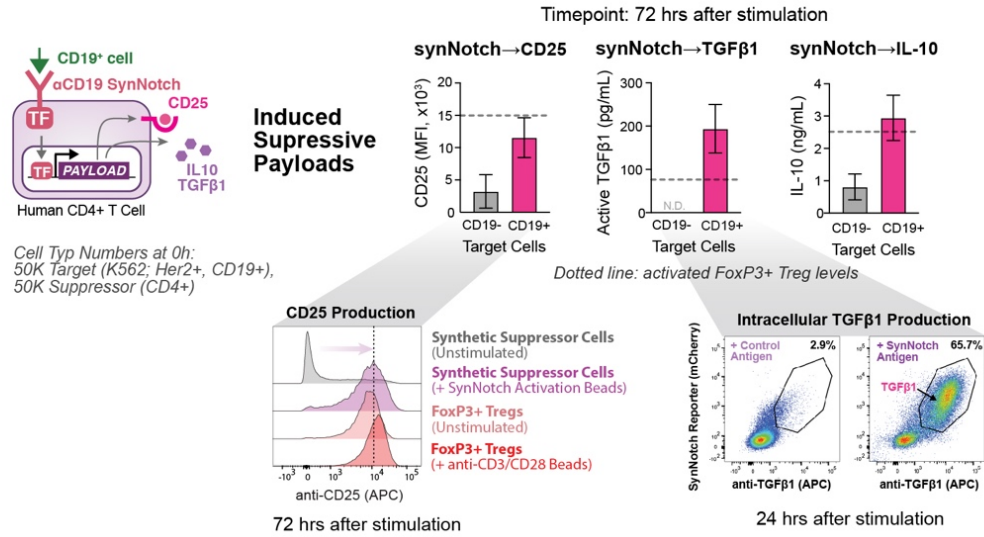
Analysis of Isolated Tumor Samples

Tumor samples were collected from mice and immediately processed. Tumors were minced and digested with 1 mg/mL collagenase IV, 20 U/mL DNase IV, and 0.1 mg/mL hyaluronidase V in RPMI for 30 min at 37°C with shaking. The digested cells were washed twice through 70 μ m cell strainers then stained for cell surface markers.

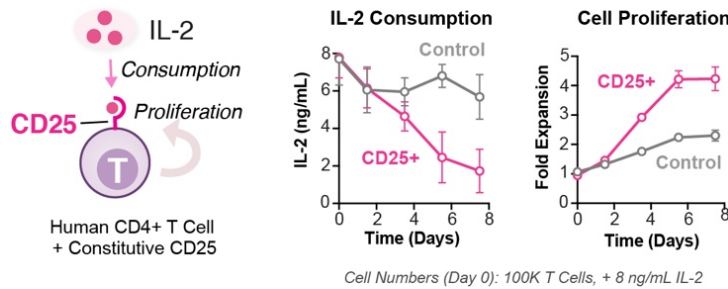
Mouse Tumor Experiments

For tumor experiments, female age 6 to 12 week old NSG (NOD-*scid* IL2Rgamma^{null}) mice were used. K562 tumors were injected in 100 μ L PBS subcutaneously into each flank. Tumors were measured by calipers. For transplant experiments, enriched beta cell clusters were transplanted into the kidney capsule of age 12 to 16 week old NSG mice. Transplants were monitored using bioluminescence imaging by an IVIS Spectrum (Perkin Elmer). Mice were injected intraperitoneally with 200 μ L of 15 mg/mL d-luciferin (Goldbio) and imaged 15 minutes after injection. In all cases, human T cells were injected intravenously by tail vein injection in 100 μ L PBS.

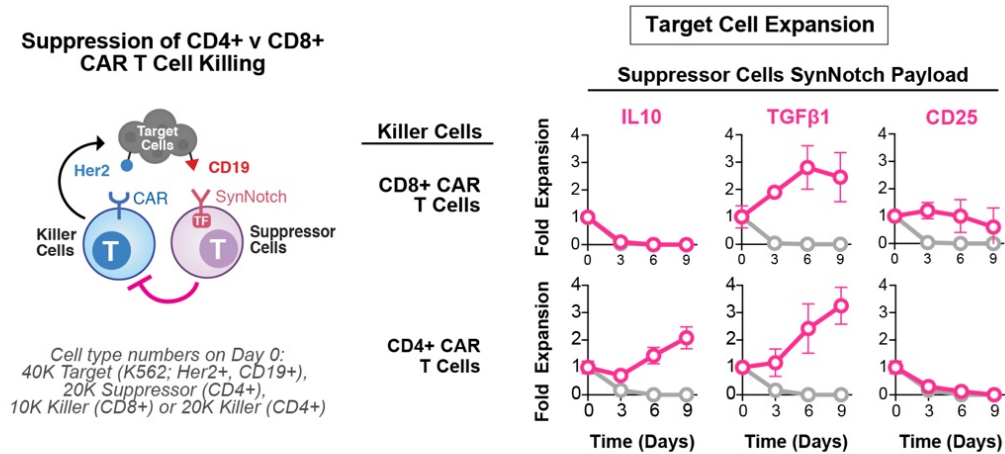
A Induced synthetic suppressor cells produce high levels of suppressive payloads comparable to those produced by stimulated FoxP3 regulatory T cells (polyclonal)



B IL-2 sink cells (constitutive CD25 expression) consume IL-2 and proliferate faster



C SynNotch payloads differentially suppress CD4+ v CD8+ CAR T cells



- IL-10 effectively inhibits CD4+, but not CD8+ T cells
- TGFβ1 effectively inhibits both CD4+ and CD8+ T cells

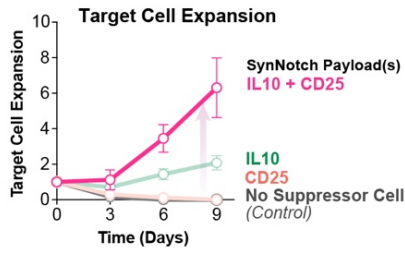
Fig. 3.S1. Analysis of synthetic suppressor cell payload production, IL-2 consumption, proliferation, and differential payload effects on CD4+ vs CD8+ CAR T cells.

(A) SynNotch-induced payloads are produced at high levels comparable to stimulated regulatory T cells. CD25 was measured by antibody staining. IL-10 and TGF β 1 was measured by ELISA of supernatant.

(B) Engineered CD25+ CD4+ T cells consume IL-2 and proliferate faster. Cell counts measured by flow cytometry and IL-2 levels measured by ELISA of supernatant.

(C) SynNotch induced IL-10 suppresses CD4+ but not CD8+ CAR T cell killing, while TGF β 1 suppresses both. Target cell survival measured by flow cytometry.

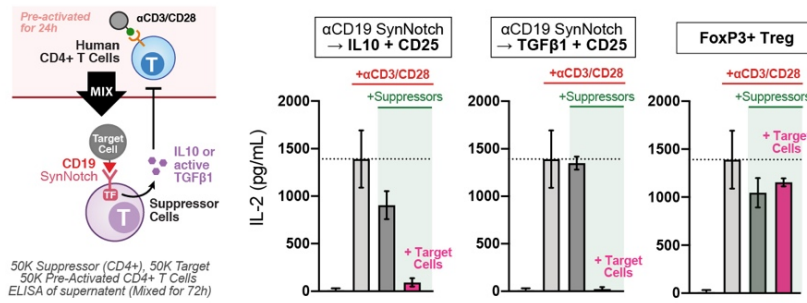
A Combination of IL-10 + CD25 payloads is more effective than single payloads



Suppressor cells making combination payloads of IL-10 + CD25 are more effective at protecting target cells from CD4+ CAR T cells than similar cells with individual payloads (TGFβ1 + CD25 combo suppression of CD8+ CAR T cells is shown in Fig. 2)

Cell type numbers on Day 0:
40K Target (K562; Her2+, CD19+),
20K Suppressor (CD4+), 20K Killer (CD4+)

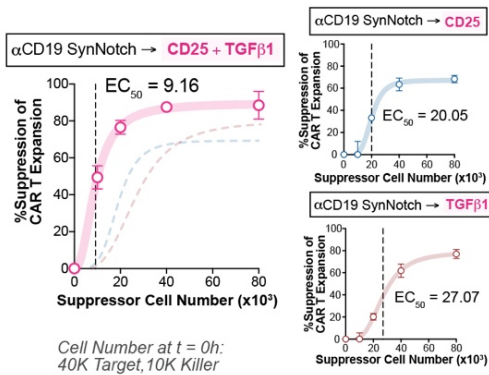
B SynNotch-induced payloads strongly suppress accumulation of IL2 produced by activated CD4+ T cells



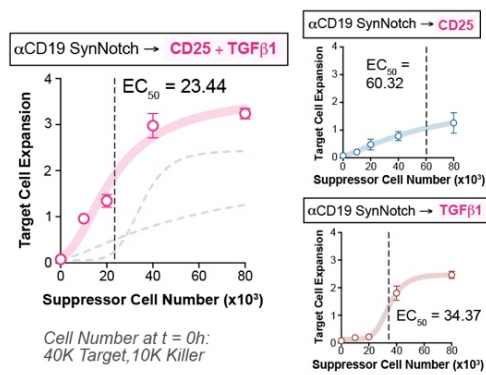
Suppressor cells making combination payloads of [IL-10 + CD25] or [TGFβ1 + CD25] are highly effective at depleting IL-2 produced by activated CD4+ T cells

C SUPPRESSION DOSE RESPONSE: comparison of single vs combo payloads

%Suppression of CAR T Cell Expansion (t = 72hrs)



Fold Expansion of Target Cells (t = 72hrs)



Suppressor cells making combination payloads of [TGFβ1 + CD25] show increased amplitude and EC50 for suppression by different metrics

Fig. 3.S2. Additional analysis of combination payload suppressor cells (synNotch → IL-10 + CD25 or synNotch → TGFβ1 + CD25).

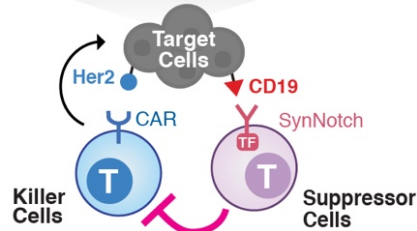
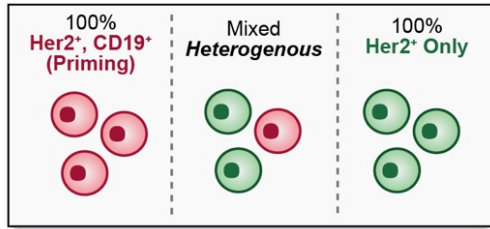
(A) Synthetic suppressor T cells with SynNotch → IL-10 + CD25 circuit block CAR CD4+ T cell killing of target cells more effectively than each payload alone. Target cell survival measured by flow cytometry.

(B) SynNotch-induced payloads block accumulation of IL-2 produced by activated CD4+ T cells. Human CD4+ T cells were activated by anti-CD3/CD28 beads and co-cultured with anti-CD19 synthetic suppressor T cells activated by CD19+ target cells. IL-2 levels in the supernatant were measured by ELISA.

(C) Suppression of CD8+ CAR T cell killing and proliferation as a dose response of the synthetic suppressor cells show that combination circuits increase the amplitude and reduce EC50 for suppression. Target cell and CAR T cell counts measured by flow cytometry.

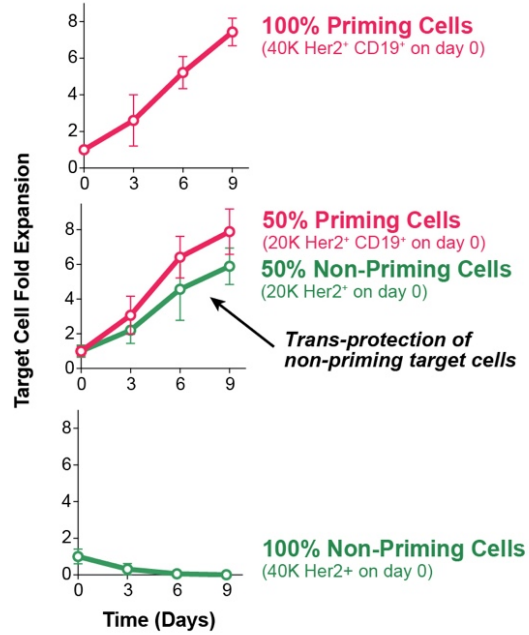
A Suppressor cells protect target cells with heterogenous priming antigen in vitro

Mix of priming and non-priming target cells

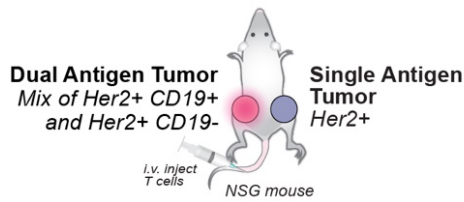


Cell type numbers on Day 0:
40K Target (K562)
20K Suppressor (CD4+),
10K Killer (CD8+)

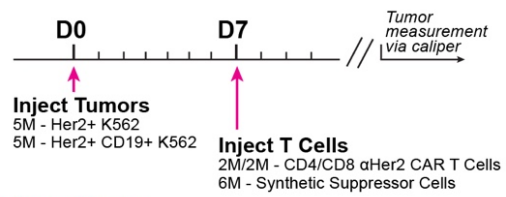
Circuit: $aCD19\ SynNotch \rightarrow CD25 + TGF\beta1$



B Suppressor cells overcome heterogeneous SynNotch priming antigen in vivo



Two Tumor Mouse Model



%Priming Cells (Her2+ CD19+) in Dual Antigen Tumor

Circuit: $aCD19\ SynNotch \rightarrow CD25 + TGF\beta1$

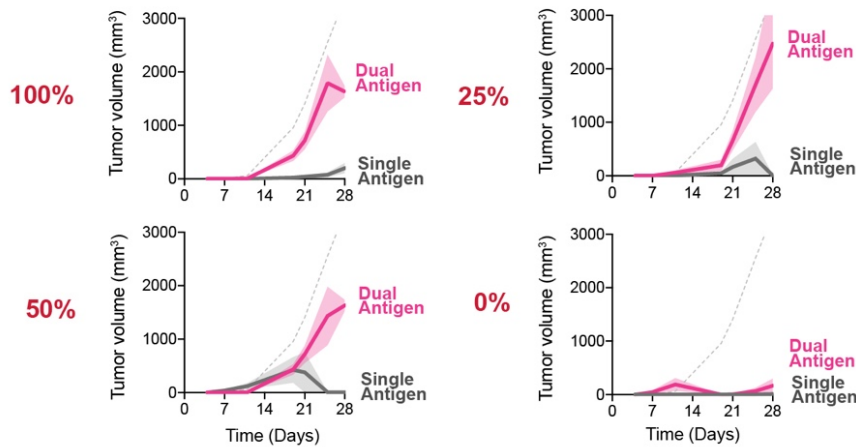


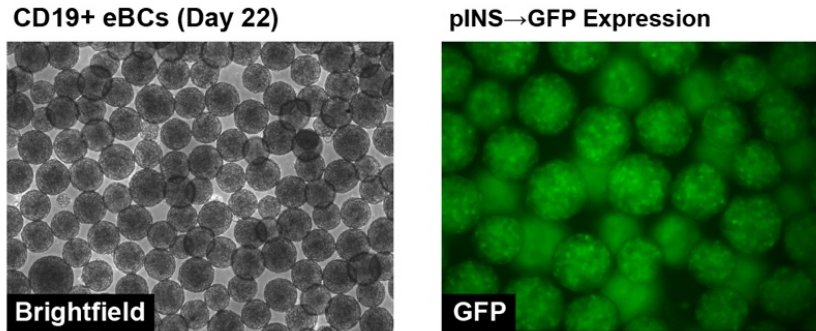
Fig. 3.S3. Synthetic suppressor cells overcome heterogeneity in SynNotch priming antigen on target cells.

(A) Synthetic suppressor T cells block killing of bystander CAR T cell target cells that lack the synNotch antigen. Target cells with or without the synNotch antigen, CD19, were mixed at different initial ratios. Cell counts were measured by flow cytometry.

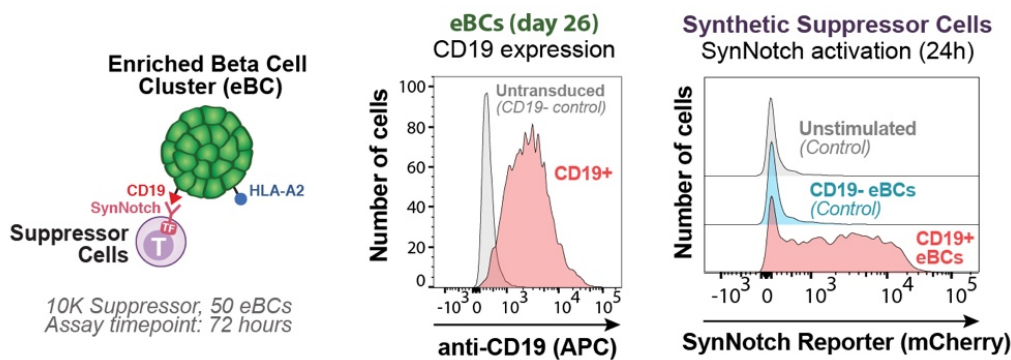
(B) Suppressor cells overcome heterogeneous SynNotch priming antigen in vivo.

Tumors containing only single antigen target cells (Her2+) or a combination of single and dual antigen (Her2+ CD19+) target cells were injected subcutaneously in NSG mice. Synthetic suppressor T cells block CAR T cell killing of tumors with as low as 25% synNotch priming cells in the tumor at the time of implantation.

A CD19+ beta cell clusters maintain structure and pINS→GFP Expression



B CD19+ beta cell clusters can activate an anti-CD19 SynNotch T cell circuit



C anti-preproinsulin (PPI) TCR T cells fail to kill beta cell clusters in vitro

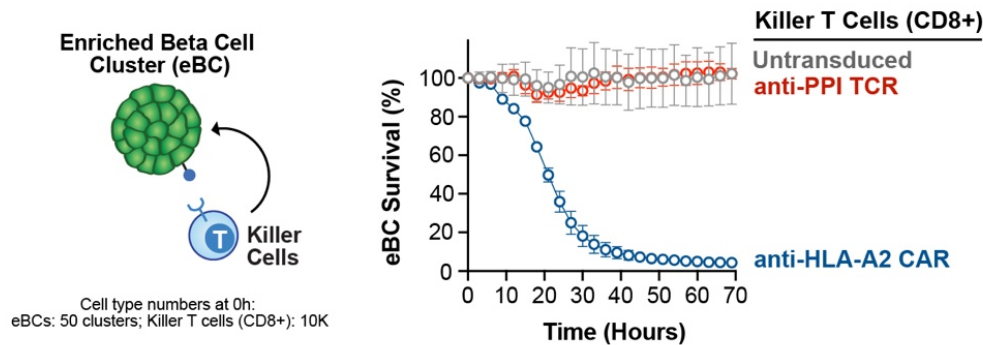
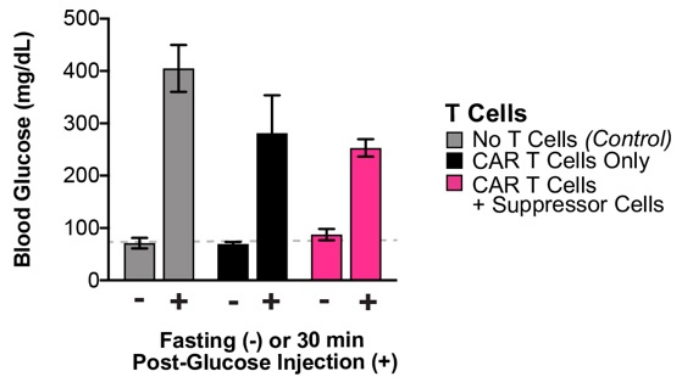


Fig. 3.S4. CD19+ enriched beta cell clusters are functional and activate synthetic suppressor cells in vitro.

(A) CD19+ eBCs maintain morphology and insulin promoter induced GFP expression.
 (B) Anti-CD19 synthetic suppressor cells can activate the expression of a synNotch reporter (mCherry) when co-cultured with CD19+ eBCs, but not untransduced (CD19) eBCs. Fluorescence measured by flow cytometry.
 (C) Anti-HLA-A2 CAR T cells and anti-PPI TCR T cells fail to kill eBCs in vitro.

A Fasting and post-glucose injection glycemia (associated with Figure 5E)



B Beta cell transplants remain intact with synthetic suppressor cells (Day 5)

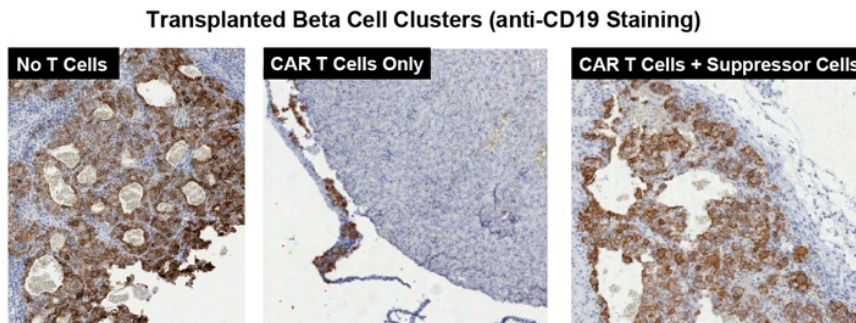


Fig. 3.S5. Analysis of hPSC-derived beta cell transplants.

(A) Blood glucose was elevated post-glucose injection for all mice (related to Fig. 3.5E)
(B) Transplanted eBCs maintain their structure in the presence of synthetic suppressor cells, but are cleared by CAR T cells alone. Anti-CD19 staining of isolated kidneys from transplanted mice 5 days after T cell injection.

Chapter 4 – Concluding Remarks

In conclusion, this thesis explored the potential of engineering immune cells to reshape immune microenvironments in various therapeutic contexts. We engineered T cell therapies with synNotch circuits to locally deliver pro-inflammatory or suppressive signals to perturb the local immune ecosystem. By programming these cells to deliver these payloads in a targeted manner, these engineered cell therapies limit off-target toxicities from systemically administration of immune modulatory agents like cytokines. This approach holds great promise for the development of novel treatments for a range of diseases, including cancer, autoimmune disorders, and transplant rejection.

Design Principles of T Cell Circuits

In addition to its potential for developing new treatments, engineering T cells with synthetic circuits also helps us to better understand the minimal components necessary to achieve particular functions. Synthetic reconstitution allows us to break down complex biological processes into their component parts and study them in isolation. By identifying the minimal set of components needed to achieve a particular function, we can gain a deeper understanding of the underlying design principles and develop more controllable and targeted therapies.

In engineering anti-tumor synthetic cytokine circuits (Chapter 2), we identify critical design rules for T cell delivery of IL-2 to tumors, particularly that TCR-independent, autocrine delivery was required for effective tumor clearance. For expansion, effector T cells need to overcome consumption of IL-2 by bystander T cells and bypass TCR signals, which can be inhibited by the tumor, to mount an effective

response. Wiring IL-2 production using a synNotch induction circuit can bypass these key points of tumor suppression and could be a general strategy to tackle challenging solid tumors.

By exploring minimal requirements for engineering immune suppressive cells (Chapter 3), we identified the design principle that a CD4⁺ T cell producing both a sink for pro-inflammatory cytokine IL-2 (CD25) and acting as a source for inhibitory cytokines (IL-10 or TGF β 1) can be sufficient to drive strong immune suppression. CD25 both acts to drive proliferation of the suppressor cells and consumption of IL-2. By driving proliferation of the suppressor cells, CD25 can amplify the level of inhibitory cytokine produced. This combination of signals may be a general way to enhance immune suppression. Other immune suppressor cells such as regulatory T cells, for example, produce both of these two signals. Although these molecular signals have been studied in isolation through genetic perturbation, reconstitution with synthetic cellular circuits allow us to study the synergies from specific combinations of components.

Major Challenges for Cell Therapies

In spite of the advances in cell therapies in recent years, there continues to be major challenges that limit the potential of these therapies:

(1) Manufacturing: Cells, such as primary human T cells, engineered with large genetic constructs remain difficult to manufacture. The capability to introduce larger constructs reproducibly and at a desired locus in the genome will enable the design of more complex synthetic circuits into cells with more consistent

behavior. Current cell therapies primarily rely on autologous cell sources.

However, allogeneic cells would allow for more accessible off-the-shelf therapies.

(2) Targeting: Precise molecular recognition of a target organ or tumor is critical for effective local therapeutic action. In this thesis, we demonstrate that this cell-based, targeted approach could be effective in treating solid tumors or inflammatory diseases using model antigens such as CD19, but identifying relevant antigens for a specific tissue will be critical to translating these therapies. In many cases, the specificity of these targets can determine the efficacy of the intervention. Combinatorial recognition of antigens (for example, using synNotch cascades) may be necessary if individual antigens are insufficiently specific for a given tissue.

(3) Pleiotropy: Inherent pleiotropy effects of induced therapeutic payloads could limit their therapeutic potential. Molecular understanding of the effects of signal molecules like IL-2 or TGF β 1 could allow us to engineer synthetic variants that limit undesired interactions. For example, IL-2 variants can be engineered to preferentially target particular immune cells or subtypes like activated T cells. Under certain physiological contexts, inhibitory cytokine TGF β 1 can cause fibrosis which may limit its use as an immune suppressive signal in certain susceptible tissues. Understanding the extent of these undesired effects can inform the design of cell therapies to more predictably control responses.

The Future of Cell Therapies

Looking to the future, there are many exciting possibilities for cell therapies. As our understanding of the underlying biology continues to advance, we may discover new ways to engineer cells that are even more effective at targeting and eliminating disease in a more controllable manner than previously possible. T cell or other immune cells can be used to drive targeted immune responses against cancer or autoimmunity. In theory, these cell therapies could be extended to regenerate damaged tissues by programming specific delivery of regenerative agents. Exploring immune signals using synthetic cellular circuits that reconstitute those functions allows us to program more predictable therapeutic action.

Overall, the field of engineered cell therapies is rapidly advancing and holds great promise for the future of medicine. As we continue to push the boundaries of what is possible, we may soon see a new era of targeted therapies that offer hope to patients with even the most challenging diseases. Beyond immune cell therapies, stem cell-based approaches hold promise for replenishing damaged or lost cells in conditions such as type 1 diabetes. Through the differentiation of stem cells into specific cell types such as islet-like organoids, we can design functional, transplantable organs. Cells could also be used in the future to precisely repair dysfunctional tissues in degenerative diseases like Parkinson's disease. Synthetic biology can help explore fundamental design principles of cellular functions and can program therapeutic cells in a more controlled and predictable manner.

Publishing Agreement

It is the policy of the University to encourage open access and broad distribution of all theses, dissertations, and manuscripts. The Graduate Division will facilitate the distribution of UCSF theses, dissertations, and manuscripts to the UCSF Library for open access and distribution. UCSF will make such theses, dissertations, and manuscripts accessible to the public and will take reasonable steps to preserve these works in perpetuity.

I hereby grant the non-exclusive, perpetual right to The Regents of the University of California to reproduce, publicly display, distribute, preserve, and publish copies of my thesis, dissertation, or manuscript in any form or media, now existing or later derived, including access online for teaching, research, and public service purposes.

DocuSigned by:

Nishitha Reddy

530AADF8A75247D...

Author Signature

5/25/2023

Date